The Thesis Committee for Tyler Katherine Wellik

Certifies that this is the approved version of the following thesis:

Evaluating Land Use Impacts of Self-Driving Vehicles and Leveraging Intelligently Charged Electrified Transit to Support a Renewable Energy Grid in the Austin, Texas Region

SUPERVISING COMMITTEE:

Kara Kockelman, Supervisor

Moataz Mohamed

Evaluating Land Use Impacts of Self-Driving Vehicles and Leveraging Intelligently Charged Electrified Transit to Support a Renewable Energy Grid in the Austin, Texas Region

by

Tyler Katherine Wellik

Thesis

Presented to the Faculty of the Graduate School of
The University of Texas at Austin
in Partial Fulfillment
of the Requirements
for the Degree of

Master of Science in Engineering

The University of Texas at Austin
December 2019

Acknowledgements

There are many I owe thanks to as I submit this thesis and prepare to graduate with my master's degree. First, I would like to thank the many faculty at the University of Texas at Austin who strengthened my experience. First and foremost, I am grateful to my advisor, Dr. Kara Kockelman, for her support and mentoring in the field of transportation engineering. I am so honored to have been a part of her lab and I have learned so much from her in such a short period of time. I am also thankful to the many professors whom I learned from in the classroom and in office hours. In addition to Dr. Kockelman, Dr. Zhanmin Zhang, Dr. Chandra Bhat, Dr. Stephen Boyles, Dr. Randy Machemehl, Dr. Gian Claudia Sciara, and Dr. Stephen Donald provided excellent instruction and advice. I believe I have grown so much as a student and as a researcher during my time at UT, in large part because of the passion and knowledge that these professors bring to the classroom and to their research.

I would also like to acknowledge several faculty members outside of UT Austin. I would like to sincerely thank Dr. Moataz Mohamed (McMaster University) for his help and guidance in the work I completed in Part Two of this thesis. If he had not been open and willing to work with us and share his electric bus expertise, this work would not have been possible. I am also honored to have him as a member of my thesis committee and for his support in editing this thesis. I would also like to thank Dr. Rolf Moeckel (Technical University of Munich) who provided an enormous amount of support and guidance during much of the work I completed in Part One of this thesis. I am thankful for the countless Skype meetings and email exchanges, and I have learned so much from him in the field of transportation and land use modeling.

I would like to thank those in the academic community outside of UT who helped me along the way. I am thankful to the National Science Foundation's Sustainable Healthy Cities Research Network for financial support of my master's degree and research. I am also grateful for the research advice I received from many colleagues in that network. I am appreciative of an additional fellowship I received that was funded through the United States Department of Transportation's Dwight D. Eisenhower Transportation Fellowship Program. This fellowship supported my attendance at the largest transportation conference in the world, the Transportation Research Board Annual Meeting. Both of these opportunities significantly enriched my education and experience.

Finally, I am grateful for my strong and vast network of support, including my family, friends, and classmates. Thank you to my parents for teaching me to work hard, manage time, and find balance in life. And thank you to my Mom for taking time out of her extremely busy schedule to help edit this thesis. Thank you to my partner, Joe, for being a fantastic teammate in Part Two of this thesis work and for keeping me balanced and grounded throughout my graduate career. And finally, thank you to my sister, Corey, for always being there and for never failing to make me laugh.

Preface

This thesis is divided into two parts, each focused on different aspects of the future of transportation.

Part One anticipates the land use and traffic impacts of self-driving vehicles across the six-county Austin, Texas region. An integrated transportation and land use model (ITLUM) fusing MATSim (the Multi-Agent Transportation Simulator) with SILO (Simple Integrated Land-Use Orchestrator) was used, along with a synthetic regional population for year 2013 based on the Census' Public Use Microdata Sample (PUMS). The land use model (SILO) was calibrated using 2015 zone-level information, estimated by the Capital Area Metropolitan Planning Organization (CAMPO), and several scenarios were run, with and without self-driving vehicle options. This work will be published with Kara Kockelman as co-author over the coming year.

Part Two looks at using the City of Austin and its transit provider, CapMetro, as a case study for determining the benefits and costs of electrified bus transit and its potential to support a grid that depends heavily on renewable energy. Texas leads the United States in wind power generation, and 37.5% of Austin's electricity comes from wind plus solar as of 2018. This is positive from a greenhouse gas emissions and climate change perspective but comes with challenges to the utility manager. Intermittent power sources have major implications for the ramping of traditional energy sources, like coal, natural gas, and nuclear power plants. This work's smart charging and discharging policies are found to offer notable emissions and power-cost benefits. This work has co-authors Joseph Griffin, Dr. Kara Kockelman, and Dr. Moataz Mohamed and is under review for publication in the *Sustainable and Renewable Energy Review Journal*. It was presented at the Sloan Foundation Workshop on Integrating New Electric Mobility Systems with the Electric Grid Infrastructure in Boston, MA on November 6, 2019, and will be presented at the 99th Transportation Research Board Annual Meeting in Washington D.C. in January 2020.

Abstract

Evaluating Land Use Impacts of Self-Driving Vehicles and Leveraging Intelligently Charged Electrified Transit to Support a Renewable Energy Grid in the Austin, Texas Region

by

Tyler Katherine Wellik, M.S.E.
The University of Texas at Austin, 2019
Supervisor: Kara M. Kockelman

This thesis is divided into two parts. The first part focuses heavily on the land use model SILO and its implementation in the Austin, Texas six-county region over a 27-year period of full adoption of self-driving vehicles. It discusses the model framework and capabilities and critically evaluates SILO's specifications. SILO was then integrated with the agent-based transportation model MATSim for the Austin region. Land use and travel results were generated for a business-as-usual case (BAU) of 0% self-driving or "autonomous" vehicles (AVs) over the model timeframe versus a scenario where households' value of travel time savings (VTTS) is reduced by 50%, to reflect the travel-burden reductions of no longer having to drive. A third scenario is also compared and examined against BAU to understand the impacts of rising vehicle occupancy (VO), and/or higher roadway capacities, due to dynamic ride-sharing (DRS) options in shared AV (SAV) fleets. Results suggest an 8.1% increase in average commute times when VTTS falls by 50% and VO remains unaffected (the 100% AV scenario), and a 33.3% increase in the number of households with "extreme commutes" (over 1 hour, each way) in the final model year (versus BAU of 0% AVs). When VO is raised to 2.0 and VTTS falls instead by 25% (the "Hi-DRS" SAV scenario), average commute times increase by 3.5% and the number of households with "extreme commutes" increase by 16.4% in the final model year (versus BAU of 0% AVs). The ITLUM also predicts 5.3% fewer households and 19.1% more available, developable land in the City of Austin

in the 100% AV scenario in the final model year relative to the BAU scenario's final year, with 5.6% more households and 10.2% less developable land outside the City. In addition, the model results predict 5.6% fewer households and 62.9% more available developable land in the City of Austin in the Hi-DRS SAV scenario in the final model year relative to the BAU scenario's final year, with 6.2% more households and 9.9% less developable land outside the City.

This thesis' second part looks at how electric buses can support a power grid that relies heavily on renewable energy sources, like wind and solar. The transportation sector is a major greenhouse gas (GHG) emitter. Concurrent electrification of vehicles and investment in renewable energy is required to deeply decarbonize this and other sectors of our economies. The introduction of intermittent renewable energy sources, like solar and wind, at a large scale presents major challenges to grid operators and utility companies. This study examines the benefits and costs that a Vehicle-to-Grid (V2G) Battery Electric Bus (BEB) fleet offers Austin, Texas by buffering against sharp shifts in renewable energy production to help smooth power demands from traditional energy sources (like coal, natural gas, and nuclear power plants). A V2G BEB "smart charging" (SC) scenario's cost and emissions were compared to those in a BEB "charge-as-needed" scenario and to those in a diesel bus scenario, for 423+ buses and over 88,000 bus-miles per day. By simply electrifying Austin's buses, without any SC strategies, the total external cost of all of Austin's electricity grid emissions and bus emissions falls by approximately 3.42%, amounting to over 21¢-savings per bus-mile, relative to the diesel-bus scenario. By using SC strategies, those same emission costs fell by 5.64% or over 35¢-savings per bus-mile. These emissions savings become very significant when summed over the course of a year. In the non-SC BEB scenario, emissions savings amount to approximately $6.86M/year, and in the SC BEB scenario, emissions savings reach approximately $11.3M/year. Such reductions are thanks to high renewable energy use in Austin's power mix and because diesel fuel is much more emitting (per kWh) than power plants. From the transit operator's perspective, a BEB fleet costs more than a diesel bus fleet, but such costs can be more than offset by renewable energy savings and emissions-costs benefits. Thanks to SC strategies, the utility manager is estimated to save 22% of their daily power-purchase cost in this case study.

Table of Contents

List of Tables xii

List of Figures xiv

PART ONE: EVALUATING LAND USE IMPACTS OF SELF-DRIVING VEHICLES IN THE AUSTIN, TEXAS REGION 1

Chapter 1: Introduction and Background to Part One 2

Chapter 2: Literature Review for Part One 5

Chapter 3: SILO's Synthetic Population Overview 8

3.1 SILO's Synthetic Population Model Framework 8

3.2 Input Files Needed for SILO's Synthetic Population Generator 9

3.2.1 Public Use Microdata Sample (PUMS) Data 9

3.2.2 Zone System 11

3.2.3 Zone Shapefile 11

3.2.4 Partially Covered PUMAs 11

3.2.5 Travel Skims 11

3.2.6 Activities File 12

3.2.7 Vacancy Rates 12

3.3 SILO's Synthetic Population Results 13

Chapter 4: SILO-MATSim Model Framework 19

4.1 SILO Model Framework 19

4.1.1 Synthetic Population 20

4.1.2 Demography Module 20

4.1.3 Real estate module 22

4.1.4 Household relocation module 25

4.2 MATSim Model Framework 28

4.3 SILO-MATSim Integration 29

4.4 SILO Input Files Needed 31

4.4.1 Synthetic Population 31

4.4.2 Available Land 32

4.4.3 Zone System 32

4.4.4 Population Forecast 33

4.4.5 Employment Forecast 33

4.4.6 Work Trip Length Frequency Distribution 33

4.4.7 Zone Shapefile 33

4.5 MATSim Input Files Needed 34

4.5.1 Transportation Network 34

4.5.2 Configuration File 34

4.6 Model Assumptions and Simplifications 34

4.6.1 SILO's Assumptions and Simplifications 34

4.6.2 Additional Assumptions and Simplifications Made for the Austin-Specific Implementation 35

Chapter 5: SILO Model Parameter Calibration ____ 38
5.1 Available, Developable Land ____ 38
5.2 Structural Vacancy Rates ____ 39
5.3 Dwelling Construction Demand ____ 40
5.4 Dwelling Price Model ____ 41
5.5 School Quality ____ 43

Chapter 6: SILO – MATSim Results ____ 46
6.1 Scenario Descriptions ____ 46
6.2 Summary of Results ____ 47
6.3 Commute Travel Time Results ____ 49
6.4 Household Location Results ____ 50
6.5 Available and Developable Land Results ____ 54

Chapter 7: Conclusions on AV Land Use Implications ____ 57

PART TWO: LEVERAGING INTELLIGENTLY CHARGED ELECTRIFIED TRANSIT TO SUPPORT A RENEWABLE ENERGY GRID ____ 61

Chapter 8: Introduction and Background to Part Two ____ 62

Chapter 9: Review of the Current State of BEBs ____ 65
9.1 Discussion About BEBs and Other Bus Alternatives ____ 65
9.1.1 Conventional Diesel Buses ____ 65
9.1.2 Compressed Natural Gas Buses ____ 66
9.1.3 Hybrid Electric Buses ____ 67
9.1.4 Battery Electric Buses ____ 67
9.2 Cost Comparisons of Battery Electric Buses to Other Bus Alternatives ____ 68
9.3 Emissions Comparisons of Battery Electric Buses to Other Bus Alternatives ____ 69
9.4 Vehicle Performance Comparisons of Battery Electric Buses to Other Bus Alternatives ____ 71
9.5 Final Notes on BEBs Compared to Other Bus Alternatives ____ 73

Chapter 10: Literature Review for Part Two ____ 75

Chapter 11: Utility-Transit Manager Model Framework ____ 79
11.1 Utility Manager Simulation Model ____ 80
11.2 BEB Simulation Model ____ 82
11.3 Cost Analysis ____ 85

Chapter 12: BEB Case Study ____ 87
12.1 Input Data ____ 87
12.2 Scenario Definition ____ 89

Chapter 13: V2G Smart-Charging Battery Electric Bus Results ____ 91

Chapter 14: Bus Costs, Energy, and Emissions Conclusions _____100
Appendix: Additional Spatial Maps for Part One _____ 102
Abbreviations _____ 110
Nomenclature for Part One _____ 112
Nomenclature for Part Two _____ 113
References _____ 114

List of Tables

Table 1: Assumed Vacancy Rates by Household Type in SILO Maryland Implementation (Moeckel, 2018g) 9

Table 2: Model Vacancy Rates by County (Moeckel, 2019a) 13

Table 3: Descriptive Statistics of Population Age in Austin 13

Table 4: Population Gender Distribution in Austin 14

Table 5: Population Relationship Distribution in Austin 14

Table 6: Race Distribution in Austin 14

Table 7: Descriptive Statistics of Working Adults' Income in Austin 15

Table 8: Distribution of Households by Size (as % of dwellings) in Austin 15

Table 9: Distribution of Households by Number of Household Vehicles (as % of occupied HHs) in Austin 16

Table 10: Job Type Distribution in Austin 16

Table 11: Dwelling Distribution by Type (as % of total dwellings) in Austin 17

Table 12: Vacant Dwellings by Type (as % of all dwellings of that type) in Austin 17

Table 13: Dwelling Distribution by Number of Bedrooms (as % of dwellings) in Austin 18

Table 14: Descriptive Statistics of Monthly Cost of Dwellings in Austin 18

Table 15: Dwelling Renovation and Deterioration Probability, Based on the Current Dwelling Quality (Moeckel, 2018f) 23

Table 16: Linear Regression Model Used to Determine Non-City Metropolitan Region Developable Land 32

Table 17: Crime Indices by County in the Austin Metropolitan Region (BestPlaces, n.d.) 37

Table 18: Vacancy Rates by Dwelling Type for the Austin Implementation of SILO 40

Table 19: School Quality Grades and Indices for School Districts in the Austin Metropolitan Region 44

Table 20: Summary of Scenario Results Comparing Model Base Year to End Year (27-year period) 47

Table 21: Cost Comparisons of Different Bus Types 69

Table 22: GHG Emissions of Different Bus Types (Mohamed et al., 2016) 71

Table 23: Vehicle performance comparisons across bus types 72

Table 24: Other vehicle performance characteristics of BEBs by battery capacity and charger power (Proterra, 2018a) 72

Table 25: Operational Information of Different Energy Sources (U.S. Energy Information Administration, 2016; Van den Bergh & Delarue, 2015) 80

Table 26: Cost Assumptions for Scenario Cost Analysis 86

Table 27: Summary of Bus Scenario Costs, Energy, and Emissions Results 92

List of Figures

Figure 1: Labeled Map of PUMAs in the Austin Metropolitan Region ____ 10

Figure 2: SILO Model Flowchart (from Moeckel, 2018e) ____ 19

Figure 3: Birth Rates of Single and Married Women, Used for Birth Probabilities in SILO (U.S. Department of Health and Human Services, 2003; from Moeckel, 2018b) ____ 20

Figure 4: Marriage Probability in SILO by Gender and Age (from Moeckel, 2018b) ____ 21

Figure 5: Marriage Age Difference Utility in SILO (from Moeckel, 2018b) ____ 21

Figure 6: Divorce Probability in SILO by Age and Gender (Moeckel, 2018b) ____ 22

Figure 7: Dwelling Demolition Probability in SILO, Based on Current Dwelling Quality and Vacancy Status (from Moeckel, 2018f) ____ 24

Figure 8: Dwelling Price Adjustments as a Function of Zonal Vacancy Rates for a Dwelling Type with 4% Structural Vacancy Rate (from Moeckel, 2018f) ____ 25

Figure 9: Frequency and Utility of Commute Travel Time from the Maryland SILO Implementation, Adopted for the Austin SILO Implementation ____ 27

Figure 10: Example of Commute Departures, arrivals, and the Corresponding Number of Persons En-Route for the BAU Model in Year 2013 (Horni et al., 2016) ____ 30

Figure 11: Construction Demand for Dwelling Types as a Function of Vacancy Rate in the Austin Implementation of SILO ____ 41

Figure 12: School Quality Index Shown Spatially in the Austin Six-County Region ____ 45

Figure 13: Commute Travel Times in Austin in the Base Model Year and 20 Years After the Base Year in Each Scenario ____ 50

Figure 17: Difference in Where Households are Located in the 100% AV Scenario Relative to the BAU Scenario in the Final Model Year ____ 51

Figure 18: Difference in Where Households are Located in the Hi-DRS SAV Scenario Relative to the BAU Scenario in the Final Model Year ____ 53

Figure 19: Difference in the Amount of Available, Developable Land in the 100% AV Scenario Relative to the BAU Scenario in the Final Model Year ____ 55

Figure 20: Difference in the Amount of Available, Developable Land in the Hi-DRS SAV Scenario Relative to the BAU Scenario in the Final Model Year ____ 56

Figure 21: EV GHG Ratings and Gasoline MPG Equivalents by Electricity Grid Region (Reichmuth, 2017) 63

Figure 22: Flowchart of Developed V2G Smart-Charging Simulation Model 79

Figure 23: Austin Bus Transit Routes Map with Charging Stations Labeled in Yellow (Remix, 2019) 87

Figure 24: Solar and Wind Production and Non-Bus Electricity Consumption Tested 89

Figure 25: Production by Source in Non-Smart-Charging (Non-SC) Scenario and Change in Production in Smart-Charging (SC) Relative to Non-SC Scenario 95

Figure 26: Electricity Generation by Type in the Diesel Case, Followed by Change in Generation by Type Relative to the Diesel Case in Non-SC and SC Scenarios 96

Figure 27: GHG Emissions by Type in the Diesel Case, Followed by Change in GHG Emissions by Type Relative to the Diesel Case in Non-SC and SC Scenarios 97

Figure 28: Battery Electric Bus (BEB) System Target vs. Achieved Consumption (from Eq. 9 & 16) 98

Figure 29: Net BEB System Energy Consumption in Non-SC and SC Scenarios 99

Figure 30: Change in Where Households are Located in the BAU Scenario from the Base Model Year to the Final Model Year 103

Figure 31: Change in Where Households are Located in the 100% AV Scenario from the Base Model Year to the Final Model Year 104

Figure 32: Change in Where Households are Located in the Hi-DRS SAV Scenario from the Base Model Year to the Final Model Year 105

Figure 33: Change in How Much Available Land is Used for Construction in the BAU Scenario from the Base Model Year to the Final Model Year 106

Figure 34: Change in How Much Available Land is Used for Construction in the 100% AV Scenario from the Base Model Year to the Final Model Year 107

Figure 35: Change in How Much Available Land is Used for Construction in the Hi-DRS SAV Scenario from the Base Model Year to the Final Model Year 108

Figure 36: Job Growth Between the Base and Final Model Year 109

PART ONE: EVALUATING LAND USE IMPACTS OF SELF-DRIVING VEHICLES IN THE AUSTIN, TEXAS REGION

Part One aims to study the potential residential land use impacts of self-driving or "autonomous" vehicles (AVs). It does so by using an integrated transportation and land use model (ITLUM) using SILO as the land use model and MATSim as the transportation model. The study region of the Austin, Texas six-county region is used in this analysis.

This section is organized as follows. Chapter 1 provides an introduction and motivation for this research. Chapter 2 reviews pertinent research in the realm of AVs and the use of ITLUMs to study the impacts of AVs. Chapter 3 examines SILO's synthetic population generator and compares the generated synthetic population to existing statistics for the region. Chapter 4 reviews the SILO-MATSim model framework. It first examines the main modules within SILO, and then discusses the MATSim implementation and its integration with SILO. This is followed by a review of the input files required and the simplifications and assumptions made in the models used. Next, Chapter 5 provides an overview of the parameter calibration that was completed for SILO. Finally, Chapter 6 reviews the model results and Chapter 7 provides conclusions and indicates where future work is needed in this realm.

Chapter 1: Introduction and Background to Part One

American cities have formed and transformed contemporaneously with transportation technologies. The suburbanization, or urban sprawl, of U.S. cities can be mainly attributed to cars and highway infrastructure. Muller (2017) has shown that, through time in American cities, the built-up urban area has maintained a rather constant 45-minute time-radius from the center. Each transportation technology has made travel easier and has therefore extended the distance of this time-radius, allowing for cheaper suburban residential areas to be unlocked. From walking horsecars in the nineteenth century to electric streetcars in the early twentieth century to the mainstream adoption of automobiles and the build-out of freeways in the mid-twentieth century, major expansions of cities have been a by-product (Muller, 2017).

A new era of urban centralization is beginning as planners find that building more freeways is either not a solution or not an option (Muller, 2017). Transportation technologies are also changing faster than ever before (Dowling & Morgan, 2019). In contrast to this era of centralization, self-driving "autonomous" vehicle (AV) technology is on the horizon which is certain to alter cities and regions significantly (Muller, 2017). Transportation economists remarks that travelers would prefer to pay less for their travel and, if they can get it for less, they will tend to travel more. These new transportation technologies, namely AVs, have the opportunity to reduce the time cost of travel compared to other travel modes because they remove the burden of driving, allowing productive time to be spent in one's vehicle. Thus, any change in transportation technology that affects travel costs will also impact land use, and changes in land use impacts travel patterns, creating a cycle of change (Dowling & Morgan, 2019). For example, it has been shown that households will tend to move to more distant regions when they have access to AVs, which has impacts on travel and land use behavior (Huang et al., 2019).

The advent of AVs makes for an interesting new transportation era because of the relatively long lead time to plan and prepare for the technology before it is expected to become widely implemented. Note that the Society of Automotive Engineers defines five levels of automation. These levels range from minor driver assistance features such as cruise control at Level 1, to fully self-driving vehicles at Level 5 (SAE International, 2018). In this thesis, when the term AV is used, the reference is to Level 4, where the vehicle is fully self-driving, but it must remain on the road infrastructure. Driverless testing on public roads has already begun in several states for major

players such as Waymo of Google and Cruise Automation of General Motors (National Conference of State Legislatures, 2019). If these major players are able to reduce travel costs significantly below the conventional human-driven taxi services (about $3/mile) there is expected to be a major adoption of AVs by the greater public. This adoption would significantly impact travelers' value of travel time savings (VTTS). This is expected to increase the distance many are willing to travel, as well as have other land use impacts such as a decreased need for parking facilities (Dowling & Morgan, 2019). Engineers, planners, and policymakers alike can use this time to ensure a successful implementation by making use of models to understand land use, energy, and transportation implications, allowing them to assess the role of policy and its impacts on these attributes.

The interaction between transportation and land use patterns are important and reinforcing. According to Hawkins and Habib (2018), the use of integrated transport and land use models (ITLUMs) are crucial to understanding and evaluating the impacts of the implementation of AVs on transportation demand, transportation supply, and residential development. Most studies expect AVs to increase urban sprawl because of more efficient driving and the decreased VTTS associated with removing the burden of driving. Modeling these impacts for the Austin, Texas six-county region is the focus of this section, but it is important to note that there are conflicting expectations on the relationship that AVs will have for urban land use. Some have claimed that shared AV fleets (SAVs) have the possibility to re-urbanize cities because parking will no longer be a necessary dwelling consideration, making more central, downtown areas more desirable (Hawkins & Habib, 2018). A limitation of the present study is that these effects are not considered. Interestingly, one recent study showed that 10% of survey recipients who were likely to move in the next few years said the availability of AVs and SAVs would mean that they would be likely to move further from the city center and 15% of survey recipients indicated that the availability of AVs and SAVs would mean that they would likely move closer to the city center (Quarles and Kockelman, 2019). So, this study limitation is a significant one.

More recent ITLUMs have focused on agent-based microsimulation modeling techniques, in contrast to traditional gravity models or econometric models. SILO (Simple Integrated Land-Use Orchestrator) was the chosen microsimulation land use model (LUM) because of its relative simplicity compared to other microsimulation LUMs, leading to reasonably short run times,

lowered data requirements, and its ease of integration with the well-established agent-based microsimulation transportation model MATSim (Hawkins & Habib, 2018).

Chapter 2: Literature Review for Part One

Transportation and land use development are in a constant feedback cycle; each informs the other and when one alters, the other adjusts, and vice versa. Because of this relationship, ITLUMs improve the reasonability of model results compared to standalone transport models. ITLUMs are not new, but there has been a new wave of interest in them because of upcoming transportation trends and technologies, such as AVs, that are expected to significantly impact land use (Dowling & Morgan, 2019). The most common concern in using an ITLUM is the intensity of data needs, which is one reason why SILO was chosen for this study. SILO integrated with MATSim is less data-intensive relative to similar ITLUMs (Moeckel, 2018a).

SILO is a simplified microsimulation model with a focus on time and budget constraints as opposed to utility maximization (Moeckel, 2019a). There is a trend towards microsimulation in LUMs and in travel demand models (TDMs). Benefits of microsimulation include that it is more flexible to a higher level of population detail, and the model is easier to explain because agents are modeled explicitly, and true decision-making is modeled more closely. These benefits come with the limitations of longer run times as well as variations in the same model runs because of the stochastic nature of the model (Moeckel, 2018a). SILO is simplified in its methodology, which decreases its data requirements and its run times. In contrast to many LUMs, SILO does not assume agents are always fully knowledgeable in making decisions (for example, they will not know information on all of the vacant dwellings in the region when looking to move). Rather than maximizing utility, agents look to satisfy requirements, within time and money constraints, that may be biased or based in habit. Further, SILO has also been integrated with MATSim in previous studies, making it a good choice of ITLUM for our needs (Hawkins & Habib, 2018).

The integration of SILO and MATSim was first published in 2016 for the Maryland study region. Because SILO and MATSim are both written in Java, integration was reported to be relatively seamless (Ziemke et al., 2016). In addition, both models are microsimulation agent-based models, so a fully agent-oriented ITLUM was proven and reasonable results were found through this methodology. Congestion levels and patterns were simulated well, even though MATSim was created based on OpenStreetMaps (OSM) data that were never altered or calibrated (Ziemke et al., 2016).

This study looks to identify land use impacts of AVs using the ITLUM of SILO and MATSim, and so similar research in this realm was reviewed. Of note is a study on congestion and accessibility impacts of AVs by Cohen and Cavoli (2019). They looked at traffic flow and accessibility implications for a range of government intervention (or non-intervention) scenarios. Using surveys and extensive literature reviews, the authors supported what many had hypothesized: that if the free market is left alone to deal with the adoption of AVs, we are likely to see a scenario that does not maximize social welfare. The authors looked at varying categories of policy intervention, including land use policies such as zoning, regulation policies such as banning the empty running of AVs, infrastructure policies such as adding walking or biking paths. They looked at nineteen interventions and determined the corresponding implications for traffic flow and accessibility, but they did not reach a final conclusion on what combination of government interventions serve the best chance at mitigating negative impacts of AV penetration (Cohen & Cavoli, 2019).

It is also important to review literature that looks at the land use-transport relationship as it pertains to AVs. A paper by Seteropoulos et al. (2019) reviewed modeling studies that looked at impacts of AVs on travel behavior and land use. The authors looked at studies between 2013 and 2018 that contained keywords of AVs, transport, land use, and modeling. Most of the studies cited examined travel behavior implications of AVs, though several examined land use impacts, mainly through the use of ITLUMs. Studies varied in whether they investigated full replacement of vehicles or a small share of vehicle trips that were modeled in an AV. A common assumption is the reduction of VTTS in AVs due to an increased productivity or comfort. Increases in roadway capacity due to AVs is another recurring assumption made in these models. For the most part, studies used vehicle miles traveled (VMT) or vehicle hours traveled (VHT) as indicators for travel changes, and varying land use impacts are analyzed, from parking needs to location choices of households and employment. Studies mostly found an increase in VMT, while VHT impacts vary based on study assumptions. In looking at the effects of AVs on households and employment, studies mostly predict that there will be an increase of population in well-connected outer regions. This is especially the case in studies with high discounts of VTTS or large increases in road capacity. It is noted that studies that examine land use impacts of AVs generally have low spatial detail, tending to only distinguish between urban and suburban areas, for example. This is the point

that this study is meant to build on, to place more weight and attention to the more complicated land use patterns that could not be interrogated in previous models (Seteropoulos et al., 2019).

Chapter 3: SILO's Synthetic Population Overview

The SILO synthetic population generator creates a simplified microscopic representation of the actual Austin population. It is simplified in that it only includes attributes deemed important to land use modeling and it is microscopic in that every person and household is represented individually. It is not identical to the actual population of Austin, but it matches various statistical distributions of the actual population, and so it is appropriate for modeling purposes. This chapter talks about the synthetic population model framework and reviews the input files needed to create the synthetic population. Then, the Austin six-county region synthetic population is analyzed, and some key results are highlighted.

3.1 SILO's Synthetic Population Model Framework

The U.S. version of SILO's synthetic population generator uses the Public Use Microdata Sample (PUMS). SILO uses the 5% PUMS sample, which provides less household characteristic details in exchange for more spatial detail, as compared to the 1% PUMS. Since these household details are sufficient for the modeling purposes, the 5% PUMS is chosen to increase spatial resolution. The spatial resolution of the 5% PUMS are called PUMAs (Public Use Microdata Areas). Besides household details, PUMS also provides information of each person in each household and the dwellings that the households live in. PUMS includes an expansion factor which describes how many households of the true population each PUMS record represents. These expansion factors are used in SILO's synthetic population generator and they were calculated specifically to match the actual population of each PUMA (Moeckel, 2018g).

By expanding household records, synthetic persons and dwellings are also expanded at the same time. Once expanded, the total number of persons matches the actual population of the region perfectly. But, because of the nature of collecting Census data, dwellings are underrepresented by this dataset. To create a complete set of dwellings, including vacant dwellings, we exogenously assume an average vacancy rate, which can vary by household type (single-family detached, single-family attached, multi-family, etc.) (Moeckel, 2018g). These vacant dwellings are added by randomly selecting existing dwellings from the PUMS and adding them without a resident. The default SILO vacancy rates for the Maryland implementation are shown in Table 1 below.

Table 1: Assumed Vacancy Rates by Household Type in SILO Maryland Implementation (Moeckel, 2018g)

Household Type	**Vacancy Rate**
Single-family detached (SFD) dwelling	1%
Single-family attached (SFA) dwelling	3%
Multi-family with up to 4 household residents (MF2-4)	5%
Multi-family with 5 or more household residents (MF5+)	4%
Mobile homes (MH)	3%

The PUMS gives dwelling location at the PUMA level. Next, dwellings must be allocated to model zones. CAMPO zonal data was used to proportionally allocate dwellings to zones, using zonal population as a proxy for dwelling allocation. Workplace locations are disaggregated similarly; PUMS data provides work locations by PUMA, and CAMPO zonal data was used to proportionally allocate jobs by zonal employment data.

The synthetic population generator creates four different files: a list of households, persons, dwellings, and jobs. Each person is part of a specific household and each household is matched to a certain dwelling. The dwelling file will have vacant dwellings as well, at the rate assumed exogenously. Finally, each working person in the synthetic population is matched with a specific job. People are assigned workplaces by drawing jobs located within their Census-specified working PUMAs (Moeckel, 2018g).

3.2 Input Files Needed for SILO's Synthetic Population Generator

3.2.1 Public Use Microdata Sample (PUMS) Data

The first input file needed for SILO's synthetic population generator is the 5% PUMS. The PUMS contains actual responses to the American Community Survey over the course of a five-year period, in this case 2013-2017. PUMS data is provided at the state level. There are two files provided by PUMS: one file representing 5% of the households in Texas and one file representing the people living in those households. Each record in the file represents either a single person or a single household (depending on which dataset), and each record is accompanied by a weight indicating how many people or households this record represents (U.S. Census Bureau, 2018).

The PUMS is aggregated spatially into PUMAs which are non-overlapping areas that contain at least 100,000 people. Since their size is determined by population, not by area, PUMAs are vastly different sizes depending on the population density of the region (U.S. Census Bureau, 2018). The six-county Austin metropolitan area consists of 16 PUMAs: 3400, 5100, 5201, 5202, 5203, 5204, 5301, 5302, 5303, 5304, 5305, 5306, 5307, 5308, 5309, and 5400. These PUMAs are shown graphically in Figure 1.

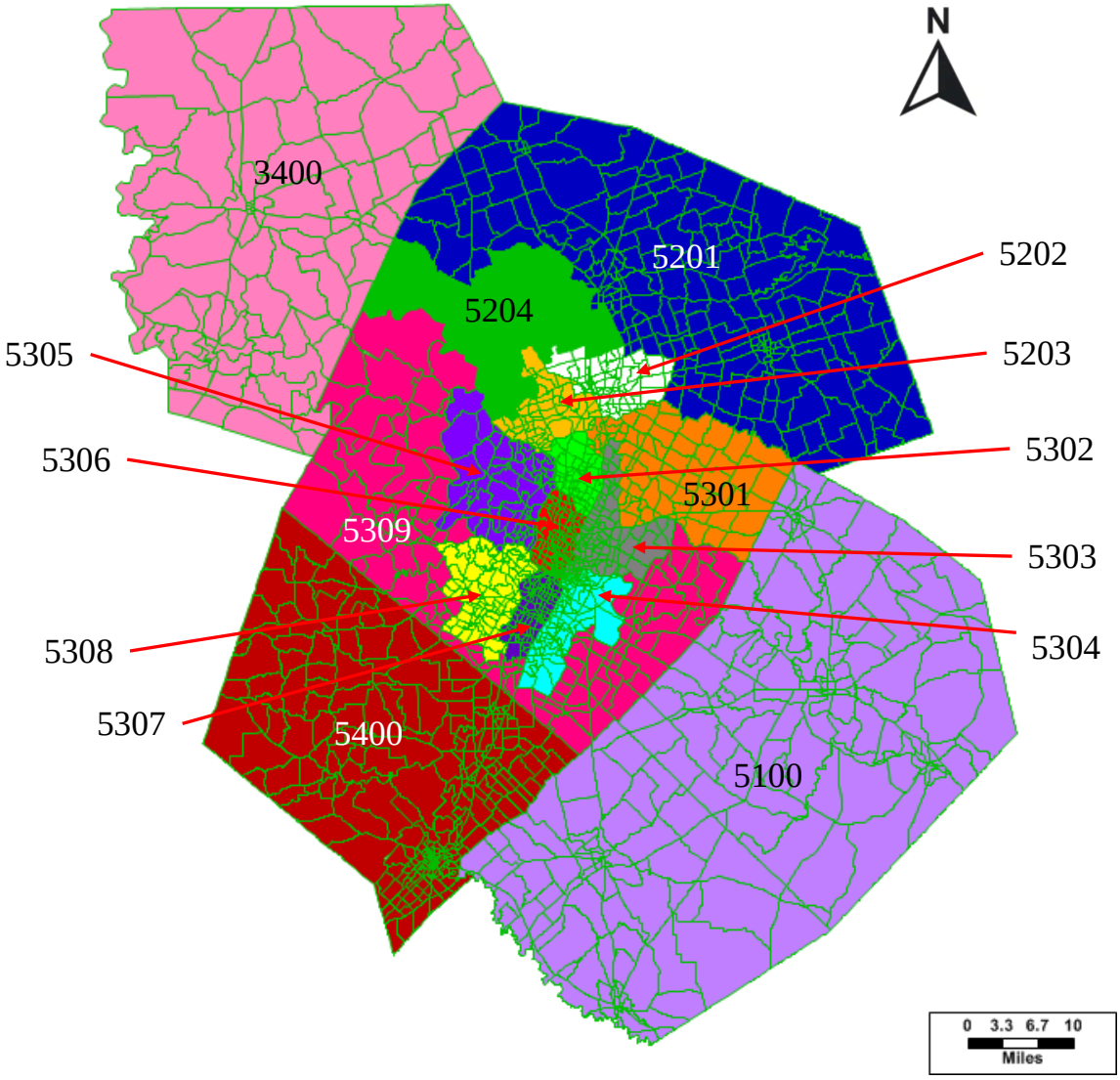

Figure 1: Labeled Map of PUMAs in the Austin Metropolitan Region

3.2.2 Zone System

The second input file needed is a file representing key features about each TAZ in the Austin six-county metropolitan area. This file gives details on zonal area as well as details on the county and PUMA(s) that the TAZ lies in (determined by majority if the TAZ spans more than one county or PUMA).

3.2.3 Zone Shapefile

Another input file needed for the synthetic population generator is a shapefile. This file gives the spatial resolution of the traffic analysis zones (TAZs). It includes information on the specific location of each TAZ as well as the area of the TAZ. This file is used to spatially allocate people, households, dwellings, and jobs.

3.2.4 Partially Covered PUMAs

There are two PUMAs in the Austin six-county metropolitan region that are only partially enclosed within the region. These zones are PUMA 3400 and 5100. In order to accurately synthesize the population, it is important to only partially expand these regions. An input file is read into SILO's synthetic population generator that indicates which PUMAs are only partially in the Austin region. This input file also shows the full population of that PUMA as well as the population that is in the study area of interest. The full population of PUMAs 3400 and 5100 was provided in the PUMS input data and was 176,700 and 153,403, respectively for the two partially covered PUMAs. To find the population in each of these PUMAs that were in the Austin metropolitan region, the populations of each TAZ that were in those PUMAs were summed. There were 42,750 people in PUMA 3400 and 112,237 people in PUMA 5100 within the Austin six-county region. The ratio of the population in the Austin area in each partially covered PUMA divided by the total PUMA population was multiplied by each household- and person-level weights (and rounded to the nearest whole number) in order to approximate the population in those two PUMA regions.

3.2.5 Travel Skims

A skim matrix gives impedances for each zone pair. The skim matrix needed for SILO's synthetic population generator is a skim of the travel times for each zone pair. That means this file

gives the travel time between every zone pair in the Austin metropolitan region of 2102 zones. This is used to assign job locations to each worker in a household. The PUMS data gives the PUMA location of each person's dwelling and of it gives the PUMA of each worker's job. PUMS data also gives the commute time for each worker. Travel skims are then used to best determine a worker's job location, based on the given PUMA and commute time.

3.2.6 Activities File

Another input file needed to generate the synthetic population for Austin is called the activities file. This file lists the number of jobs of each type and the number of households in each TAZ in the Austin region for the base year. This is used to appropriately disaggregate jobs and households from the PUMA scale to the TAZ-level.

3.2.7 Vacancy Rates

The final file needed for the synthetic population generator is a file that gives dwelling vacancy rates at the county level. These vacancy rates were determined based on the vacancy rates used in the Maryland-region implementation. Because Travis county is the most densely populated county in the region, the lower end of the range of Maryland's vacancy rates was used, which was 2.1%. An upper range of vacancy rates of 10% was used. Population density was used as a proxy for vacancy rates, where lower population density led to higher vacancy rates. A linear relationship between vacancy rates and population density was assumed, and Table 2 below gives the vacancy rates used for each county in the region.

Table 2: Model Vacancy Rates by County (Moeckel, 2019a)

County	Population density (people/mile$_2$)	Vacancy rate
Travis	1150.13	2.10%
Williamson	448.25	7.11%
Hays	286.53	8.27%
Bastrop	89.63	9.68%
Caldwell	74.12	9.78%
Burnet	44.09	10.0%

3.3 SILO's Synthetic Population Results

Using SILO's synthetic population generator, the four synthetic population files for the Austin, Texas six-county metropolitan region were created. The 2017 Texas PUMS was used to create this synthetic population. The first of the four files provides details on the population at the person-level. It created a population of 1,916,060 people. Table 3 shows summary statistics of the population age. The synthetic population generator created a population between the ages of zero and ninety-two, with an average age of 36.5 years old. The summarized Census PUMS data is also shown in Table 3 and gives similar results.

Table 3: Descriptive Statistics of Population Age in Austin

	Mean	Median	Maximum	Minimum	Std. Dev.
Synthetic Population	36.5 yr	36	92	0	21.3
PUMS	36.0 yr	38	92	0	22.5

The synthetic population generated a population that was 49% male and 51% female, compared to the Census PUMS data which has 50% male and 50% female (Table 4).

Table 4: Population Gender Distribution in Austin

	Male	Female
Synthetic Population	938,295 (48.97%)	977,765 (51.03%)
PUMS	958,400 (50.02%)	957,660 (49.98%)

In the person-specific population file, 29% of the population is under 18, and 71% of the population is adults. Of the adults, 62% are married and 38% are single. This is quite similar to the Census PUMS, though the model seems to over-estimate married adults. See Table 5 for more details.

Table 5: Population Relationship Distribution in Austin

	Child (under 18)	Married Adult	Single Adult
Synthetic Population	551,954 (28.81%)	845,462 (44.13%)	518,644 (27.07%)
PUMS	499,629 (26.07%)	690,434 (36.03%)	725,997 (37.90%)

Table 6 shows that the synthetic population produces a population that is 54% white, 31% Hispanic, 6% black, and 9% other races. This reflect the PUMS fairly well, with black Austinites being slightly over-represented and other races being slightly under-represented in the synthetic population.

Table 6: Race Distribution in Austin

	White	Hispanic	Black	Other
Synthetic Population	1,026,710 (53.58%)	602,740 (31.46%)	115,653 (6.04%)	170,958 (8.92%)
PUMS	1,027,775 (53.64%)	520,594 (27.17%)	137,765 (7.19%)	229,927 (12.00%)

The synthetic population contains 1.04 million workers, which is just over 54% of the total population. Table 7 shows the summary statistics of income for working adults. The average personal income is about $40.4k and the median income is $22k. The maximum income is $742k

and the minimum is $0. This matches the PUMS well, though the mean income is over-represented by about 10% in the synthetic population.

Table 7: Descriptive Statistics of Working Adults' Income in Austin

	Mean	Median	Maximum	Minimum	Std. Dev.
Synthetic Population	$40,423	$22,000	$742,000	0	$72,685
PUMS	$36,574	$22,470	$812,000	0	$70,255

The next file that SILO's synthetic population generator creates is a household-level file. It creates 768,950 households to represent all of the households in the Austin Metropolitan region. The mean household size is 2.49 people and the median household size is two people. The Census PUMS shows that this is close to the true household size, which was a mean of 2.21 and a median of two in 2017. See Table 8 for the distribution of households by size for the synthetic population as compared to the PUMS. They match quite well.

Table 8: Distribution of Households by Size (as % of dwellings) in Austin

	Vacant Dwellings	1-Person Households	2-Person Households	3-Person Households	4-Person Households	5-Person Households	6+-Person Households
Synthetic Population	83,290 (9.77%)	207,593 (24.36%)	265,672 (31.18%)	120,508 (14.14%)	103,097 (12.10%)	45,760 (5.37%)	26,320 (3.09%)
PUMS	97,808 (11.47%)	202,733 (23.78%)	261,141 (30.63%)	118,779 (13.93%)	101,091 (11.86%)	45,072 (5.29%)	25916 (3.04%)

The household-level file also provides the number of household vehicles. The average number of household vehicles in the synthetic population is 1.87 and the median is two cars. This is close to the values provided by the Census PUMS, which are an average of 1.67 and a median of two household cars. Table 9 shows the distribution of the number of household vehicles for the synthetic population and provided by the PUMS. The synthetic population matches the PUMS extremely well on this measure.

Table 9: Distribution of Households by Number of Household Vehicles (as % of occupied HHs) in Austin

	0- vehicle Households	**1- vehicle Households**	**2- vehicle Households**	**3-vehicle Households**	**4-vehicle Households**	**5+-vehicle Households**
Synthetic Population	31,656 (4.12%)	253,613 (32.98%)	331,051 (43.05%)	105,555 (13.73%)	33,257 (4.32%)	13,818 (1.80%)
PUMS	31,358 (4.08%)	250,386 (32.56%)	332,717 (43.27%)	106,333 (13.83%)	34,068 (4.43%)	14,088 (1.83%)

The third file created in SILO's synthetic population generator is a job-level file. The generator created 918,981 jobs in the six-county region, which is a bit less than the true number of jobs in the region according to the CAMPO model, which is 991,373 jobs. Just over half the jobs in the region were categorized as service jobs, 23% were categorized as retail jobs, 21% were deemed basic jobs, and the remaining 5% were education-related jobs (see Table 10). This distribution of jobs by type comes from the CAMPO model and the proportions match up well between the synthetic population and the CAMPO population.

Table 10: Job Type Distribution in Austin

	Retail	**Service**	**Basic**	**Education**
Synthetic Population	204,937 (22.33%)	461,963 (50.27%)	197,081 (21.45%)	48,584 (5.29%)
PUMS	228,823 (23.08%)	496,931 (50.13%)	213,106 (21.50%)	52,511 (5.30%)

The final file created in SILO's synthetic population generator is a list of all dwellings in the region. It created a total of 852,552 dwellings, with nearly 60% of those being single-family detached dwellings, over 25% were multi-family units with five or more households, and the remaining 15% being approximately evenly split between single-family attached units, multi-family units with less than five households, and those living in mobile homes (see Table 11). The PUMS gave a similar distribution of households by type.

Table 11: Dwelling Distribution by Type (as % of total dwellings) in Austin

	SFA	SFD	MF2-4	MF5+	MH
Synthetic Population	32,455 (3.81%)	507,466 (59.52%)	48,529 (5.69%)	222,273 (26.07%)	41,828 (4.91%)
PUMS	33,613 (3.87%)	526,111 (60.53%)	50,009 (5.75%)	208,949 (24.04%)	49,506 (5.70%)

The average vacancy rate in the synthetic population of dwellings is 11.5% which matches exactly the vacancy rate of the PUMS. Vacancy rates by type are given in Table 12. The synthetic population matches the PUMS quite well in this regard, although it underestimates the vacancy rates of single-family dwellings by a couple of percentage points.

Table 12: Vacant Dwellings by Type (as % of all dwellings of that type) in Austin

	SFA	SFD	MF2-4	MF5+	MH
Synthetic Population	3,916 (12.07%)	36,006 (7.10%)	5,571 (11.48%)	32,305 (14.53%)	5,803 (13.87%)
PUMS	5,346 (15.91%)	48,166 (9.16%)	6,527 (13.05%)	30,998 (14.84%)	8,677 (17.53%)

The model created 3% of the dwellings with zero bedrooms, 15% of the dwellings with one bedroom, 22% with two, 37% with three, 19% with four, and 4% with five or more bedrooms. This is quite similar to what the PUMS indicates (see Table 13).

Table 13: Dwelling Distribution by Number of Bedrooms (as % of dwellings) in Austin

	0	**1**	**2**	**3**	**4**	**5+**
Synthetic Population	26,203 (3.07%)	129,125 (15.15%)	187,311 (21.97%)	314,971 (36.94%)	161,967 (19.00%)	32,974 (3.87%)
PUMS	26,579 (3.06%)	125,024 (14.38%)	190,658 (21.94%)	331,468 (38.14%)	162,938 (18.75%)	32,496 (3.74%)

Finally, the average cost of dwellings in the synthetic population was $1,143 per month and the median cost was $1,000 per month. See Table 14 for a comparison to the PUMS. They follow closely, with the median slightly underestimated in the synthetic population.

Table 14: Descriptive Statistics of Monthly Cost of Dwellings in Austin

	Mean	**Median**	**Maximum**	**Minimum**	**Std. Dev.**
Synthetic Population	$1,143	$1,000	$4,800	$4	$715
PUMS	$1,099	$1,100	$4,800	$4	$771

Chapter 4: SILO-MATSim Model Framework

SILO is a microscopic land use orchestrator that is fully integrated with the transport model MATSim. This chapter discusses the SILO and MATSim model frameworks, and their integration. Then the input files needed for each model are reviewed, and the model simplifications are examined.

4.1 SILO Model Framework

SILO is a discrete choice microsimulation LUM. It is a discrete choice model in that decisions are modeled based on the utilities of the choice set. It is a microsimulation model in that each household and person is simulated individually. All spatial decisions are modeled with Logit models, and other non-spatial decisions are modeled using Markov models that apply transition probabilities (Moeckel, 2018h). The SILO framework is shown below in Figure 2 in flowchart form. See https://github.com/msmobility/silo/ for the SILO code base and to see updates to the code made for the Austin implementation.

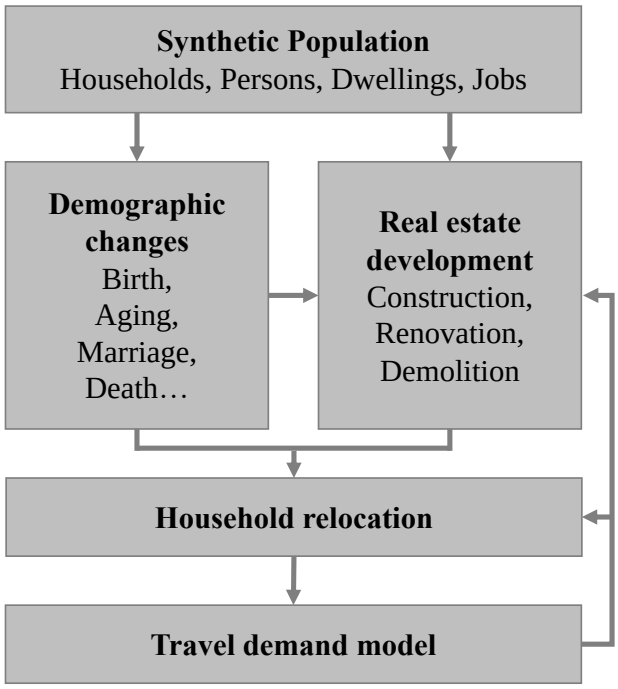

Figure 2: SILO Model Flowchart (from Moeckel, 2018e)

4.1.1 Synthetic Population

The synthetic population is created as described in Chapter 3. This is created once for the base year and is provided as input to the model in the base year. It is then updated by other modules in subsequent years (Moeckel, 2018e).

4.1.2 Demography Module

The demography module simulates all non-spatial changes in households. These include person events such as aging, death, giving birth, getting married or divorced, and changing jobs. Aging is the simplest of these simulated events. Each model year, every person's age is increased by one year. Death probabilities are based on survival rates from the World Health Organization in the United States. These probabilities are different based on a person's age and gender. Those who are older have higher death probabilities, and death probabilities are slightly higher for men compared to women. The probability of a woman giving birth is dependent on the woman's age and whether she is married or living with a man. See Figure 3 below to understand how these birth probabilities change with these two factors (Moeckel, 2018b).

Figure 3: Birth Rates of Single and Married Women, Used for Birth Probabilities in SILO (U.S. Department of Health and Human Services, 2003; from Moeckel, 2018b)

The probability of getting married in SILO depends on the age and gender of the person, with women more likely to get married at a slightly younger age than men. See Figure 4 below for

more details. Currently, SILO only models heterosexual marriages and relationships. Each simulation period, SILO considers all single persons between the ages of fifteen and seventy-nine to have the possibility of marrying. If an unmarried person decides to get married, a person of the opposite gender is selected. Only age is used as a "utility" to find a partner, and marriage statistics suggest that the groom is an average of 2.3 years older than the bride. This means that a 28-year-old man looking for a female partner will most likely select a 26-year-old woman. These marriage age utilities are shown below in Figure 5 (Moeckel, 2018b).

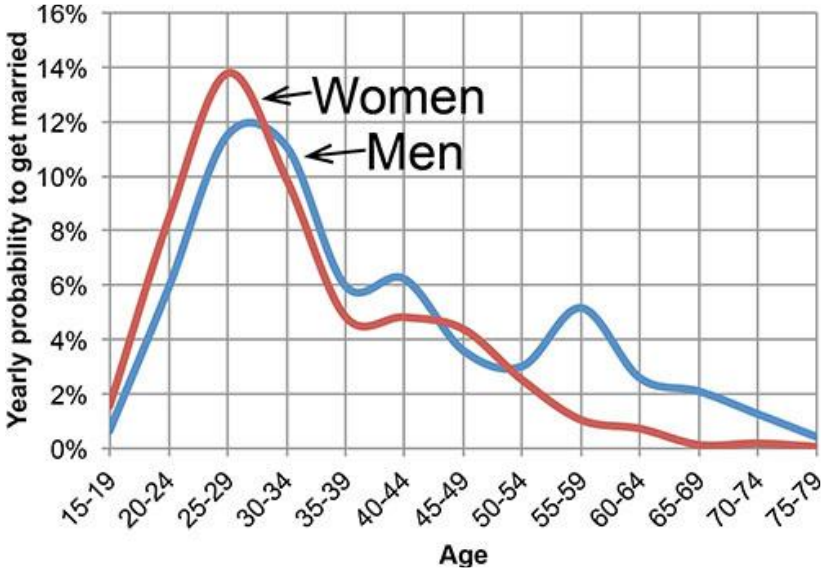

Figure 4: Marriage Probability in SILO by Gender and Age (from Moeckel, 2018b)

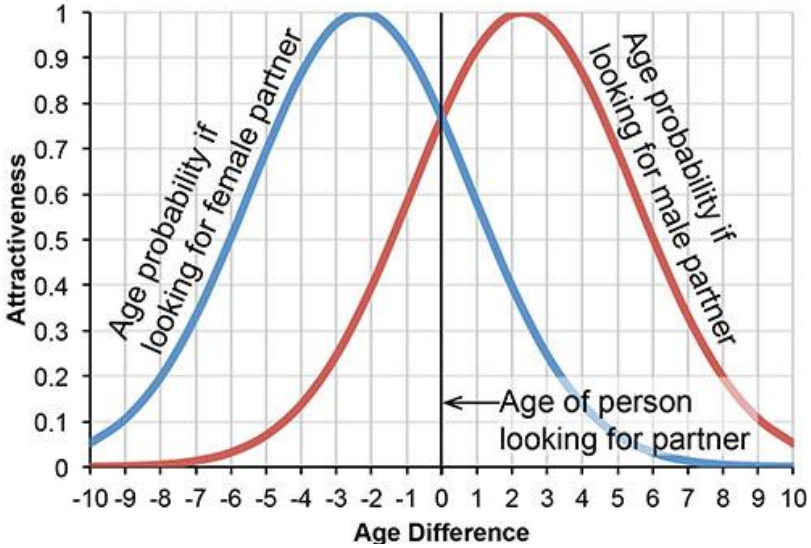

Figure 5: Marriage Age Difference Utility in SILO (from Moeckel, 2018b)

Every cohabitating or married couple has the possibility of separating or divorcing each model year. Divorce probabilities are used to determine these separations every simulation period. This probability is a function of age and gender. Note that women have a higher divorce rate in the younger ages because women are more likely to be married at those younger ages (Moeckel, 2018b).

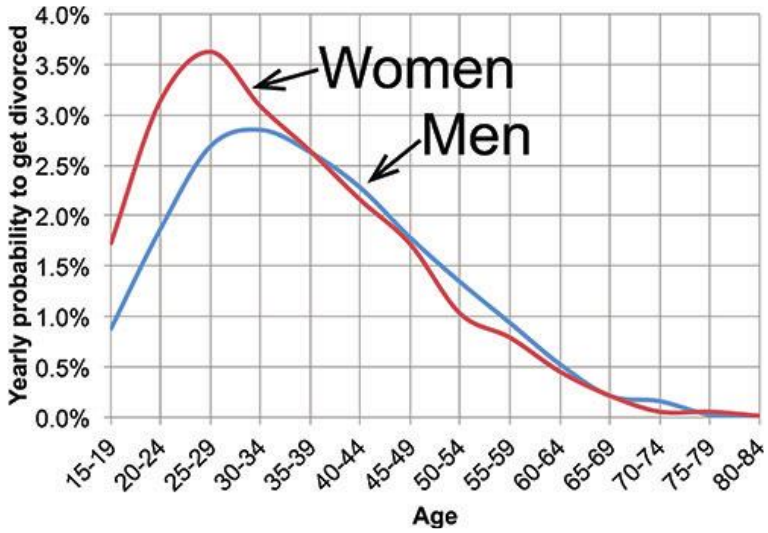

Figure 6: Divorce Probability in SILO by Age and Gender (Moeckel, 2018b)

A zonal-level static exogenous employment forecast is provided to SILO. Every simulation period, this forecast is compared to the number of jobs by zone in SILO. If SILO has fewer jobs than the forecast suggests, new jobs are created. If SILO has more jobs than the forecast, SILO cuts jobs from that zone until it matches the forecast. It first cuts vacant jobs, and then randomly removes additional jobs if necessary, leaving those workers unemployed (Moeckel, 2018b).

4.1.3 Real estate module

This module updates dwellings each model year based on demand for different dwelling types. Five event types are simulated in this module each simulation period: construction of new dwellings, renovation of dwellings, deterioration of dwellings, demolition of dwellings, and dwelling price adjustments (Moeckel, 2018f).

Each model year, developers look at the current demand by region and dwelling type, conveyed by the vacancy rate. If the vacancy rate is low for a particular dwelling type in a region, the model understands that demand is high for that dwelling type in that region, and developers

look for available, developable land to build more of that dwelling type. To find the best locations, developers use similar location choice decision models as homeowners to choose development locations. Dwellings developed in one simulation period are released into the housing market the following simulation period, to reflect the lag in development due to planning and construction (Moeckel, 2018f).

Each dwelling in SILO has an associated quality attribute, representing the condition of the dwelling. Quality levels are integer values ranging from one to four, with one being the poorest quality and four being the highest quality dwelling. Each model year, dwellings have a possibility to improve in quality, or be renovated; to digress in quality, or to deteriorate; or to remain unchanged in their quality level. These probabilities depend on the current quality level and are shown in Table 15 (Moeckel, 2018f).

Table 15: Dwelling Renovation and Deterioration Probability, Based on the Current Dwelling Quality (Moeckel, 2018f)

Current Quality Level	Deteriorate 2	Deteriorate 1	Unchanged	Improve 1	Improve 2
1	0	0	0.93	0.05	0.02
2	0	0.10	0.75	0.10	0.05
3	0.05	0.10	0.75	0.10	0
4	0.02	0.05	0.93	0	0

It is also assumed that the share of dwellings by quality remains relatively unchanged over time. This means that if there is an increase in the number of high-quality dwellings relative to the number of dwellings of lower qualities, the probability of deterioration is slightly higher to maintain approximately the same share of dwelling qualities over time. This is important because new dwellings are constantly being released into the market, so if this constraint were not applied, the quality of dwellings would continually improve over time (Moeckel, 2018f).

Some dwellings are also demolished each model year. Dwellings of lower quality are much more likely to be demolished than those of higher quality, as shown in Figure 7. Further, dwellings that are occupied should be demolished very rarely, and that is shown in Figure 7 as well. If an

occupied dwelling is selected for demolition, that household enters the household relocation module and must find an alternative dwelling immediately (Moeckel, 2018f).

Figure 7: Dwelling Demolition Probability in SILO, Based on Current Dwelling Quality and Vacancy Status (from Moeckel, 2018f)

Finally, the real estate module updates dwelling costs based on the current demand, which again is expressed by the vacancy rate. Structural vacancy rates are defined to state an average regionwide vacancy rate by dwelling type, and vacancy rates in each zone are compared to these structural vacancy rates to determine price adjustments. The structural vacancy rates for the Austin metropolitan region will be discussed in Chapter 5. If vacancy rates are below the structural vacancy rate, landlords will increase rent and quickly adjust their prices upwards. However, if vacancy rates are above structural vacancy rates, prices decline, but they decline much more slowly than the price increases that occur if vacancy rates are relatively low. This reflects the observed behavior of landlords to try to keep rent prices high even if demand is somewhat low. Figure 8 shows these price adjustments for an example dwelling type with a structural vacancy rate of 4%. If the vacancy rate equals the structural vacancy rate of 4%, prices do not change. Vacancy rates that are somewhat higher than 4% show a slow decrease in prices. However, vacancy rates that are somewhat lower than 4% show a much quicker increase in prices (Moeckel, 2018f).

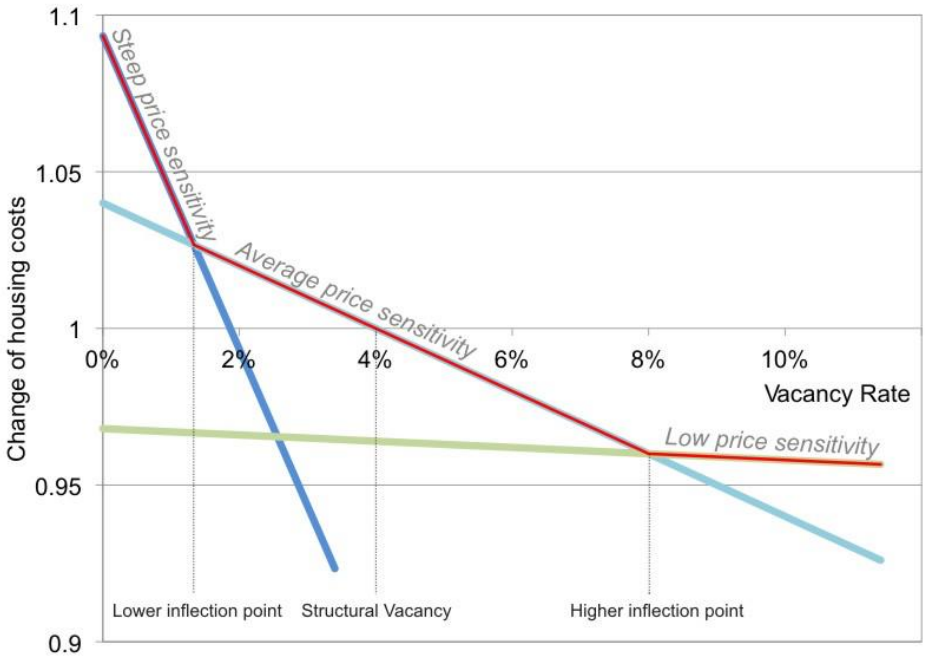

Figure 8: Dwelling Price Adjustments as a Function of Zonal Vacancy Rates for a Dwelling Type with 4% Structural Vacancy Rate (from Moeckel, 2018f)

4.1.4 Household relocation module

Each simulation period, every household evaluates whether it wants to move or not. This decision is made with three logit models that select if and where to a household may choose to move. The first is a binomial logit model that decides whether or not the household wants to move. The household assesses its satisfaction or utility from its current dwelling and compares that to the potential utility from alternative, currently vacant dwellings. If the household has the opportunity to improve its satisfaction significantly, it will continue on in the relocation module and look for a new dwelling. Most households will decide not to move and will exit this module after making this decision (Moeckel, 2018d).

If a household decides it wants to move, it proceeds to the next two logit models in the household relocation module. Because logit models are meant to select between a somewhat narrow set of alternatives, choosing between all vacant dwellings would be inappropriate. Instead, a two-step dwelling selection process was designed for SILO. In the first logit model, a region is chosen. The regions defined for the Austin metropolitan area are the seventeen PUMAs that lie in the region, as shown in Figure 1. Then, after a region is chosen, the household chooses between

all vacant dwellings in that region in the final logit model. The utilities of dwellings are calculated differently for households of different size and income (Moeckel, 2018d).

There are three main location considerations that households consider when choosing a household: housing costs, commute travel times, and transportation costs. These are considered the essential factors. The Cobb-Douglas function is used to consider these utilities, shown below in Eq. 1. Note that in this equation form, if any one of these utilities is zero, the utility for the dwelling is zero and so it will not be considered (Moeckel, 2017).

$$u_d = u_p^{\alpha} * u_c^{\beta} * u_t^{\gamma} * u_{oth}^{(1-\alpha-\beta-\gamma)} \quad (1)$$

where u_d is the utility of the dwelling, u_p is the utility of the price of the dwelling, u_c is the utility of the commute time from the dwelling, u_t is the utility of the transportation costs required for the dwelling, and u_{oth} is the utility of non-essential factors of the dwelling, and α, β, and γ vary for households of different sizes and income levels (Moeckel, 2017).

The utility of the price u_p of the dwelling is an important constraint, as household income needs to get along with the mortgage or rent payment in the long-run. The distribution of rent or mortgage payments for households of different income levels was used to determine how much households are willing to pay. Eq. 2 below is used to determine this utility of price of the dwelling. Higher prices mean for lower utilities, and households in higher income categories see these utilities decrease slower than those in lower income categories (Moeckel, 2017).

$$u_p = 1 - \frac{\sum_{p=0}^{price_j} hhCount_{p;\,inc}}{\sum_{p=0}^{\infty} hhCount_{p;\,inc}} \quad (2)$$

where $price_j$ is the price that the household is considering paying, $hhCount_{p;\,inc}$ is the number of households in the same income class that paid a mortgage or rent of p (Moeckel, 2017).

The utility of the commute time from the dwelling u_t is another essential household location constraint and consideration. The utility of a commute travel time is based on observed data from the Baltimore-Washington region, fit to a gamma function. The utility of a commute time follows the same shape as the frequency from which that commute time was observed, as shown in Figure 9 below. When households are making a dwelling location or relocation decision, the commute time of all workers in the household are considered (Moeckel, 2017).

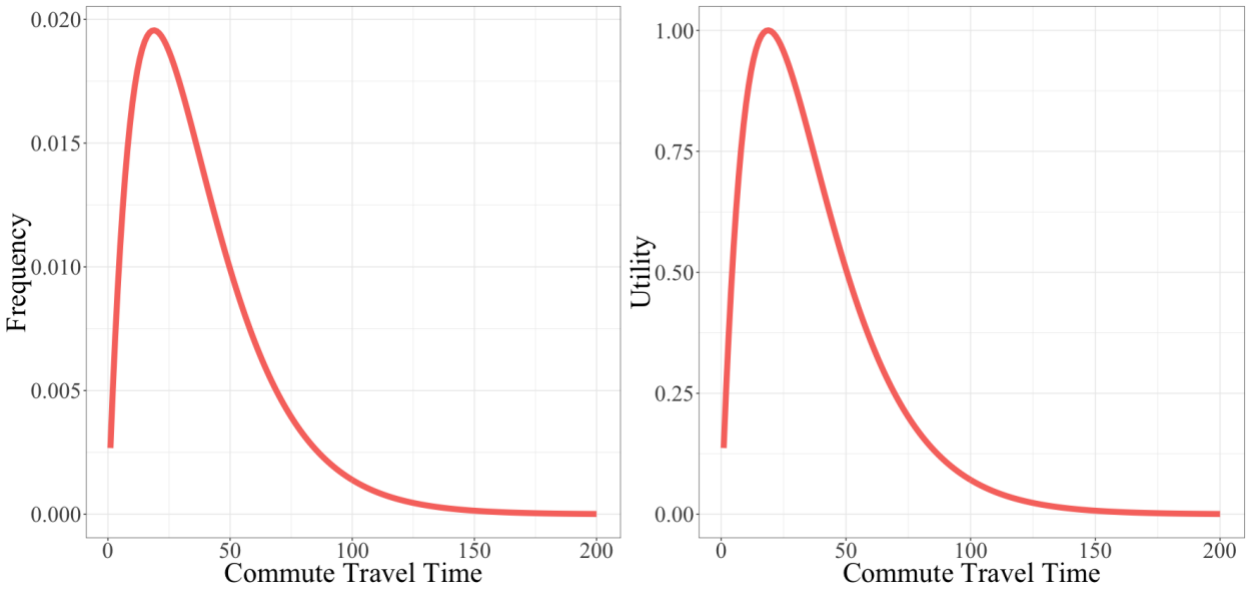

Figure 9: Frequency and Utility of Commute Travel Time from the Maryland SILO Implementation, Adopted for the Austin SILO Implementation

The final essential location factor is the transportation budget. It has been found that households spend an average of 18% of their after-tax income on transportation, and low-income households spend as much as 36% of their after-tax income on transportation. Transportation costs must be considered when choosing a new dwelling. The transportation expenditures are given by Eq. 3 below (Moeckel, 2017).

$$et_h = tc_s \left(1 + \frac{tc_s - tc_r}{tc_r} * el\right) \qquad (3)$$

where et_h is the transportation expenditures for household h, tc is the transportation costs (r for the reference case and s for the alternative scenario), and el is the elasticity of travel demand on transportation costs (Moeckel, 2017). This was set to -0.25 based on a study by Litman (2013) which showed that fuel price elasticity is between -0.2 and -0.3 for medium-run adjustments.

Finally, a binomial logit model is used to calculate the utility of transportation costs u_t. Note that if the discretionary income and savings are not enough to cover transportation costs of a dwelling, the utility is set to zero (Eq. 4). Otherwise, the utility is given by Eq. 5. These values of discretionary expenditures and savings are approximated based on data from the Consumer Expenditures Survey for households of different incomes (Moeckel, 2017).

$$if\ \left(e_{dis,h} + s_h < tc\right): u_t = 0 \qquad (4)$$

$$if\ \left(e_{dis,h} + s_h > tc\right): u_t = \frac{1}{1+\exp\left(\zeta * \frac{e_{dis,h}+s_h}{tc}\right)} \quad (5)$$

where $e_{dis,h}$ is the discretionary expenditures of household *h*, s_h is the savings of household *h*, ζ is a parameter describing the sensitivity of increased transportation costs, which varies by household income (Moeckel, 2017).

Lastly, the utility of the other, non-essential dwelling factors u_{oth} is characterized by Eq. 6 below.

$$u_{oth} = \theta_1 * u_{size} + \theta_2 * u_{quality} + \theta_3 * u_{autoAccess} + \theta_4 * u_{transitAccess} + (1 - \theta_1 - \theta_2 - \theta_3 - \theta_4) * u_{crimeIndex} \quad (6)$$

where θ_1, θ_2 ... are parameters that vary by household income and size, u_{size} is the utility of dwelling size, $u_{quality}$ is the utility of dwelling quality, $u_{autoAccess}$ is the utility of auto access, $u_{transitAccess}$ is the utility of transit access, and $u_{crimeIndex}$ is the utility of county-level crime index (Moeckel, 2017).

4.2 MATSim Model Framework

MATSim is an activity-based, agent-based transportation simulation model implemented in Java. MATSim was designed for large-scale scenarios, which means that the model features are simplified to avoid very long run times. A scenario in MATSim is defined by the agent populations, their original plans and their activity locations (such as their home, workplace, and grocery store), and the network and facilities where they compete in time and space. Agents have initial plans that often shifts at least slightly while the system is searching for user equilibrium (Horni et al., 2016). User equilibrium makes two main assumptions. The first is the shortest path assumption, which assumes that every driver aims to choose the path with the least travel time. Some may argue that drivers consider more factors than travel time when deciding on a route, but most will agree that this is the most important consideration in route choice, making this a decent assumption, given its simplicity. The second is that drivers have perfect knowledge of travel times. This is also a simplifying assumption that is not fully realistic, but this is actually becoming more realistic now since many of travelers use smartphone GPS devices that select our route for us, with accurate understanding of the travel times other routes would provide (Boyles et al., 2019).

MATSim is based on the co-evolutionary principle, meaning that each agent iteratively optimizes its activity schedule in unison with all other agents that are competing in time and space

for the use of the transportation facilities. Plan modification is performed with four dimensions considered: departure time, route, mode, and destination. Each iteration, agents evaluate their plans, and the day is repeated until the average score remains relatively constant. For the scenarios considered in this thesis, 50 iterations are used as plan scores sufficiently stabilized at this point. For more details on the inner workings of MATSim, please refer to the book *The Multi-Agent Transport Simulation MATSim* (Horni et al., 2016).

For this implementation of MATSim for the Austin, Texas six-county metropolitan region, OpenStreetMap data was used to create the network. Default values are used to set speeds and other network attributes. In addition, only car travel is modeled in MATSim. A 5% sample of the total population was used to simulate traffic. Since the population on the network is 5% of the true expected population on the network, roadway capacity factors must scale down as well to reflect true congestion in the region. There are two capacity factors considered in MATSim's standard traffic flow model QSim, which are used here. The first is storage capacity, which defines the number of cars that can fit on each link in the network. The second is flow capacity, which indicates the outflow capacity of each link in the network. In other words, the flow capacity specifies how many travelers can leave a link in a given time increment (Horni et al., 2016). In general, flow capacity is scaled down proportionally to the population, but storage capacity is left slightly higher than the population scaling for small sample sizes. According to Dr. Kai Nagel, for small sample sizes it is generally appropriate to scale storage capacity to $s^{0.75}$, where s is the population scaling. Because of this, storage capacity factor was set to 0.11. See https://github.com/matsim-org for the MATSim code base used in this thesis.

4.3 SILO-MATSim Integration

As mentioned previously, SILO runs every year and MATSim runs every ten years. This means that there are many years where SILO runs without any transportation feedback. However, when the model is at a year where MATSim runs (which occurs in the base year and every ten years until the model terminates), a feedback between the two models is necessary. On a year when MATSim is run, SILO takes a list of all of the persons modeled in the region and mostly-randomly selects 5% of this list. Those selected will be created as a MATSim agent. I say "mostly-randomly" because a SILO person is only chosen to become a MATSim agent if they are employed, they have a workplace in the six-county region, and their household has at least one car (meaning that they

have the possibility to commute by car). The SILO Person Java object stores IDs of home and work zones, and so a random coordinate within those zones is selected and assigned as the home and workplace locations of the agent (Ziemke et al., 2016).

Trip start times are needed in order to create trips from this information. As a crude approximation, these trip start times are chosen randomly within a Normal distribution between 6 and 9 am for the morning peak commute and between 3 and 6 pm for the afternoon commute. An example of these departures and arrivals for the BAU scenario in the base year for the model region is shown in Figure 10 below.

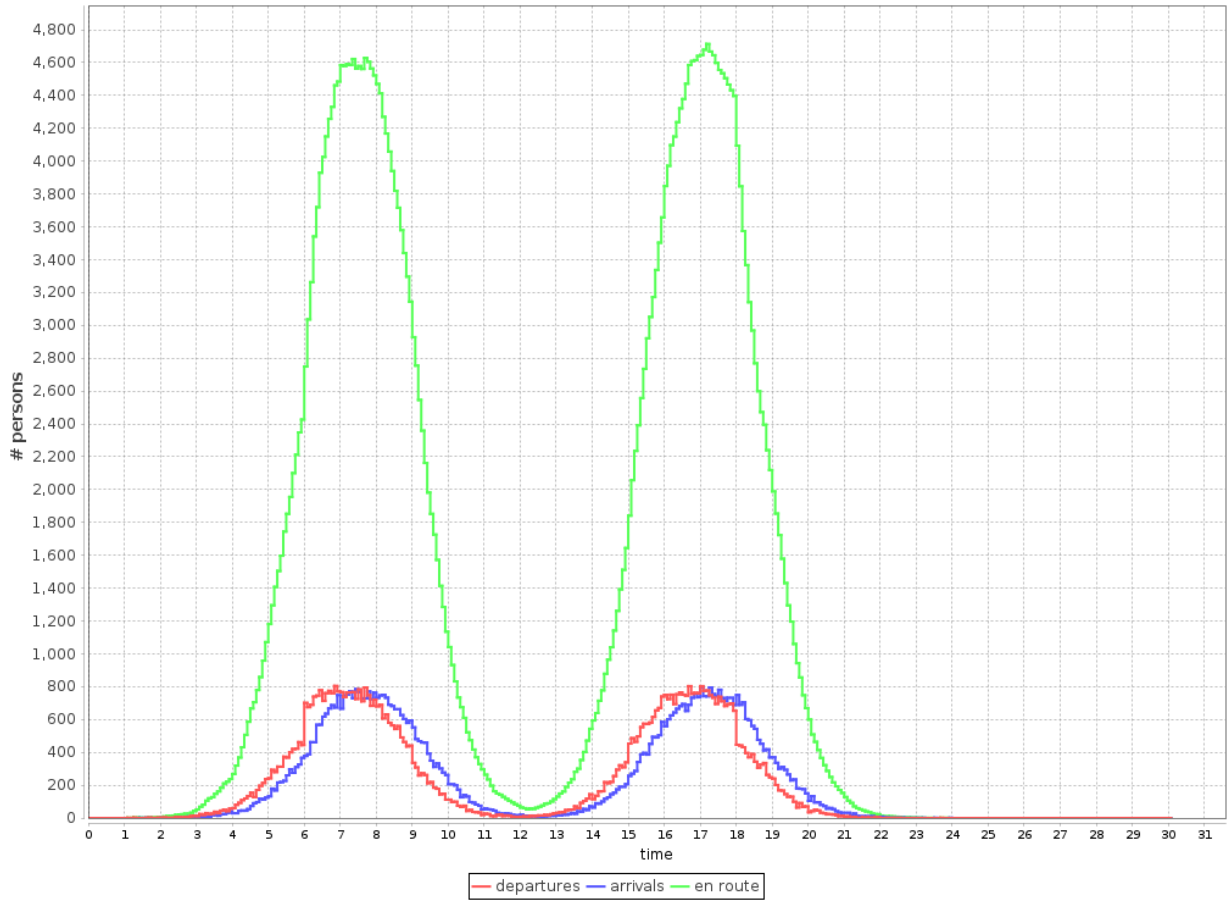

Figure 10: Example of Commute Departures, arrivals, and the Corresponding Number of Persons En-Route for the BAU Model in Year 2013 (Horni et al., 2016)

Once MATSim completes its 50 iterations, it must transfer the travel time information to SILO. SILO requires travel times at the zonal level. Travel times can be computed in an efficient

manner in MATSim using least-cost-path trees. It chooses random coordinates within each zone and calculates the traffic-condition-dependent travel times. It uses averages for all zone-to-zone travel times to create the travel time skim. These travel times are used to determine dwelling satisfaction and commute disutilities in current dwellings, which can be taken into account in household relocation decisions (Ziemke et al., 2016).

4.4 SILO Input Files Needed

Several input files are needed to help SILO understand the particulars of the Austin metropolitan region. These include four files that describe the synthetic population, a file indicating developable land availability, a zone system, a population and employment forecast, a commute trip frequency distribution, and a zone shapefile. These are discussed in more detail below.

4.4.1 Synthetic Population

As discussed in Chapter 3, the synthetic population generator creates four different files which are meant to represent a simplified microscopic representation of the actual Austin population. The first represents the persons in the study area, and contains key characteristics of each individual including age, gender, relationship, race, and occupation. The second represents households in the study area and contains attributes for every household including the TAZ that the household is in and the number of household vehicles. Persons from the person file are each assigned to households. The third represents dwellings in the study area, and contains key characteristics of each dwelling, such as the dwelling type, number of bedrooms, and monthly cost. Each household is assigned to a dwelling, however there are more dwellings than households, representing dwelling vacancies for the region. The final synthetic population file is one representing jobs and contains pertinent qualities of every job including the zone location of the job, the job type, and whether it is vacant or not. A working person is assigned to each job that is not vacant. For more detail on the data used to construct the synthetic population files, please see Chapter 3.

4.4.2 Available Land

The second input file needed for SILO is available, developable land at the TAZ-level. This is an important input file to SILO because it indicates where the model is able to add residential developments. CAMPO collects a detailed land use inventory for the City of Austin and publishes this every year (Land Use Inventory Detailed, 2019). The land that was categorized as 'undeveloped' was determined to be land that was available to develop residentially. The database defines 'undeveloped' as parcels without structures that have the potential for development. A GIS overlay of this categorized land was used to aggregate this information to determine the total developable land at the TAZ-level for the TAZs in the City of Austin. Unfortunately, there was not the same level of detailed data available for the non-city metropolitan region of Austin. A linear regression model was used to make reasonable assumptions for available land in these non-city regions of Austin. Several iterations of linear regression models were run until only statistically significant ($\alpha = 0.05$) variables were left. The values determined from this linear regression model were modified some during the parameter calibration process (see Table 16 below). See Chapter 5 for more details.

Table 16: Linear Regression Model Used to Determine Non-City Metropolitan Region Developable Land

Explanatory Variables	**Coefficient**	**Std. Err.**	**t-statistic**	**p-value**
Constant	9.89E-2	8.34E-3	11.86	0.000
Population Density	-5.88E-3	1.04E-3	-5.66	0.000
Population Density Squared	1.39E-4	3.50E-5	3.96	0.000
Employment Density	-1.25E-3	5.35E-4	-2.33	0.020
Median Income	-3.39E-7	8.25E-8	-4.11	0.000
Suburban (binary variable)	3.55E-2	7.98E-3	4.44	0.000

4.4.3 Zone System

See Section 3.2.2 Zone System for details on this file.

4.4.4 Population Forecast

Population is forecasted exogenously in SILO, so this file defines the population forecast for each model year. It is an aggregated forecast of the entire Austin metropolitan study region, so it does not forecast the population at the zonal level. This data on population forecast through 2040 was obtained from the CAMPO transportation model forecasts (Zhao, 2018). Years between the CAMPO forecasts were linearly extrapolated.

4.4.5 Employment Forecast

The employment forecast is also defined exogenously, but this time these forecasts are made at the zonal level and there are separate forecasts for each job type. SILO automatically interpolates between the forecast years provided. These employment forecasts were also obtained from the CAMPO transportation model forecasts (Zhao, 2018).

4.4.6 Work Trip Length Frequency Distribution

This file was adopted from the Maryland implementation of SILO and describes the trip length frequency distribution of commute trips. For each commute travel time from one minute to 200 minutes, a frequency of this commute travel time and a disutility of this commute travel time are given. This is used by SILO so that commute length can be considered in one's dwelling satisfaction evaluation. The file ends at a travel time of 200 minutes, because it is assumed that practically no one commutes that far on a daily basis. This means that dwellings that are further than 200 minutes away from a household member's workplace are not considered to be in the choice set for that household. It was determined that the Maryland commute frequency distribution was acceptable for the Austin area because they have similar average commute times. The average commute travel time in Maryland is 31 minutes compared to the average commute travel time in Austin of 27 minutes (Reschovsky, 2004; U.S. Census Bureau, 2017).

4.4.7 Zone Shapefile

See section 3.2.3 Zone Shapefile for details on this file.

4.5 MATSim Input Files Needed

There are two basic input files needed in order for MATSim to run. The first is a transport network that contains nodes and links that represent the Austin transportation facilities. The second is a configuration file. These are discussed in more detail in the following two sections.

4.5.1 Transportation Network

The transportation network describes the transportation infrastructure on which agents can move around, or the supply, and the plans describe the demand. A network consists of nodes and links. Nodes are described by coordinate values. Links have more features, including the length of the link, the flow and storage capacity, the free speed, the number of lanes, and the modes allowed on the link.

4.5.2 Configuration File

The configuration file defines the MATSim model run. It defines the number of iterations to run and locates the network file to be used. It also defines the flow and storage capacity factors as 0.05 and 0.11 respectively.

4.6 Model Assumptions and Simplifications

This section is broken up into two sub-sections. The first talks about the simplifications and assumptions that SILO makes in general. The second talks about simplifications and assumptions made for the Austin-specific implementation.

4.6.1 SILO's Assumptions and Simplifications

SILO is known as a middle-weight land use model. It is more involved than a sketch-planning model and can be integrated with a transportation model. However, it makes several simplifications in the interest of fewer data requirements, faster run times, and ease of implementation. SILO is a microsimulation model because all persons and households are simulated individually (Moeckel, 2018c). However, it really models land use changes at the zonal-level and disaggregates those to the household and person level.

SILO also does not aim to predict the total population growth nor the employment group across the entire region. It is fairly standard to have these two be exogenous to the model. However,

a simplification worth noting in SILO is that it also assumes job placement at the zonal level are also exogenous. Because of this, it can really only be considered a *residential* land use model, since it does not attempt to predict employment locations.

Another major simplification of SILO is in its integration with transportation models, in this case MATSim. Neither SILO nor MATSim aims to predict or generate travel demand. Instead, it just sends every worker to work between the hours of 6 am to 9 am in the morning peak. This is assumed to represent traffic congestion and traffic patterns in MATSim fairly well because in reality, not every worker goes to work each day. A significant portion of workers do not make their commute trip on any given day because they are either sick, on vacation, or working from home. On the other hand, there are more travelers on the roads during the peak hour than just the workers. There may be non-workers that run errands between those hours, for example. So, it is assumed that by sending all workers to work, it reasonably reflects the true number of travelers on the road during the peak periods.

Further, only the peak periods are modeled in MATSim because it is assumed that most households make their household location and relocation decisions focused around the commute trip, not so much on other trips they may take. Of course, there are other factors households consider such as dwelling size, quality, and price, but when it comes to travel-related considerations, SILO assumes that the commute distance is all that is taken into account. This is a simplification because there are often other travel-related considerations many of us make when choosing a new dwelling, such as proximity to restaurants and grocery stores. Moreover, there are households that contain no workers, such as retired couples, who then have no travel-related factors in their household location and relocation decision-making, which is probably not realistic.

Finally, school quality is an important factor for households with children in them when making household location and relocation decisions. While SILO does consider school quality in the moving decision, it unfortunately does not look at the age of the people in the household. Instead, it varies the importance of school quality based on just the number of persons in the household and on the household income.

4.6.2 Additional Assumptions and Simplifications Made for the Austin-Specific Implementation

In addition to the simplifications that SILO makes innately, there were generalizations made in the Austin-specific implementation that need to be discussed in order to fully understand

the results that were produced. The first and most major simplification made was that there were many parameters that were not calibrated for the Austin region. This was mostly due to project time constraints. For example, all demographic parameters were the same as the Maryland implementation of SILO. This means that the probability of death, giving birth, getting married or divorced, etc., was assumed to be the same in Austin as in Maryland. This is a fairly reasonable assumption because it is expected that most of these demographics should be reasonably similar. These demographic results are also not of the utmost interest to this project, and so it was deemed acceptable to leave them calibrated to a different U.S. region. Another parameter left uncalibrated was the disutility of a commute based on commute time. The commute times in Maryland and its shoulder regions are fairly similar to the commute times experienced in Austin, so this was also left over from the Maryland implementation. For more details on which parameters were calibrated and which were not, see Chapter 5.

Another assumption made in the Austin implementation of SILO relates to the classification of available, developable land. CAMPO collects a detailed land use inventory for the City of Austin each year. The land that CAMPO categorized as 'undeveloped' was assumed to be land that was able to develop residentially. The CAMPO database defines 'undeveloped' land as parcels without structures that have the potential for development. This is an assumption to consider this land to all be available to develop residentially because of additional zoning laws, but it was assumed to be a reasonable enough assumption. Unfortunately, there was not the same level of detailed data available for the non-city metropolitan region of Austin. A linear regression model was trained on the City of Austin data to make defensible assumptions for available land in these non-city regions of Austin. See Table 16 for more details. This is another major assumption because there is likely to be more land available under the same conditions in the metropolitan regions than in the City of Austin. For this reason, the values that were determined from the linear regression model shown in Table 16 were modified some during the parameter calibration process. See Chapter 5 for more details on this process.

Some other more minor assumptions were made. In SILO, there is room to include a crime index in the household location decision-making. However, SILO looks at crime indices at the county-scale, which is a very coarse view, particularly in the Austin implementation which is only a six-county region. Because the crime indices by county are very similar in the Austin six-county region, this was left out of the model. See Table 17 below for these details. Because SILO looks

at crime indices between 0 and 1, and these indices are relative instead of absolute, it was decided that this should not be considered in the household relocation process, in fear that it may inaccurately push households away from dwellings in counties that have slightly higher crime indices.

Table 17: Crime Indices by County in the Austin Metropolitan Region (BestPlaces, n.d.)

County	**Violent Crime Index**	**Property Crime Index**
Williamson	13.2	26.2
Travis	17.6	37.8
Hays	15.6	33.5
Bastrop	17.4	39.6
Caldwell	20.0	34.6
Burnet	15.7	30.4
U.S. Average	22.7	35.4

The final assumption of note in the Austin implementation of SILO is that the CAMPO model forecasts were used for the population and employment growth assumptions Note that the total population growth forecasts from CAMPO were used, and SILO determined where those people and households would live and where they would move over the course of the model period. However, SILO used CAMPO's employment forecast by zone since job locations are exogenous to the model.

Chapter 5: SILO Model Parameter Calibration

This chapter goes into detail on some of the main parameters that were adjusted in the Austin implementation of SILO in order for the model to better reflect the Austin six-county region. First, this chapter talks about calibrating the available and developable land for the non-city metropolitan areas of the region for which data was not available. Then, it reviews the calibration of the region-wide structural vacancy rates, followed by a discussion of the calibration of dwelling construction demand parameters. Next, it talks about parameters calibrated in the dwelling pricing model, followed by a discussion about the school quality parameters. Finally, this chapter discusses the parameters that were not calibrated for this region.

5.1 Available, Developable Land

According to Dr. Rolf Moeckel, the lead researcher and professor who developed SILO, available land is the most sensitive parameter to the results of SILO (Moeckel, 2019b). Because of this, the most amount of calibration time was spent on tuning this parameter. As was discussed in Section 4.4.2., CAMPO collects a detailed land use inventory for the City of Austin every year. The land in the City of Austin that was categorized as 'undeveloped' was determined to be land that was available to develop residentially. The database defines 'undeveloped' as parcels without structures that have the potential for development. However, there was no comparable dataset for the non-city Metropolitan region of Austin. Section 4.4.2 discusses a linear regression model (see Table 16) that was used to obtain reasonable assumptions for non-city zones in the model region.

While this is a defensible approach, it is easy to imagine how this may be biased and how it could underestimate the amount of available land in the non-city metropolitan regions. This is because non-city regions by definition are more rural, and so one would expect there to be more undeveloped land than in the city. Considering this fact, it is not terribly appropriate to train a linear regression model on data whose predictor variable takes certain values in one particular region and apply it to data whose predictor variable takes different values in another region. In this case, a linear regression model is trained on data with relatively less available land, and then applied to regions that one expects to have more available land. As such, the regression has some inherent bias.

Given these two motivations of (1) high parameter sensitivity and (2) concerns with using a linear regression model outside of its reasonable range, it is important to calibrate the available land values that are obtained for the non-city metropolitan regions. To perform this calibration, the model was run with varying percentages of the regression model results for these non-city Metropolitan regions. It was run with 50%, 75%, 100%, 125%, 150%, 175%, 200%, 250%, and 300% of the available, developable land that was output from the linear regression model for the model base year of 2013. Then, available land is calibrated by comparing the household distribution in subsequent model years. In particular, the household distribution results for each of these model runs were compared to the household distribution from the CAMPO model in 2015, as well as for the CAMPO model household forecast for 2040.

To aggregate this calibration to a more digestible size, household distribution was compared at the county level for each model run to the CAMPO household distribution values in 2015 and 2040. As expected, decreasing the amount of available land in the non-city Metropolitan regions was further from the results in the CAMPO model, and increasing the amount of land in these regions helped, but only to a certain point. It was found that multiplying the developable land obtained from the linear regression model by 175% or 1.75 came the closest to the CAMPO model in 2015 and 2040. As such, these values for available and developable land were used in all scenarios discussed in Chapter 6.

5.2 Structural Vacancy Rates

The dwelling price model updates monthly costs based on vacancy rate, which is meant to be a proxy for current demand. Vacancy rates are calculated every year for each dwelling type in every zone. Structural vacancy rates are defined for each dwelling type and are meant to reflect the average region-wide vacancy rate for each dwelling type. The structural vacancy rates for the Austin implementation of SILO reflected the average region-wide vacancy rate for each dwelling type in the base year. These are shown in Table 18 below. If vacancy rates are above the structural vacancy rate in a given zone, prices decrease; if vacancy rates are below the structural vacancy rate, prices increase. See Section 4.1.3 for more details on how structural vacancy rates impact the dwelling price.

Table 18: Vacancy Rates by Dwelling Type for the Austin Implementation of SILO

Dwelling Type	Structural Vacancy Rate
Single-Family Dwelling	3.7%
Single-Family Attached Dwelling	6.4%
Multi-Family with 5+ Families	7.8%
Multi-Family with 2 – 4 Families	6.1%
Mobile Homes	7.4%

5.3 Dwelling Construction Demand

Every model year in SILO, developers evaluate the demand for each dwelling type in each region. Demand is expressed by vacancy rate, so lower vacancy rates signify higher construction demand. This demand as a function of vacancy rate for each dwelling type for the Austin implementation of SILO is shown below in Figure 11. The values of these parameters were adopted from the Maryland implementation, but the order of their sensitivity was changed. So, in the figure below, multi-family dwellings with five or more dwellings are the least sensitive to vacancy rates while mobile homes are the most sensitive. In the Maryland implementation, the order from least to most sensitive was multi-family dwellings with two to four dwellings, multi-family dwellings with five or more dwellings, mobile homes and single-family attached dwellings were tied, and single-family detached were the most sensitive to vacancy rates. This order was switched to reflect the number of dwellings of each type that have been built in Austin in the recent past (New Residential Units: Summary by Calendar Year and Type, 2019).

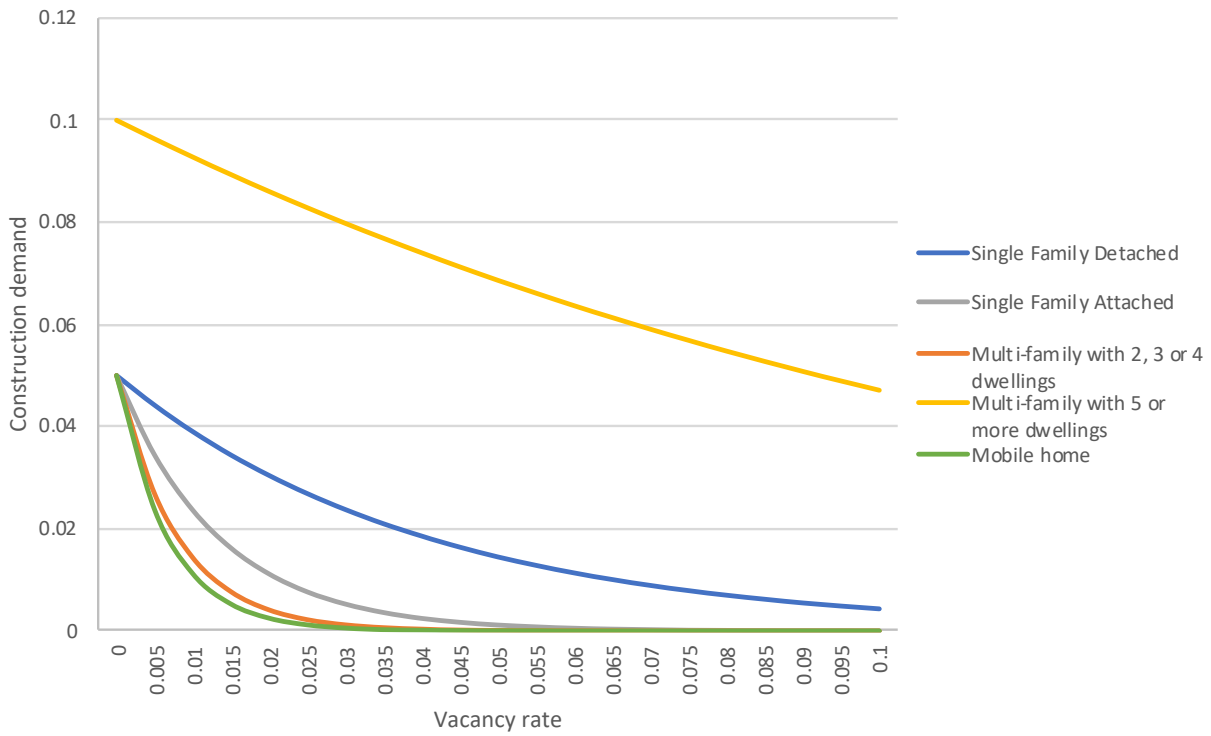

Figure 11: Construction Demand for Dwelling Types as a Function of Vacancy Rate in the Austin Implementation of SILO

5.4 Dwelling Price Model

There are six main parameters associated with the dwelling pricing model. The dwelling pricing model uses vacancy rates as a proxy for dwelling demand, and it considers vacancy rates by dwelling type and by region for this demand. The first main parameter used in the dwelling pricing model is the average price sensitivity or the "main slope". This parameter describes the linear relationship between dwelling price and vacancy rate when vacancy rates are near the structural vacancy rates. This main slope was left the same as it was in the Maryland implementation of SILO at -1.0. This means that as vacancy rates decrease by 1% for a certain dwelling type in a specific region, the price increases by 1% when the vacancy rate is near enough to the structural vacancy rate. There are parameters that define how near is near enough to the structural vacancy rates such that this slope is used. That will be discussed later in this section.

The second parameter associated with the dwelling price model is the low-vacancy price sensitivity. This parameter describes the linear relationship between dwelling price and vacancy rate when vacancy rates are substantially lower than the structural vacancy rates. So, it gives a steeper slope than the average price sensitivity slope. Lower vacancy rates are meant to signal

higher demand and so developers and renters will be eager to increase prices significantly in response. This parameter was set to -10.0 in the Austin implementation which is twice the value that was used in the Maryland implementation. This means that as vacancy rates decrease by 1% for a certain dwelling type in a specific region, the price increases by 10% when the vacancy rate is significantly lower than the structural vacancy rate. This reflects the dramatic increase in dwelling prices that Austin has seen in the recent past and is expected to see in the future model years as the population nearly doubles.

On the other end of the spectrum, the third parameter associated with the dwelling price model is the high-vacancy price sensitivity. This parameter describes the linear relationship between dwelling price and vacancy rate when vacancy rates are substantially higher than the structural vacancy rates. Higher vacancy rates signal relatively low demand, but developers and renters will not be keen on dramatically lower dwelling prices. So, this slope is less steep than both the low-vacancy price sensitivity and the average price sensitivity slopes. This slope was left the same as it was in the Maryland implementation of SILO at -0.1. This means that as vacancy rates increase by 1% for a certain dwelling type in a specific region, the price decreases by 0.1% when the vacancy rate is significantly higher than the structural vacancy rate.

Next, these inflection points that define when each of the above slopes are used to determine changes in dwelling prices as a function of vacancy rate must be defined. A value of 0.9 or 90% was used to define the lower inflection point. This means that at vacancy rates below 90% of the structural vacancy rate, the steeper low-vacancy price sensitivity slope of -10 is used to reflect changes in dwelling cost. A value of 2.0 or 200% was used to define the upper inflection point. This means that at vacancy rates above 200% of the structural vacancy rate, the shallower high-vacancy price sensitivity slope of -0.1 is used to reflect changes in dwelling costs. That means that between 90% and 200% of the structural vacancy rate, the average price sensitivity slope is used to describe the linear relationship between dwelling price and vacancy rate.

Finally, the pricing model defines a maximum change in dwelling prices that can occur over one year. This was set to 0.02 or 2% in the Maryland implementation of SILO. A maximum year over year dwelling price increase of 2% is much too low for the Austin implementation of SILO. From December 2013 to December 2018, Austin's median home price increased by 33%, from $226,000 to $301,391 (Silver, 2019). This equates to an average of a 6% increase in the median home price. Because this just represents the average increase, the maximum allowable

increase must be set quite a bit higher to allow quickly growing neighborhoods to reflect the true increase in real estate value. Thus, the maximum change in dwelling prices that can occur in over one year was set to 10% or 0.10 in the Austin implementation of SILO.

5.5 School Quality

School quality is an important household location and relocation factor for households with children living in the house. SILO considers school quality to be an increasingly important household location factor as household size and income increase. In order to include school quality in relocation decision-making, the overall school grade for each school district in the model region, calculated by a company called Niche, was converted to a number between 0 and 1 and was assumed to be the school quality index for all dwellings in that school district's coverage area (Niche, 2019). This "grade" is calculated by using dozens of public data sources, including the U.S. Department of Education graduation rates and state level test scores, Common Core Data from the National Center for Education Statistics, which gives information such as enrollment figures, and many more sources (Niche, 2019). It also considers reviews from parents and students. The scores for each school district in the model region are shown below in Table 19. The school quality indices are also shown spatially in Figure 12 below.

Table 19: School Quality Grades and Indices for School Districts in the Austin Metropolitan Region

School District	Overall Grade	School Quality Index
Austin ISD	A-	0.8
Bartlett ISD	C+	0.4
Bastrop ISD	C+	0.4
Blanco ISD	B+	0.7
Burnet Consolidated ISD	B-	0.5
Comal ISD	A-	0.8
Del Valle ISD	C	0.3
Dripping Springs ISD	A	0.9
Eanes ISD	A+	1.0
Elgin ISD	C-	0.2
Florence ISD	C	0.3
Georgetown ISD	B+	0.7
Gonzales ISD	B-	0.5
Granger ISD	B	0.6
Hays ISD	B-	0.5
Hutto ISD	B	0.6
Jarrell ISD	C+	0.4
Johnson City ISD	B	0.6
Lake Travis ISD	A+	1.0
Lampasas ISD	B	0.6
Lago Vista ISD	B	0.6
Leander ISD	A+	1.0
Liberty Hill ISD	A-	0.8
Llano ISD	B	0.6
Lockhart ISD	C-	0.2
Luling ISD	C	0.3
Manor ISD	C	0.3
Marble Falls ISD	B-	0.5
McDade ISD	B	0.6
Pfugerville ISD	A-	0.8
Prairie Lea	C+	0.4
Round Rock ISD	A	0.9
San Marcos Consolidated ISD	C+	0.4
Smithville ISD	B-	0.5
Taylor ISD	B-	0.5
Thrall ISD	B+	0.7
Thorndale ISD	B+	0.7
Waelder ISD	C-	0.2
Wimberly ISD	A	0.9

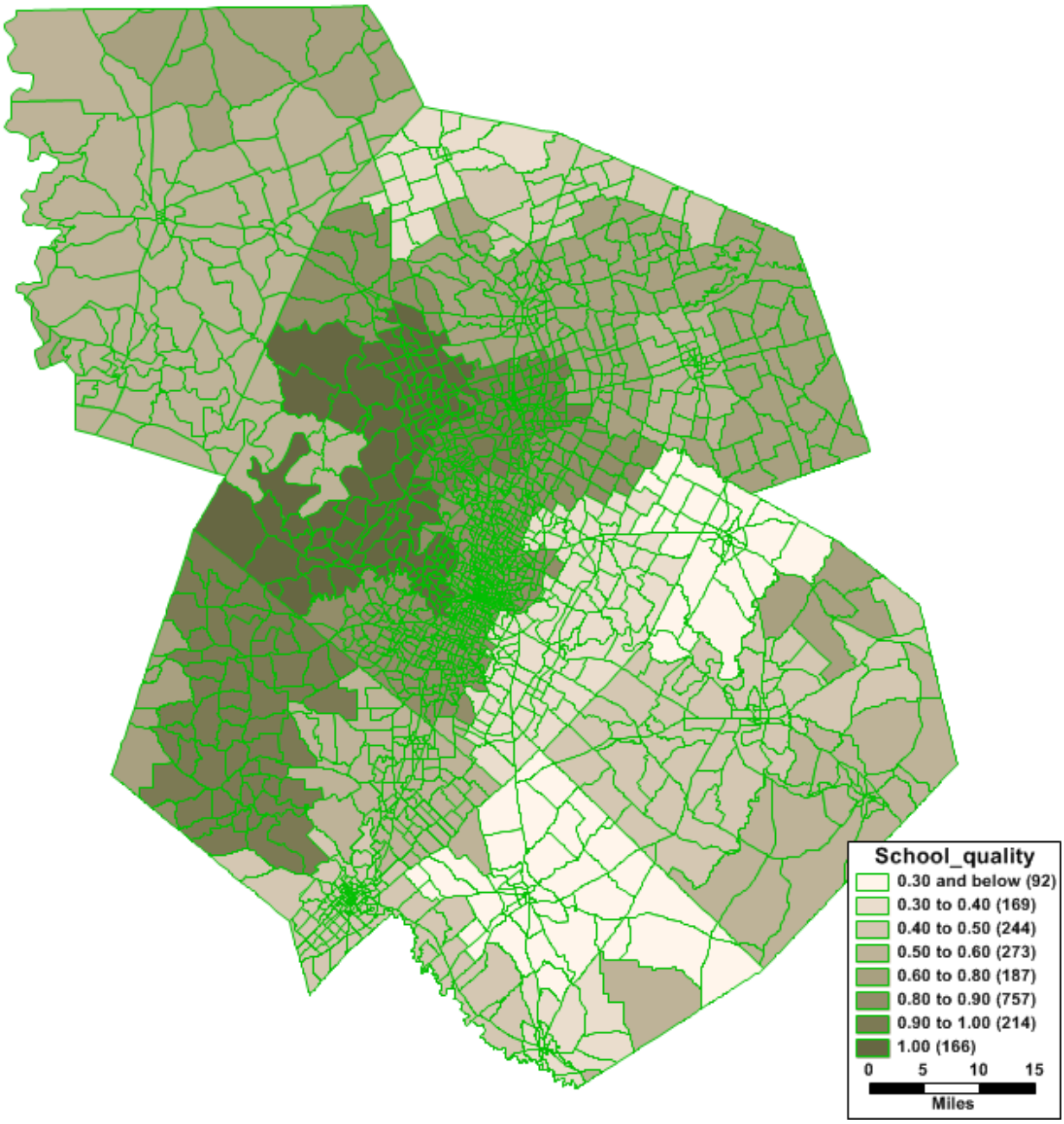

Figure 12: School Quality Index Shown Spatially in the Austin Six-County Region

Chapter 6: SILO – MATSim Results

This chapter presents and explains the results from part one of this thesis. It starts by describing the scenarios that were simulated over a 27-year period. Next, it gives a summary of the results that came out of the modeling. Then, this section dives into key results in more detail, namely, commute travel time, household location, and available land results.

6.1 Scenario Descriptions

Three main scenarios are defined and analyzed over a 27-year period. First is a business-as-usual (BAU) 0% AV scenario where the traditional passenger car is the main travel mode and commute travel time is a major driver in household location and relocation decision making. The second case, the "100% AV" scenario, looks at a scenario where personal AVs are used across the network. To model this simply, SILO was updated so that households value their commute travel time at half the amount they do in the BAU scenario, with respect to their household location and relocation decision making. This means that, when households are evaluating their satisfaction with their current dwelling, or when households are moving and considering new dwellings, the workers' commute travel time factors into the decision-making at a 50% lower priority than it did in the BAU scenario. This second scenario is meant to represent the changes in the value of travel time that are expected when self-driving technologies emerge assuming workers travel privately by AVs, and can work, sleep, or do some other task of value while commuting. Note that vehicle occupancy is unaltered in the 100% AV scenario. Finally, the third case looks at the case of shared AV (SAV) implementation with a high penetration of dynamic ride sharing (DRS). This scenario is called the "Hi-DRS SAV" scenario from here forward. This is modeled in a simplified fashion by updating SILO so that households value their commute travel time at 25% the level they do in the BAU scenario, with respect to their household location and relocation decision making. In addition, MATSim is updated in this scenario to have twice the capacity. This is meant to model a situation where there are 50% fewer vehicles on the road, meaning the average vehicle occupancy is about two, which is double the average vehicle occupancy assumed in the first two scenarios.

6.2 Summary of Results

The three scenarios are compared on various measures relative to the base year, summarized below in Table 20.

Table 20: Summary of Scenario Results Comparing Model Base Year to End Year (27-year period)

	Base year	**BAU (0% AV) – end year**	**100% AV scenario – end year**	**Hi-DRS SAV scenario – end year**
Household-Level Statistics				
Number of households	768,950	1,798,924	1,798,648	1,799,542
Number of households in the City of Austin (CoA)	462,465	944,520	894,744	892,711
Number of households in non-CoA Metro area	306,485	854,404	903,904	907,182
Dwelling-Level Statistics				
Number of SFD dwellings	489,673	863,756	921,076	921,947
Number of SFA dwellings	30,497	32,880	33,507	33,638
Number of MF5+ dwellings	206,120	837,169	820,462	824,533
Number of MF2-4 dwellings	45,744	52,245	51,760	51,983
Number of MH dwellings	38,927	48,559	52,516	53,227
Available, Developable Land				
Total available, developable land	426.9 mi_2	245.2	222.9	227.4
Available, developable land in the CoA	69.0 mi_2	8.9	10.6	14.5
Available, developable land in metro areas	358.0 mi_2	236.3	212.3	212.9
Commute Statistics				
Average commute time	31.4 mins	38.5	41.6	39.8
Average commute time for those living in the CoA	22.3 mins	25.7	25.6	25.6
Avg. commute time for those living in metro areas	41.4 mins	48.4	52.1	50.5
Number of commuters with 60+ minute commutes	2639	6006	8007	6993

The above table gives a summary of some major results that can be drawn from the three scenarios that are run from the base to the final model year in SILO, with MATSim running every ten model years to update commute travel times. The first thing to note from Table 20 is that the Austin, Texas six-county region is growing dramatically over the model time period. More than a million households are expected to move to the region in the 27 years between the base and final

model year, which is a 134% increase in the total number of households. Another major result of note in this realm is that many more of these households live in the City of Austin in the BAU scenario than in the 100% AV or the Hi-DRS SAV scenarios, meaning that there are many fewer households living in the non-City Metropolitan region in the BAU scenario than there are in the 100% AV or the Hi-DRS SAV scenarios. This will be discussed more in Section 6.4.

There are also more single-family dwellings in the 100% AV and the Hi-DRS SAV scenarios as compared to the BAU scenario in the final model year. This is because people care more about dwelling size and quality in the 100% AV and the Hi-DRS SAV scenarios relative to the BAU scenario (0% AV), so there is more demand for, and thus more construction of, single-family dwellings. Similarly, there are more multi-family dwellings with five or more dwellings in them in all scenarios because there are more of these dwellings constructed (see Figure 11). New dwellings have the highest quality, and since this is more valued on a relative basis in the 100% AV scenario relative to the BAU scenario, more people move into these MF5+ dwellings, and thus there is higher demand, and more yet are constructed.

There is a 42.6% reduction in available developable land in the 27-year period between the base to final model year in the BAU scenario (0% AV), a 47.8% reduction in the same period in the 100% AV scenario, and a 46.7% reduction in the Hi-DRS SAV scenario. There is a larger total reduction in the 100% AV and the Hi-DRS SAV scenarios than in the BAU scenario because households care relatively more about size than they do in the BAU scenario, so there are more SFDs which are on larger plots of land. There is also a larger reduction in available land in the CoA in the BAU scenario than there is in the 100% AV and the Hi-DRS SAV scenarios. On a related note, there are more households living in the CoA in the BAU scenario than there are in the 100% AV and the Hi-DRS SAV scenarios, and less living in the metro regions in the BAU scenario than in the 100% AV and the Hi-DRS SAV scenarios. This is discussed in more detail in Section 6.5.

Finally, commute travel times increase significantly in all three scenarios in the 27-year period between the base and final model year. However, they increase significantly more in the Hi-DRS SAV scenario, and even more so in the 100% AV scenario, by the final model year as compared to the BAU scenario (0% AV) in the final model year, on average. In addition, there are many more people with extreme commutes of over one hour in the 100% AV and the Hi-DRS

SAV scenario in the final model year, compared to the BAU scenario in the final model year. This is discussed in more detail in Section 6.3.

6.3 Commute Travel Time Results

In this section, commute travel time results are compared across the three scenarios. Figure 13 shows the distribution of commute travel times across all workers living and working in the Austin six-county metropolitan region in the base model year and 20 years after the base year in each scenario. The base year is shown in orange in Figure 13, and the average commute travel time in the base year is 31.4 minutes.

The BAU scenario 20 years after the base year is shown in green in Figure 13. In this scenario, each bin seems pretty uniformly stretched upwards, so the distribution looks similar but there are more travelers in each bin. The average commute travel time 20 years after the base year in the BAU scenario is 38.5 minutes, so commute times are nearly five minutes longer across all workers, relative to the base model year.

The 100% AV scenario 20 years after the base year is shown in yellow in Figure 13. The major distinction of note in this figure is how many more workers are commuting sixty minutes or more to work. This makes sense because households are no longer considering this commute time as strongly in their household location and relocation decisions, making other dwelling attributes such as dwelling size and quality more important. The average commute travel time 20 years after the base year in the 100% AV scenario is 41.6 minutes, so commute times are over ten minutes longer across all workers, relative to the base model year.

The Hi-DRS SAV scenario 20 years after the base year is shown in blue in Figure 13. The main difference between the 100% AV and the Hi-DRS SAV scenario is that there is a 12.7% decrease in the number of extreme commutes of 60 minutes or more one-way. The average commute travel time 20 years after the base year in the Hi-DRS SAV scenario is 39.8 minutes, so commute times are over eight minutes longer across all workers, relative to the base model year.

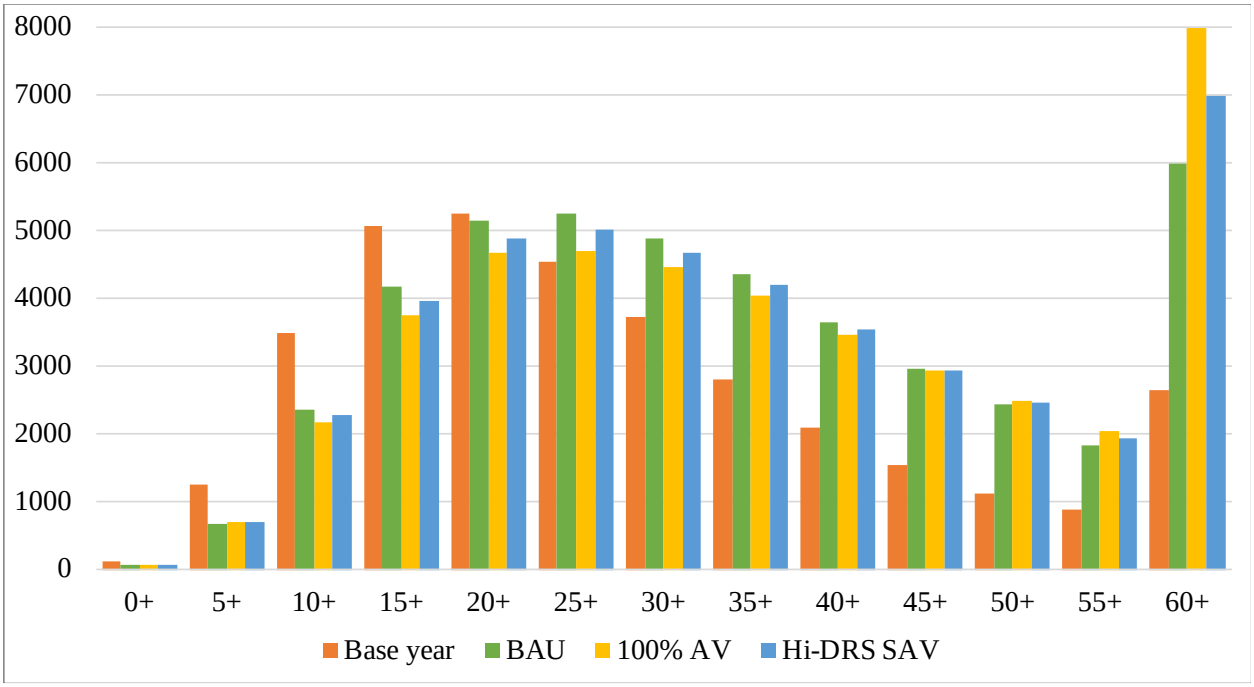

Figure 13: Commute Travel Times in Austin in the Base Model Year and 20 Years After the Base Year in Each Scenario

6.4 Household Location Results

The total number of households in the region increases by 134% in both scenarios. This is a major growth from around 769,000 households in the BAU model year to 1.80 million households in the final model year. In the 100% AV scenario, more of this growth is happening in the less-central non-city metropolitan regions than the BAU scenario (0% AV). The number of households in the non-city metro regions in the 100% AV scenario grows by 194.9% from the base to the final model year, compared to the BAU scenario which grows by 178.8% in the same area over the same time period. Similarly, there is then less growth happening in the City of Austin in the 100% AV scenario than in the BAU scenario. In the 100% AV scenario, the number of households in the City of Austin grows by 93.5% from the base to the final model year, compared to the BAU scenario which grows by 104.2% in the same area over the same time period. Figure 14 below shows the spatial layout of the difference in the number of households by zone in the final model year of the 100% AV scenario relative to the final model year of the BAU scenario (0% AV). Positive values in the figure (shown in dark orange) indicate more households in that zone in the 100% AV scenario relative to the BAU scenario in the final model year. Negative values in the figure (shown in white) indicate fewer households in that zone in the 100% AV

scenario relative to the BAU scenario in the final model year. The change in number of households by zone over the course of the model timeframe for each scenario is shown in the Appendix.

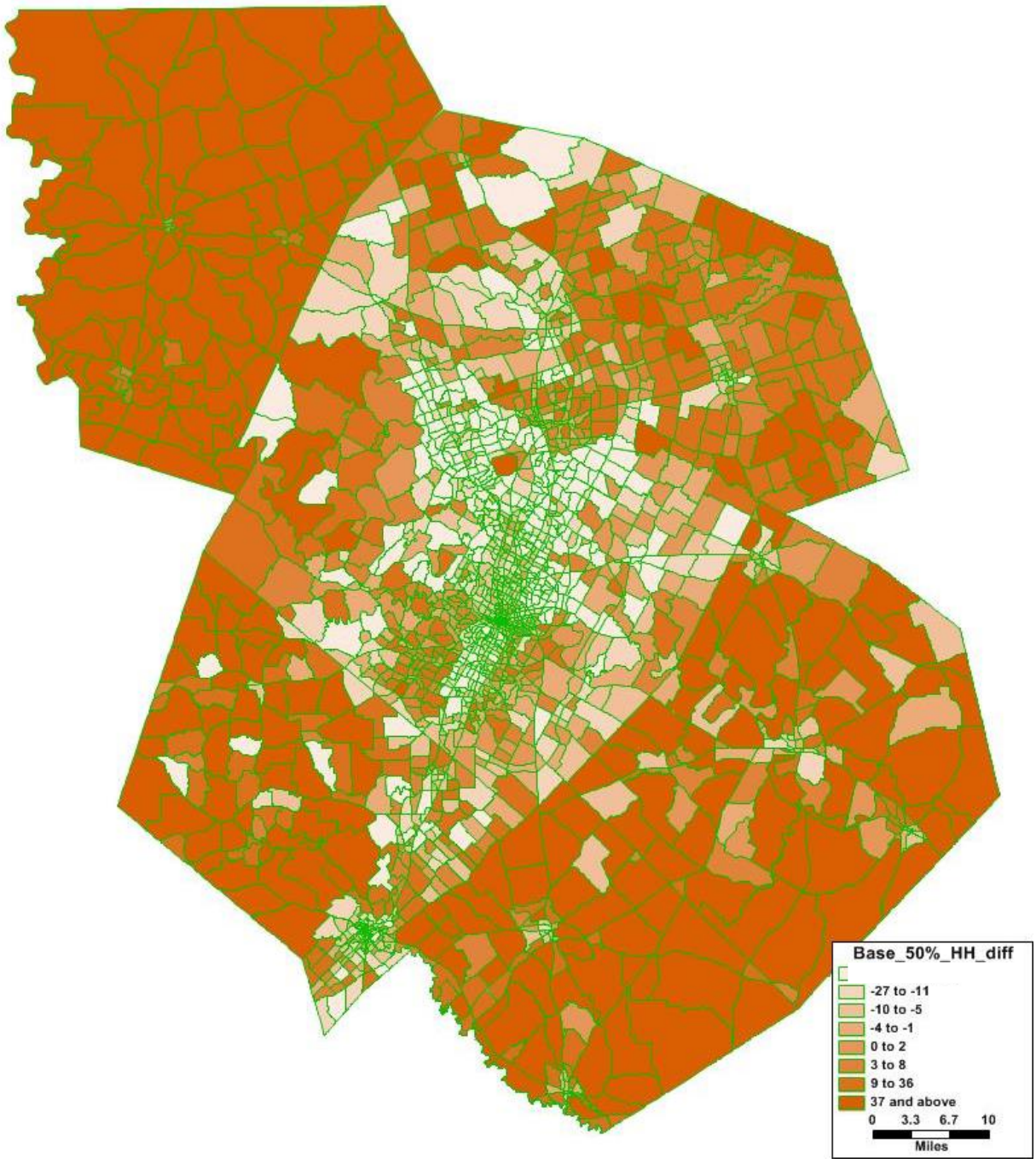

Figure 14: Difference in Where Households are Located in the 100% AV Scenario Relative to the BAU Scenario in the Final Model Year

In the Hi-DRS SAV scenario, more of this growth is happening in the non-city metropolitan regions than the BAU scenario (0% AV). There is also slightly more growth happening in the non-city metropolitan regions in the Hi-DRS SAV scenario relative to the 100% AV scenario. In the Hi-DRS SAV scenario, the number of households in the non-city metro regions grows by 196.0% from the base to the final model year, compared to the BAU scenario which grows by 178.8% in the same area over the same time period. Similarly, there is then less growth happening in the City of Austin in the Hi-DRS SAV scenario than in the BAU scenario. In the Hi-DRS SAV scenario, the number of households in the City of Austin grows by 93.0% from the base to the final model year, compared to the BAU scenario which grows by 104.2% in the same area over the same time period. Figure 15 below shows the spatial layout of the difference in the number of households by zone in the final model year of the Hi-DRS SAV scenario relative to the BAU scenario. Positive values in the figure (shown in dark orange) indicate more households in that zone in the Hi-DRS SAV scenario relative to the BAU scenario in the final model year. Negative values in the figure (shown in white) indicate fewer households in that zone in the Hi-DRS SAV scenario relative to the BAU scenario in the final model year.

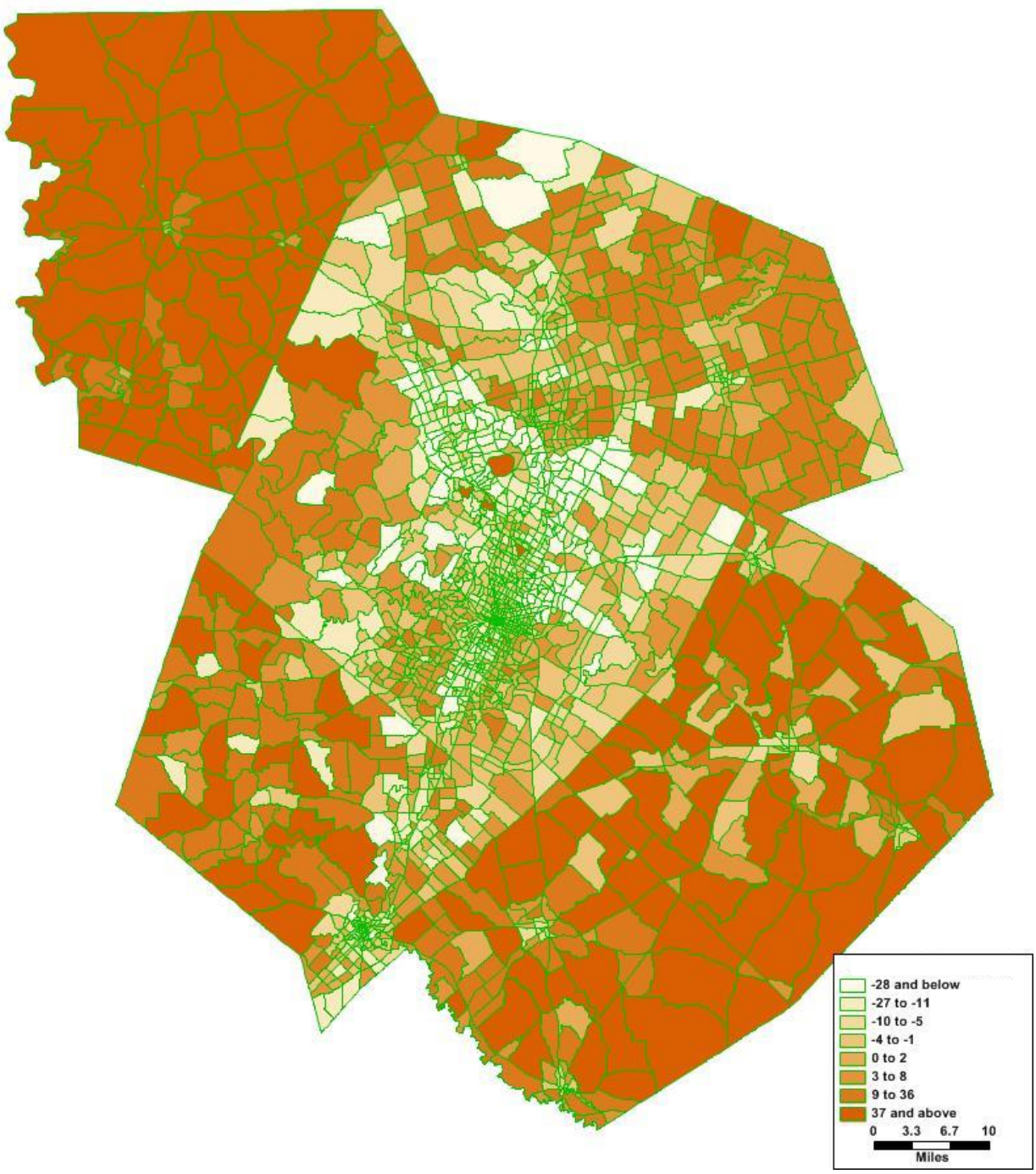

Figure 15: Difference in Where Households are Located in the Hi-DRS SAV Scenario Relative to the BAU Scenario in the Final Model Year

6.5 Available and Developable Land Results

Austin-Round Rock, Texas is number four on the list of the fastest growing cities in America according to USA Today (2019). Because of this, it is expected that available and developable land will decrease significantly over the model period of the base to the final model year. This is seen through a 42.6% reduction in developable land over the model time period in the BAU scenario (0% AV), a 47.8% reduction in the 100% AV scenario, and a 46.7% reduction in the Hi-DRS SAV scenario. This larger reduction in developable land in the 100% AV and in the Hi-DRS SAV scenarios compared to the BAU scenario is because households care relatively more about size than they do in the BAU scenario, so there are more single-family dwellings constructed, which take up more land.

There is also a larger reduction in available land in the City of Austin in the BAU scenario (0% AV) than there is in the city in the 100% AV and in the Hi-DRS SAV scenarios. This is because households are more willing to live in the less central regions and less willing to pay higher prices to live in the city in both of the AV scenarios, because they do not care as much about their commute distance to work. In the BAU scenario, there is an 87.1% reduction in available land in the city and a 34.0% reduction in available land in the non-city metropolitan regions. In the 100% AV scenario, there is an 84.7% reduction in available land in the city and a 40.7% reduction in available land in the non-city metropolitan regions. In the Hi-DRS SAV scenario, there is an 78.9% reduction in available land in the city and a 40.5% reduction in available land in the non-city metropolitan regions. Figure 16 below indicates the spatial distribution of available land by zone in the final model year in the 100% AV scenario relative to the BAU scenario and Figure 17 indicates the spatial distribution of available land by zone in the final model year in the 100% AV scenario relative to the BAU scenario. Positive values in the figure (shown in dark green) indicate more available land in that zone in the respective AV scenario relative to the BAU scenario in the final model year. Negative values in the figure (shown in white) indicate less available land in that zone in the respective AV scenario relative to the BAU scenario in the final model year. The change in available, developable land by zone over the course of the model timeframe for each scenario individually is shown in the Appendix.

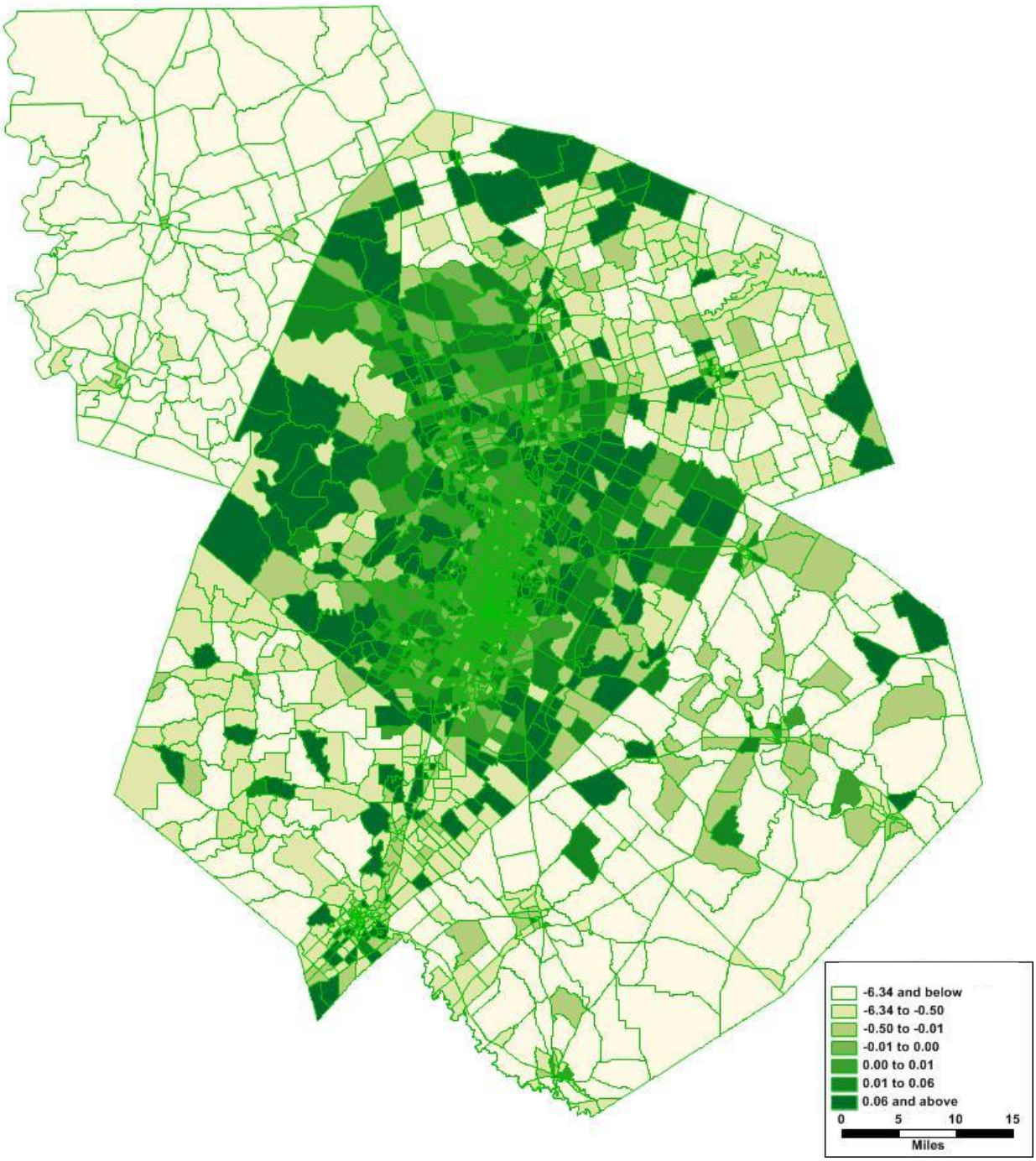

Figure 16: Difference in the Amount of Available, Developable Land in the 100% AV Scenario Relative to the BAU Scenario in the Final Model Year

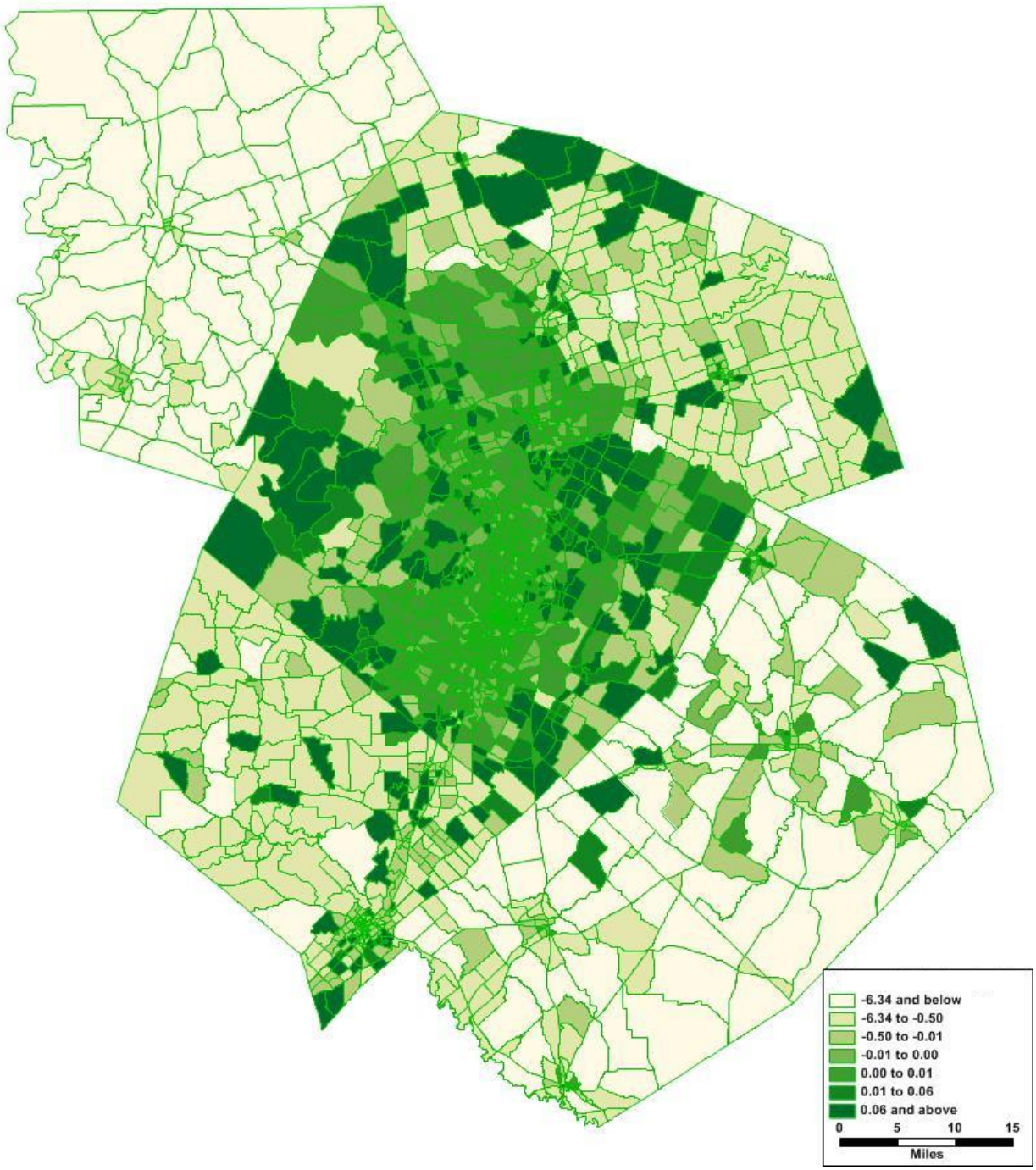

Figure 17: Difference in the Amount of Available, Developable Land in the Hi-DRS SAV Scenario Relative to the BAU Scenario in the Final Model Year

Chapter 7: Conclusions on AV Land Use Implications

The adoption of AVs is fast approaching as many companies are hard at work on their version of the technology. As such, engineers and planners must begin to plan and prepare for important impacts of their adoption. There are many benefits one could imagine from the advent of AVs, including safety improvements, increased economic productivity, and improved quality of life. However, there are also secondary negative impacts of these technological changes that are plausible if appropriate action is not taken to mitigate them. This includes the impacts of urban sprawl as are discussed in this thesis, which has negative consequences including increased emissions and congestion. There are many other negative impacts one could envision of AV technology adoption that are not the focus of this thesis but require future work. This includes induced demand for travel, issues with equity surrounding the technology, and safety and privacy issues. There are many opportunities for important research in the area of AV impacts.

The study discussed in this thesis provides an initial look at potential residential land use implications from a reduction in the value of the time it takes to complete one's commute which will be expected in a future of fully automated vehicles. Because this model is not fully calibrated for the model region, one should really only consider the relative differences between the BAU scenario and the two AV scenario results, rather than the true values, and make conclusions based on those.

Of major note, it was seen that commute travel times increase quite significantly in the 100% AV scenario relative to the BAU scenario (0% AV) 20 years after the base year. There was also an increase in commute travel times in the Hi-DRS SAV scenario relative to the BAU scenario 20 years after the base year, to a lesser degree. Specifically, average commute travel times increase by 3.1 minutes in the 100% AV scenario relative to the BAU scenario (0% AV) in the final model year, which is an 8.1% increase. Additionally, average commute travel times increase by 1.3 minutes in the Hi-DRS SAV scenario relative to the BAU scenario in the final model year, which is a 3.4% increase. There is also an increase in the number of "extreme" commutes of 60 minutes or more. There are 2,001 more workers in the model region with an extreme commute in the 100% AV scenario relative to the BAU scenario in the final model year, which is a 33.3% increase. There are also 987 more workers in the model region with an extreme commute in the 100% AV scenario relative to the BAU scenario in the final model year, which is a 16.4% increase.

The work in this thesis also found differences in the distribution of households across the model region between the two AV scenarios relative to the BAU scenario as well. There were 49,776 fewer households in the City of Austin in the 100% AV scenario relative to the BAU scenario (0% AV) in the final model year, which is a 5.3% decrease. Similarly, there were 51,809 fewer households in the City of Austin in the Hi-DRS SAV scenario relative to the BAU in the final model year, which is a 5.5% decrease. On this same note, there were 49,500 more households that were located in the non-city metropolitan regions of the Austin six-county region in the 100% AV scenario relative to the BAU scenario in the final model year, which is a 5.8% decrease. Similarly, there were 52,778 more households that were located in the non-city metropolitan regions of the Austin six-county region in the Hi-DRS SAV scenario relative to the BAU scenario in the final model year, which is a 6.2% decrease.

Also related to these results are the differences in available and developable land. There is relatively more available land in the City of Austin in the 100% AV and the Hi-DRS SAV scenarios relative to the BAU scenario in the final model year and relatively less available land in the City of Austin in the 100% AV and the Hi-DRS SAV scenarios relative to the BAU scenario in the final model year. Namely, there was 24.0 square miles less land located in the non-city metropolitan regions of the Austin six-county region in the 100% AV scenario relative to the BAU scenario (0% AV) in the final model year, which is a 10.2% decrease. Additionally, there was 23.4 square miles less land located in the non-city metropolitan regions of the Austin six-county region in the Hi-DRS SAV scenario relative to the BAU scenario in the final model year, which is a 9.9% decrease. Along the same lines, there was 1.7 square miles more land located in the City of Austin in the 100% AV scenario relative to the BAU scenario in the final model year, which is a 19.1% increase. Additionally, there was 5.6 square miles more land located in the City of Austin in the Hi-DRS SAV scenario relative to the BAU scenario in the final model year, which is a 62.9% increase. All of these are directionally what one would expect when AVs and SAVs are deployed and commute times are not as strong of a consideration in household location and relocation decision-making.

It is interesting that commute travel times do not increase as dramatically in the Hi-DRS SAV scenario as they do in the 100% AV scenario relative to the BAU scenario, but the land use impacts are similar and even more pronounced in the Hi-DRS SAV scenario than they are in the 100% AV scenario. This makes sense because sharing rides in the SAV scenario leads to shorter

travel times because of the reduction in the number of vehicles on the road relative to the AV scenario. Because these travel times decrease, households are willing to live further distances from their workplaces, increasing urban sprawl. It is worth noting that, although the sprawl is more significant in the Hi-DRS SAV scenario, the emissions implications would be lower than the 100% AV scenario because the rides are shared, meaning there are fewer vehicles traveling those longer distances.

It is also important to understand some of the limitations to our study. For one, there are major simplifications made in the scenario definitions for the "100% AV" and the "Hi-DRS SAV" scenarios, so these results must be considered taking into account these simplifications. In addition, AVs, and particularly SAVs, have major implications for parking needs. Currently, parking is an important housing choice consideration, and if you don't need to worry about parking because you can easily use SAVs on-demand, this could cause conflicting results to our study, such as re-urbanization. These factors are not considered. In addition, telework is becoming a more common trend in workplaces, and is unfortunately not represented by SILO as an option for workers. As a final limitation of note, SILO does not account for any new travelers that may occur in response to the introduction of AV technology, such as those currently without driver's licenses. There are other limitations in the way SILO operates as discussed in Section 4.6. This includes assumptions in the SILO model framework such as the fact that the only transportation consideration in the household location and relocation decision-making is the commute travel time.

This is a crude initial look at some of the residential land use and transportation impacts that could occur in a future of self-driving vehicles. Further research is needed in this area. It would be beneficial future work to increase the complexity of the integration of the land use and transportation model. This could include using AV and/or SAV MATSim plug-ins to both generate AV/SAV travel demand and to simulate all of the traffic in the system, not just commute trips. Then, one could also model a mix of AVs and traditional passenger cars. It would of course be beneficial to spend the time to fully calibrate the LUM for the model region too. Though this is very time-consuming, it would improve the reasonability of results. Finally, it would be constructive to increase the complexity of the LUM to include more accessibility and transportation characteristics into the household location and relocation decision-making. For example, many households care about the distance to the nearest grocery store and proximity to restaurants and retail, not just their commute distance. As more complexity is added to these

ITLUMs, there is of course further calibration and data needs. However, this is where the field of ITLUMs should be headed.

PART TWO: LEVERAGING INTELLIGENTLY CHARGED ELECTRIFIED TRANSIT TO SUPPORT A RENEWABLE ENERGY GRID

Part Two looks at the opportunity smart-charging electric buses provide to support an electricity grid that depends heavily on renewable energy sources of solar and wind. A paper based on this research is under review for publication in the *Sustainable and Renewable Energy Reviews*, was presented at the Sloan Foundation Workshop on Integrating New Electric Mobility Systems with the Electric Grid Infrastructure in Boston, MA on November 6, 2019, and will be presented at the 99th Transportation Research Board Annual Meeting in Washington D.C. in January 2020. Co-authors on this paper include Joseph Griffin, Dr. Kara Kockelman, and Dr. Moataz Mohamed (Wellik et al., 2019).

The section is organized as follows. Chapter 8 provides an introduction and motivation for the electrification of bus fleets and their opportunity to support the electricity grid. Chapter 9 reviews the current state of battery electric buses (BEBs) on the market and how they compare on cost, emissions, and vehicle performance perspectives. Chapter 10 narrows in on BEBs and reviews the state-of-the-art literature related to nexuses between EV and BEB or EV systems and utility grids. Chapter 11 describes the proposed methods, including a utility model, a transit system model for BEBs, and cost estimation details. The case study is detailed in Chapter 12 along with the Austin transit and power data. Chapter 13 reports the results of three different integration scenarios between utility and bus systems. The study concludes with Chapter 14, which contains a discussion and concluding remarks for future research.

Chapter 8: Introduction and Background to Part Two[1]

The transportation sector is the largest greenhouse gas (GHG) emitting sector in the United States, constituting 28.9% of all GHG emissions nationally. Carbon dioxide is the major GHG emitter from the transportation sector, due to the combustion of petroleum-based fuels in vehicles' internal combustion engines. Therefore, moving away from petroleum-based products is a key to reducing emissions. From 1990 to 2017, GHG emissions from the transportation sector have risen for a number of reasons including population and economic growth, urban sprawl, and greater travel distances per capita (Environmental Protection Agency, 2017).

Alternative, clean technology in all modes of transportation are needed to keep the earth from critical 1.5°C warming. Transit buses are good candidates for electrification because of their fixed schedules and routes, making it straightforward to plan around battery range constraints (Mohamed et al., 2017). Adoption of battery electric buses (BEBs) has been limited in scale and scope with the high upfront cost being the major barrier to entry. However, BEBs have the opportunity to minimize this initial cost discrepancy by minimizing operation and maintenance costs. In addition, given the stop-and-go nature of transit operation, BEBs capitalize on regenerative braking to capture energy that is otherwise lost to heat during traditional braking. Finally, BEB systems offer lowered and more predictable operating costs, delivering an important advantage over diesel buses, which can face volatile petroleum prices (Li et al., 2018).

It is important to note that even though BEBs do not emit GHG emissions directly, they do not necessarily operate "carbon-free". One must consider the carbon intensity of the electricity grid supporting BEBs operation. Depending on this carbon intensity, GHG emissions savings can be minimal when switching from diesel- or gasoline-powered vehicles to EVs (Kennedy, 2015). However, a study by the Union of Concerned Scientists (2017) showed that EVs perform better than a gasoline-powered vehicle that gets 50 mpg from a GHG perspective for 70% of American consumers (see Figure 18 below). Because of this relationship between the electricity grid and EV emissions, it is important to reduce the carbon intensity of electricity grid systems in tandem with electrifying transportation. This could be achieved by increasing renewable energy source capacity

[1] This chapter is adopted from a publication submission that is under review for publication in the *Sustainable and Renewable Energy Reviews* with co-authors Joseph Griffin, Dr. Kara Kockelman, and Dr. Moataz Mohamed.

to power our grids, namely, sources of solar and wind energy. Electric powertrains are carbon-free only if the energy is produced through renewable resources.

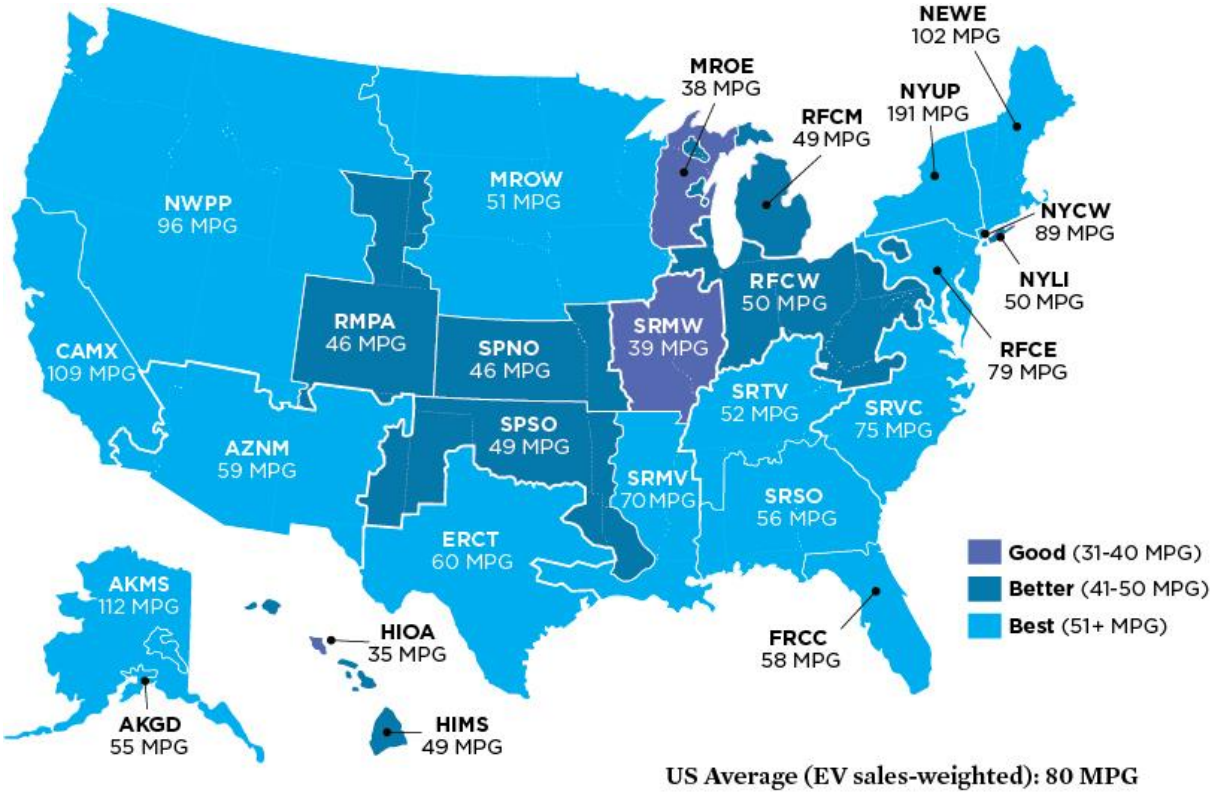

Figure 18: EV GHG Ratings and Gasoline MPG Equivalents by Electricity Grid Region (Reichmuth, 2017)

RESs offer major reductions in GHG emissions while presenting some challenges. Sun and wind are intermittent sources that vary dramatically over the course of each day (with the sun shining during the daytime, and wind blowing stronger at night) and throughout the year (across seasons and weather patterns). Utility managers require backup power generation during times when renewables are producing insufficient energy. It is costly to ramp up and down traditional energy sources, so managers seek to avoid this (Phuangpornpitak & Tia, 2013). This is to name some of the fundamental challenges in the utilization of renewables.

With the overall aim to jointly promote the use of renewables and electric transportation options, this study develops a methodology for vehicle-to-grid (V2G) electrified transportation systems to respond to daily utility operational challenges in utilizing renewables. Put another way, we investigate opportunities for a utility-transportation energy nexus that benefits both utility and

transit systems. In this study, we look at the application of electrifying Austin's bus transit fleet, and the focus of the methodology is to optimally charge and discharge BEBs to shave minute-to-minute renewable production peaks and valleys, thereby reducing the ramping of traditional energy sources. In future studies, this methodology could be expanded to other electrified transportation systems.

Although details on the case study are provided later, in a nutshell, Texas leads the country in wind power with 37.5% of Austin's electricity coming from a combination of wind plus solar, compared to a national average of 10.4% in the United States (Austin Energy, 2018b; REN21, 2018). In addition, Austin has plans to achieve at least 55% renewable energy generation by 2025 and 65% by 2027 (Austin Energy, 2017). One could conceptualize a partnership between the transit provider and the utility manager wherein the transit provider receives discounted electricity prices in exchange for responding to power requests from the utility manager. This proposed method is implemented in a case study of electrifying the Austin, Texas bus transit fleet, modeling this partnership between the utility and transit managers.

Chapter 9: Review of the Current State of BEBs

In the past decade, battery electric vehicles (BEVs) have made a splash in the personal vehicle market. Automobile companies like Tesla have generated a lot of buzz and have also advanced BEV technology significantly (Levy, 2019). The main barrier in purchasing electric vehicles for many consumers is the range anxiety that is associated with long recharging times. However, this has been an area of drastic improvement. Where BEVs previously took 8 – 12 hours to fully charge, Tesla BEVs now take around 50 minutes to fully charge at superchargers (Gent, 2019). Improvements on range, performance, and cost of BEVs are the focus of many companies right now, so while the technology is not currently on par with internal combustion engine (ICE) powered vehicles, the industry is improving rapidly.

With all of the buzz around the personal EV market, one may wonder if battery electric buses (BEBs) can follow suit. The electric bus market is expected to reach a market value of $71.9 billion by 2024, with the key players of BYD, CRRC, Alexander Dennis Limited, Solaris Bus and Coach, Zhengzhou Yutong, New Flyer, Volvo, and Proterra (Wood, 2019). This chapter looks at the current state of BEBs on the market and how they compare to alternatives such as diesel buses (DBs), hybrid electric buses (HEBs), and compressed natural gas (CNG) buses.

9.1 Discussion About BEBs and Other Bus Alternatives

9.1.1 Conventional Diesel Buses

DBs are the most common bus type in the U.S. and globally by a large margin. In 2012, DBs accounted for 89% of the global transit bus market of new bus purchases. However, it is projected that this market share will decrease steadily as more efficient vehicle technology improves in performance and affordability (Mohamed et al., 2016).

DBs are powered by diesel engines which are a type of ICE. Diesel engines work by compressing air in the cylinder using a piston until it gets very hot (often at least 500°C or 1,000°F), at which point a combination of diesel fuel and air is sprayed into the cylinder. Because the air is so hot, the fuel immediately ignites and explodes. This explosion pushes the piston back out of the cylinder, producing the power that is then used to drive the vehicle. This repeats hundreds or thousands of times per minute. Diesel engines are up to twice as efficient as gasoline engines, at around 40% efficiency. This is partially because diesel is more energy dense than

gasoline, but it is also because diesel engines compress more and operate at higher temperatures, and because they do not require a spark plug ignition system, allowing for a simpler, more efficient design (Woodford, 2019).

Pollution is one of the biggest drawbacks of diesel. Diesel engines produce a lot of unburned soot particles that are dirty and hazardous to human health and contribute substantially to climate change. Another major drawback to DBs is that they are extremely noisy (Woodford, 2019).

9.1.2 Compressed Natural Gas Buses

CNG buses make up a small but significant share of bus fleets across the world. In 2012, CNG and liquified natural gas (LNG) accounted for 5% of global transit bus new bus purchases, and this share is growing. CNG and LNG buses combined are projected to account for 13% of the new bus market share in 2020. CNG is cheaper than diesel fuel, and CNG buses are also less emitting than DBs (Mohamed et al., 2016).

Natural gas vehicles (NGVs) use the same basic principles as gasoline-powered vehicles. This means that the natural gas is mixed with air in the cylinder and then ignited using a spark plug to move the piston in the cylinder up and down. However, there are some fundamental differences between gasoline and natural gas in terms of flammability which require some modifications to make NGVs run efficiently. First, most NGVs operate using CNG so that the fuel takes up less space. These fuel storage tanks for CNG used to be bulky and heavy, but advances in lightweight materials in these cylinders have made CNG vehicles more appealing. Second, engines require an extra component between the storage cylinder and the engine called a regulator that reduces the pressure (CarsDirect, 2012; The Fuel Cells and Hydrogen Joint Undertaking, 2012).

The benefits of CNG are that it burns cleaner and reduces carbon monoxide emissions by 80% and produces 44% fewer hydrocarbons in its exhaust relative to traditional petrol and diesel. Also, in the case of a leak, CNG is non-toxic, so it does not present dangers to ground water contamination. Another benefit is the reduced fuel price—it is about 40% cheaper than diesel on a per-gallon basis. It is also safer because it is less flammable, and it damages your car less, leading to lower maintenance costs. Finally, NGVs tend to have better performance because of higher octane ratings (Ramdass, 2017). Disadvantages of NGVs or CNG buses include that the CNG tanks require a significant about of storage space and can add additional weight to the vehicle

compared to a diesel fuel tank. Other disadvantages include the higher purchase cost of CNG buses relative to DBs and limited CNG filling station availability (CNG United, n.d.).

9.1.3 Hybrid Electric Buses

An HEB is powered by an electric motor and a relatively smaller ICE compared to DB's ICEs. A major benefit of HEBs is that the battery powered electric motor allows the ICE to operate at optimal efficiency. Diesel is the most common fuel that powers HEBs' ICE. There are two different type of HEB systems: parallel HEBs and series HEBs. In a parallel HEB, the ICE and electric motor are connected to the transmission independently. In this setup, the electric motor is designed to provide the majority of the power in stop-and-go traffic and the ICE provides most of the power at highway speeds. In this setup, energy that is traditionally lost due to braking is captured and used to charge the battery through a process called regenerative braking. A series HEB is entirely powered by the electric motor, and the ICE is connected to an electric generator which converts the energy produced by the ICE into electric power. This same generator also recharges the battery which provides added power to the motor. With the ICE disconnected from the wheels, it can operate at an optimal rate and can even be switched off for periods. Parallel HEBs are more efficient than series HEBs at constant highway speeds and series HEBs are more efficient than parallel HEBs in stop-and-go driving (Ranganathan, n.d.).

HEB benefits include a reduction in emissions of up to 75% compared to conventional DBs, including an almost-90% reduction in PM which is the most harmful emission to human health. HEBs have comparable performance to other non-hybrid buses and many transit agencies report smoother acceleration due to the increased low-end torque capabilities of electric motors. Hybrid buses offer reduced maintenance and fueling costs due to an average increase in fuel efficiency of 37%. The most notable disadvantage of HEBs is their higher purchase cost (Ranganathan, n.d.).

9.1.4 Battery Electric Buses

BEBs use electricity stored in an onboard battery which powers an electric motor. This motor is then used to turn the wheels and power the vehicle. When the battery is depleted of charge, the batteries can be recharged using electricity from the grid. Nearly all BEBs use lithium ion batteries (Union of Concerned Scientists, 2018).

The major benefit of BEBs is that they operate with zero local emissions. This is great for city air quality (Weeberb et al., 2018). Other major benefits of BEBs include that minimal energy is wasted by turning the bus off when stopped, which is called "idle off", and that energy that is traditionally lost to heat during braking is captured and that energy is used to charge the battery. These two features are even more beneficial for buses as compared to passenger EVs because they stop often and for fairly extended periods of time. In addition, electric motors are simply fundamentally more energy efficient than gasoline or diesel engines. Finally, the driving experience in BEBs tends to be reported as smoother and more enjoyable because electric motors can provide nearly instant torque, allowing for increased low-end torque capabilities (Union of Concerned Scientists, 2018). This is a shared benefit with HEBs, when they are operating with the electric motor. Another benefit to BEBs pertinent to the analysis that will come in later chapters is that the onboard battery allows for V2G charging, which is another way to make up the delta in purchase cost between BEBs and DBs and can also be beneficial to the electricity grid manager. The most notable disadvantage of HEBs is their higher purchase cost, their relatively slow recharging times, and their limited ranges.

9.2 Cost Comparisons of Battery Electric Buses to Other Bus Alternatives

Bus purchases are the main capital investment cost for transit agencies. While DBs beat out other bus types when it comes to purchase cost, more efficient bus types have the opportunity to be competitive and minimize this initial cost discrepancy through their leaner and cheaper operating costs. In HEBs, this is accomplished through increased fuel economy, which improves from 25 – 52% relative to DBs (Ranganathan, n.d.). In BEBs, this is realized through lower electricity costs compared to diesel fuel costs (Union of Concerned Scientists, 2018). Additionally, costs can be reduced in more efficient bus types of HEBs and BEBs due to lowered maintenance costs. In HEBs, these lowered costs result from reduced stress and maintenance on mechanical components. In addition, there are simply fewer moving parts in electric drive chains in HEBs and BEBs which require less maintenance than a traditional transmission (Ranganathan, n.d.). This is a larger benefit for BEBs, which do not contain a traditional transmission at all, but it is also significant for HEBs because their transmissions run less often and tend to operate at their most efficient rate as well.

Table 21 below summarizes differences in purchase costs, fueling costs, and maintenance costs across the different bus types of DBs, CNG buses, HEBs, and BEBs. Note that a majority of the operating costs of transit agencies is made up of employee wages and benefits. In fact, these employee costs make up almost 40% of the total operating cost for transit agencies (University of Wisconsin-Milwaukee, 2006). However, it is assumed these costs do not vary by bus type, so those personnel costs are not considered.

Table 21: Cost Comparisons of Different Bus Types

Bus Type	Bus Purchase Cost	Bus Fueling Cost	Bus Maintenance Cost
DB	$290,000	$1.22/mi* (2.5 mpg)	$0.46/mi
CNG Bus	$319,000	$1.30/mi* (1.70 mpg)	$0.46/mi
HEB	$500,000	$0.96/mi* (3.17 mpg)	$0.44/mi
BEB	$600,000†	$0.23/mi† (1.24 kWh/mi)	$0.23/mi†

*Based on a diesel fuel price of $3.04/gallon and a CNG fuel price of $2.21/gallon
†Average of three major BEBs on the market: Proterra Catalyst 500 kW, New Flyer XE40 250 kW, and BYD 40-Electric 80 kW
Sources for this table: Mohamed et al., 2016; Ranganathan, n.d.; New Flyer-XE40, 2015; BYD-40E, 2014; Proterra-E40, 2015; U.S. Department of Energy, 2019.

9.3 Emissions Comparisons of Battery Electric Buses to Other Bus Alternatives

One of the major touted benefits of BEBs is their environmental benefit. However, it is important to realize that just because the bus does not emit GHGs directly does not mean that they can be considered to operate carbon-free. One must look to the carbon-intensity of the grid to understand the GHG implications. For this reason, a well-to-wheel (WTW) approach is taken to compare the GHG emissions across bus types. This WTW assessment considers GHG emissions in two stages: (1) well-to-tank (WTT) and (2) tank-to-wheel (TTW) (Environmental Protection Agency, 2017).

WTT measures the GHG emissions during the energy production and distribution processes. For DBs, CNG buses, and HEBs, this involves the production and transport of the fuel that the buses receive at the gas station. In the case of BEBs, the GHG emissions are dependent on

the mix of energy types that are used to power the electricity grid from which the BEBs get their power. This, of course, varies significantly based on the electricity mix—when there is mainly coal plants that power the grid, these emissions are high; when there is mainly nuclear plants and solar and wind farms that power the grid, these emissions are very low. Because of this, three electricity mixes are considered in Table 22 below. The table lists GHG emissions for an average United States mix of energy source production, an average European Union (EU) mix of energy sources, and a best-case all-renewable energy source production. The WTT GHG emissions vary drastically depending on this energy mix (Environmental Protection Agency, 2017; Mohamed et al., 2016). Note that all emissions in Table 22 are converted to CO_2 equivalent-emissions (CO_2e) so that one number can be compared across all bus types.

In looking at WTT GHG emissions, BEBs do not seem like a very good option from an emissions perspective. However, WTT emissions do not tell the whole story. TTW emissions are important to consider as these are the local emissions that are produced by the bus type. This is the emission-type where BEBs shine—BEBs produce no local emissions, providing a major benefit to the air quality of the city in which they provide service. DBs, CNG buses, and HEBs all have quite high TTW GHG emissions, though HEBs are about 20% lower than the other two bus types. See Table 22 below for these details.

WTW GHG emissions for each bus type are the sum of that bus type's WTT and TTW GHG emissions. Table 22 shows that DBs perform the worst when all GHG emissions are considered, and CNG buses are only slightly better. When BEBs are charged using the average U.S. mix of energy sources, HEBs are actually more positive from a GHG emissions perspective than BEBs. However, BEBs have an opportunity to reduce GHG emissions dramatically as electricity grids become increasingly dependent on nuclear power and solar and wind energy. For example, with the average EU mix of energy sources to power the electricity grid, WTW GHG emissions are reduced by over 41%. Further, if a grid was fully powered by nuclear power and wind and solar energy, the WTW GHG emissions could be almost totally eliminated. This is a very positive result and a motivation for cities and transit agencies to begin transitioning to BEBs.

Table 22: GHG Emissions of Different Bus Types (Mohamed et al., 2016)

Bus Type	**WTT GHGs (CO_2e/mi)**	**TTW GHGs (CO_2e/mi)**	**WTW GHGs (CO_2e/mi)**	**Avg. % reduction of WTW GHGs compared to DB**
DB	218	1004	1222	N/A
CNG Bus	157	1014	1171	4.17%
HEB	180	833	1013	17.10%
BEB – US mix	1070	0	1070	12.44%
BEB – EU mix	720	0	720	41.08%
BEB – renew.	20	0	20	98.36%

9.4 Vehicle Performance Comparisons of Battery Electric Buses to Other Bus Alternatives

In this section, the vehicle performance is compared between BEBs and the alternatives of DBs, CNG buses, and HEBs. Table 23 compares the average performance of several BEBs on the market to an approximate average of DBs, CNG buses, and HEBs based on the literature. Table 23 shows that BEB ranges can be competitive with the other bus types, but many of them are much lower. This is all dependent on the capacity of the battery in the bus, and higher capacity batteries (which mean for higher ranges) are the largest driver of cost in BEBs. In looking at vehicle performance characteristics other than range, BEBs outperform other bus types. They have higher horsepower and acceleration rates, as can be seen in Table 23.

Table 23: Vehicle performance comparisons across bus types

Bus Type	Range (miles)	Horsepower (peak)	Horsepower (continuous)	Acceleration (from 0 to 20 mph/sec)	Acceleration (from 20 to 50 mph/sec)
DB, CNG bus, and HEB	> 300	200 – 380		2 – 2.5	1.25
BEB (average)	97 – 327	338 – 510	170 – 338	4	1.875 – 2.5

Sources for this table: Proterra, 2019a; Madison BRT Transit Corridor Study Proposed BRT Travel Time Estimation Approach; Legislative & Strategic Planning Committee (HART), 2017; The Fuel Cells and Hydrogen Joint Undertaking, 2012.

Table 24 below shows a few other BEB vehicle performance characteristics broken out by BEB battery capacity and charger power. This helps one understand how range and operating efficiency vary based on the battery capacity (220 – 660 kWh battery capacities are shown). It also indicates how fast different charging types (overhead and plug-in) are for these different battery capacities.

Table 24: Other vehicle performance characteristics of BEBs by battery capacity and charger power (Proterra, 2018a)

	220 kWh BEB	440 kWh BEB	660 kWh BEB
Operating efficiency	1.49-1.82	1.53-2.19	1.61-2.28
Operating range	97-118	161-230	232-328
Max plug-in charge rate at 200A	72	132	132
Max overhead charge rate	166	331	397
Overhead charging (miles replenished per 10 mins)	16	27	31
Overhead charging (hours to full charge)	2.7	2.7	2.8
Plug-in charging (time to full charge)	2.8	3.2	4.5

9.5 Final Notes on BEBs Compared to Other Bus Alternatives

This section compared BEBs on several aspects to other bus alternatives including DBs, CNG buses, and HEBs. From an initial purchase cost perspective, BEBs are hard to persuade. However, when you look at operational costs of fueling and maintenance, BEBs become much more attractive to transit agencies. They are cheaper to fuel because of the lowered electricity cost per unit energy as compared to diesel. In addition, they are cheaper from a maintenance cost perspective because of fewer moving parts.

BEBs also offer additional features that make them more attractive than traditional DBs or CNG buses. They are very operationally efficient due to features including "idle off" and "regenerative braking" which both minimize wasted energy. Another positive feature of BEBs (and HEBs to a lesser extend) is that electric motors have increased low-end torque capabilities, offering a more pleasant ride due to smoother acceleration from stops, improving passenger comfort.

Another major benefit of BEBs is that they operate with zero local emissions, which is great for city air quality. However, one needs to consider the carbon-intensity of the grid from which the BEBs get their electricity to charge when considering the total emissions produced. Emissions of BEBs in nearly any city will be significantly more positive than DBs and CNG buses, even if the grid relies very heavily on coal. However, depending on the energy source mix that powers the grid, HEBs can be more positive than BEBs from an emissions perspective. This is not the case in Austin, Texas though, as 37.5% of Austin's energy generation by fuel type comes from a combination of solar and wind energy and 23% comes from nuclear energy as of 2018 (Austin Energy, 2018b). This is much higher than the U.S. national average of 10.4% from solar and wind energy and 20% from nuclear (REN21, 2018). In addition, Austin has plans to achieve at least 55% renewable energy generation by 2025 and 65% by 2027, so BEBs will only become a much more positive option over the years from an emissions perspective.

From a vehicle performance perspective, BEBs can be competitive or they can even outperform other bus types, but it's mostly dependent on the capacity of the battery in the BEB. Higher capacities mean longer ranges, but they increase the cost of the BEB dramatically. Other vehicle performance characteristics such as horsepower and acceleration tend to outperform other bus types regardless of the battery capacity. Finally, one major deterrence in switching to BEBs from other bus types is their charge times. The best on the market perform quite well, replenishing

over 30 miles in ten minutes of overhead charging, but these overhead “flash” chargers are expensive to install, and this still does not compare to bus types that refuel their full range as a gas station in less than ten minutes.

At this point, BEBs make sense for shorter routes that operate at slow speeds and stop and go often. Under this route profile long-range BEBs could likely operate all day without charging. Shorter-range BEBs could also be good candidates for these route profiles if there is a charging station on-route. For longer routes, HEBs may make the most sense from a cost and operational perspective, particularly in regions that depend heavily on coal and natural gas to power their electricity grid. However, with on-route charging, BEBs are good candidates for these longer routes as well. DBs and CNG buses perform the worst across all perspectives.

Chapter 10: Literature Review for Part Two[2]

Now that background has been provided on BEBs and how they compare and contrast to other bus alternatives, this next chapter performs a literature review on studies that have looked at the relationship between electrified transportation and the electricity grid. There have been several major studies of note on the topic of electric fleet (bus or otherwise) operations and their interactions with the grid. One such study useful to the present work was a review of alternative powertrains for electric buses by Mohamed, Garnett, Ferguson, and Kanaroglou (2016). This study provides an expansive review of different electric buses types and their prospective for replacing traditional diesel-powered buses. They compared diesel buses to five major electric bus alternatives: hybrid electric buses (HEBs) in parallel and series configuration, fuel cell electric buses (FCEBs), opportunity BEBs (charge on route using flash charging), and overnight-charging BEBs. It compared each electric bus alternative to diesel buses with respect to the following: economic aspects such as capital and operational costs; operational aspects including range and charging time; environmental aspects such as GHG emissions; and energy aspects including energy consumption and efficiency. Given these range of considerations, the study finds that overnight BEBs are the best option for bus transit but notes that this result is context sensitive; in particular, the grid energy profile has a significant impact on which technology is optimal. For example, BEBs perform better in regions that have a large renewable-based energy profile, whereas FCEBs may be optimal for regions with dirtier, less renewable energy profiles (Mohamed et al., 2016).

García-Olivares et al. (2018), study what transportation systems would look like in a 100% renewable economy. For many reasons, including that electric motors are more efficient than fuel cell motors, as well as the fact that hydrogen energy produced from wind power is relatively expensive, these authors also propose BEBs over FCEBs or hydrogen-powered vehicles. They also note that BEBs in their current state have comparable carrying capacity and ranges to traditional gasoline-powered buses, making the transition easier. The charging infrastructure is the main missing piece, and this would be fairly easy to build out for the transit application (Garcia-Olivares et al., 2018).

[2] This chapter is adopted from a publication submission that is under review for publication in the *Sustainable and Renewable Energy Reviews* with co-authors Joseph Griffin, Dr. Kara Kockelman, and Dr. Moataz Mohamed.

A study from the University of Virginia built a framework for shared autonomous electric vehicle (SAEV) smart-charging (SC), aimed at reducing electricity costs (Chen & Zhang, 2019). They simulated an SAEV fleet, comparing an unmanaged, charge-as-needed, BAU scenario and to an SC scenario, both under a two-tier time-of-use electricity pricing structure. They found that unmanaged charging peaks occur between 6 and 8 pm, aligned with the end of the evening travel demand peak. This timing occurs at the same time as an increase in residential electricity demand. When fleets were managed to maximize off-peak charging, they found that SAEVs could reduce average electricity costs by 11.5% in short-range EVs and 32.8% in long-range EVs. As expected, long-range EVs are able to be more flexible and responsive to SC incentives. They found that short-range EVs often used up their battery capacity during the peak travel hours, forcing them to either charge during the peak hours or pull themselves out of commission until they can charge during off-peak hours (Chen & Zhang, 2019).

Foley et al. (2013) looked at the effect of EVs on the operation of the wholesale electricity market in Ireland. They simulated the electricity market, and emissions impacts were also analyzed under a single generation portfolio for peak (charging immediately after work) and off-peak (charging later in the night) charging scenarios. A baseline scenario was also run without any EV loads. They found that the key factor in determining emissions results was the generation portfolio, as many other studies have found. Regions with high penetration of coal power generation show the highest increase in emissions relative to the baseline scenario, although the off-peak charging scenario had reduced cycling compared to the peak charging scenario. In contrast, areas with high renewable generation showed positive emission results, particularly when EV charging occurred in the off-peak. They concluded that EV off-peak charging is for grid operational efficiency, due to night-time valley filling and better wind power usage in the off-peak, when wind is strongest (Foley et al., 2013).

Cheng, Wang, Ding, and He (2019) propose an integrated resource planning model that optimizes investment and operations of a BEB system. In one case study, they found that aggregating charging station locations reduced the total cost of the public transportation system by 17% compared to having one charging station per route. This is mainly due to construction cost, which is reduced by 51%. Additionally, operation cost decreased by 0.4% (Cheng et al., 2019). Their case study only had five routes, so in a larger bus system with more aggregation, we would expect this cost to be reduced further.

Mwasilu et al. (2014) reviewed V2G applications with renewable integration. They raised concerns with personal EVs being a useful V2G application because many people charge at home, and this decentralized method would be challenging for power distribution systems (Mwasilu et al., 2014). However, if the integration is planned and organized carefully, mainly in public charging stations, there is the potential to add large value in terms of grid performance and efficiency. BEBs have more potential in this manner because one can define relatively few charging locations and BEBs have more energy capacity. However, the challenge with BEBs is that they are more heavily utilized than a personal vehicle, which sits idle 95% of the time, so they are less flexible in charge times (Barter, 2019).

Mwasilu et al (2014), also point to the importance of SC schemes when it comes to V2G applications. Uncontrolled EV charging has detrimental impacts, mainly through increased energy demand during peak energy usage periods, which can lead to overloading the power system, meaning a less efficient electricity supply. This must be avoided as EV presence scales up. This is particularly important as RESs of wind and solar also increasingly power our electric systems, because of their less predictable, intermittent supply of energy. renewable integration requires energy storage systems (ESSs) to absorb or supply electricity when there is excess or low energy generation. SC EVs provide the opportunity to avoid a high-cost investment in dedicated ESSs as they can act as ESSs when they are parked (Mwasilu et al., 2014).

A study out of Utah State University looks at demand charges of BEBs and its impact on the transit system cost. Electricity bills are based on the peak power demand during a billing period, referred to as the demand charge. These results show that demand charges account for a significant portion of the total cost of a BEB system, so this must be considered when planning and designing these system (He et al., 2019).

A final important study for this study is the simulation of BEBs in Belleville, Ontario, Canada. This study looks at the operational feasibility and grid impacts of electrifying a bus fleet to determine the best application of BEBs. There are two simulation models at play in this study. First there is a BEB simulation model which calculates energy consumption for each route, and then bus, and assigns a charging priority based on this. Simultaneously, it models the charging stations and minimizes the number of chargers for each scenario. Then, a real-time simulation of the BEB system is run. Thus, this model creates a load profile for the operation of the BEB system for each scenario. This information is fed in to the second simulation model, the grid impact model,

where impacts of BEB charging on the grid is analyzed. This study found that, for this case study in Canada, overnight BEBs were more feasible than flash-charged or opportunity on-route BEBs because of the latter's major impact on the grid (Mohamed et al., 2017).

This literature review provided a thorough background that aided in this study's methodology development and case study design. This research focuses on BEBs instead of FCEBs or HEBs based on the findings from Mohamed et al. (2016) Garcia-Olivares et al. (2018), and Foley et al. (2013), which reported that BEBs were the optimal fuel source for electrifying bus transit, especially for grids with high renewable penetration. This study compares diesel, non-SC, and SC scenarios because of the findings from Chen and Zhang (2019) and Mwasilu et al. (2014) and it aggregates charging stations such that transit lines share as few stations as possible, based on cost results from Cheng et al. (2019) and Mwasilu et al. (2014). In addition, there is a possibility of high demand charges that could make fueling BEBs prohibitively expensive. The findings in He et al. (2019) highlight the need to reduce electricity costs and avoid peak charge for transit managers, thereby avoiding peak demand for utility managers. Finally, this study builds off of the work from Mohamed et al. (2017) in part, using the same BEB energy equations to determine the consumed energy per trip length for the Austin bus transit routes, and using a similar model framework.

Chapter 11: Utility-Transit Manager Model Framework[3]

This section describes the methods and the methodological framework, with two main models developed. The first is a utility manager model, which simulates the combination of energy sources under different energy demands. The overarching goal of the utility manager model is to minimize the operational cost of delivering the required power. The second model is a BEB simulation, which models the energy status of the BEB system over the course of the day, including energy consumption and charging. The overarching goal of the BEB model is to smooth the generation of the utility's traditional energy sources of coal, natural gas, and nuclear. See Figure 19 for a flow chart of the integration of the two models.

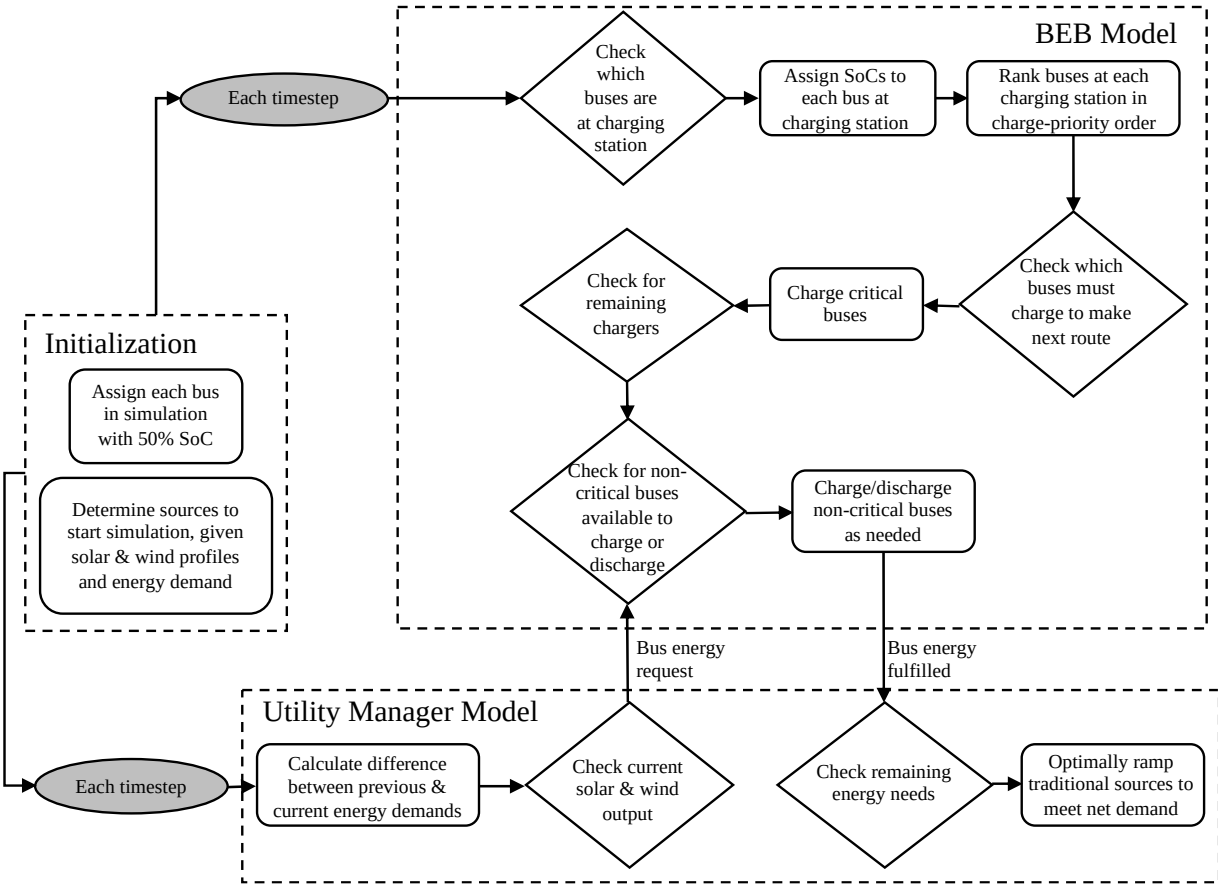

Figure 19: Flowchart of Developed V2G Smart-Charging Simulation Model

[3] This chapter is adopted from a publication submission that is under review for publication in the *Sustainable and Renewable Energy Reviews* with co-authors Joseph Griffin, Dr. Kara Kockelman, and Dr. Moataz Mohamed.

11.1 Utility Manager Simulation Model

This model uses Gurobi optimization (Gurobi Optimization, Inc., 2019) to simulate the energy sources used to meet the demands of the model region. It assumes that the utility manager's sole aim is to minimize cost to meet such energy demands, meaning that GHG emissions or other potential motivations are not considered in this decision-making. The inputs to this model are the energy sources available to the utility manager, and each of those sources' energy type, maximum capacity, minimum running load, variable operating and maintenance (O&M) cost, ramp rate, ramping cost, and startup cost. For the model region, the available energy sources and their maximum capacities are publicly available (Austin Energy, 2018b). These sources consist of coal, simple cycle natural gas (SCNG), combined cycle natural gas (CCNG), steam-powered natural gas, and nuclear plants, as well as wind and solar installations. Operational information for each energy type is shown in Table 25 below.

With the different energy sources as inputs, at each timestep the model reads in solar and wind generation, as well as energy demands from the BEB charging and non-BEB energy demands (Austin Energy, 2018a; Sargent, 2018). The model assumes that energy sources are always available to run up to the maximum specified capacity, with ramp rates constraining their rates.

Table 25: Operational Information of Different Energy Sources (U.S. Energy Information Administration, 2016; Van den Bergh & Delarue, 2015)

Energy Source Type	***Variable O&M Cost ($/MWh)***	***Minimum Load (% maximum capacity/min)***	***Ramp Rate (% maximum capacity/min)***	***Ramping Cost ($/ΔMW)***	***Startup Cost ($/ΔMW)***
Coal (steam)	4.33	32.5	2.330	2.227	98.960
SC Natural Gas	4.93	35	12.92	0.9896	52.449
CC Natural Gas	4.93	40	5.415	0.6185	55.665
Natural Gas (steam)	4.93	40	3.415	1.732	90.301
Nuclear	2.30	45	2.625	0	43.295
Wind	0	0	100	0	0
Solar	0	0	100	0	0

The timestep used in this study is one minute and the total model run time is 24 hours. At each timestep, the utility manager determines how much energy is required and the means to provide the energy. As is shown in Eq. (1), at each timestep *t* the sum of the power production $P_{i,t}$ (MW) of each energy source *i* that is currently on must be between 100% and 105% of the total power required from bus and non-bus related loads, D_t (MW). This upper buffer in energy production ensures grid reliability and reduces the rigidity of the optimization solution. $O_{i,t}$ is a binary indicator of energy source *i* being on ($O_{i,t} = 1$) or off ($O_{i,t} = 0$).

$$D_t \leq \sum_i P_{i,t} * O_{i,t} \leq 1.05 * D_t \quad (1)$$

To determine how to fulfill the power required in each timestep, the utility manager uses the objective function in Eq. (2) subject to constraints in Eq. (1) and (3), where C_i is the variable O&M cost of source *i* ($/MWmin), RC_i is the ramping cost ($/ΔMW) and SC_i is the startup cost ($/ΔMW), each of energy source *i*.

$$Minimize\{\sum_i(O_{i,t}C_iP_{i,t} + max\,(0, P_{i,t} - P_{i,t-1}) * RC_i + max(0, O_{i,t} - O_{i,t-1}) * Q_{i,min} * SC_i)\} \quad (2)$$

$$L_{i,min} \leq P_{i,t} \leq L_{i,max} \text{ for all } i \text{ with } O_{i,t} = 1 \quad (3)$$

$L_{i,max}$ and $L_{i,min}$ are the maximum and minimum power (MW) that energy source *i* is capable of producing at the current timestep, constrained by ramp rates and maximum and minimum capacities (Eq. (4) – (7)).

$$L_{i,min} = P_{i,t-1} - R_i \quad (4)$$

$$L_{i,min} \geq Q_{i,min} \quad (5)$$

$$L_{i,max} = P_{i,t-1} + R_i \quad (6)$$

$$L_{i,max} \leq Q_{i,max} \quad (7)$$

where R_i is the maximum change in power (MW) in one minute, $Q_{i,min}$ is the minimum power capacity (MW), and $Q_{i,max}$ is the maximum power capacity (MW), each of energy source *i*. If an energy source was off ($O_{i,t} = 0$) in the previous timestep, then it can produce $Q_{i,min}$ power in the current timestep. Additionally, an energy source can turn off if $L_{i,min} = Q_{i,min}$.

Note that to initialize the model (when $t = 0$), the utility manager does not consider ramp rates or startup costs; it just runs the energy sources with the lowest variable O&M cost to reach

the required production levels at the model start time. This effectively means that, during initialization, constraints in Eq. (4) and (6) are not considered and $RC_i = SC_i = 0$.

Each timestep, the model issues a power request to the bus manager. The goal of this power request is to use BEB charging to buffer sharp changes in renewable production, allowing for smoother generation from traditional energy sources, thereby reducing the utility manager's costs. To develop the power request, the model first uses Eq. (8), which defines G_t, the total renewable generation, as the sum of W_t and S_t, the wind and solar production, all at time *t* in MW.

$$G_t = W_t + S_t \tag{8}$$

The power request, $R_{buses,t}$, is then given in Eq. (9), where $\bar{B}$ is the average bus energy consumption given by Eq. (10) and $\widetilde{G_t}$ is the filtered G_t using a low-pass filter given by Eq. (11), each in MW, where $f = 0.52$ is the filter factor used. This filter factor was optimized to minimize the cost to the utility manager. $\widetilde{G_t}$ is initialized as G_t at $t = 0$, and is updated by Eq. (11) in each subsequent timestep.

$$R_{buses,t} = \bar{B} + G_t - \widetilde{G_t} \tag{9}$$

$$\bar{B} = \frac{1}{t_f - t_i} * \frac{1\,MWh}{1000\,kWh} * \sum_b d_b * c_b \tag{10}$$

$$\widetilde{G_t} = f * \widetilde{G_{t-1}} + (1 - f) * G_t \tag{11}$$

where t_f is the final model timestep, t_i is the initial model timestep, d_b is the total distance traveled by bus b over the course of the day (miles), and c_b is the consumption rate of bus b (kWh/mile).

11.2 BEB Simulation Model

This model simulates the BEB system over the course of the day. It should be noted that simplifications were made at the bus level in order to focus at the system-level on the broader research question: can a large-scale BEB system help support an electricity grid, particularly one that relies significantly on RESs of solar and wind? To do this, an average value of BEB energy consumption per-mile was extracted from the literature based on bus weights and battery compositions, averaged for different terrain types. Charge rates were also averaged and assumed to be constant, regardless of BEB state of charge (SoC). This study did not directly optimize bus routing and charging station locations; these parameters were considered exogenously.

In this respect, three bus types are considered in the analysis. The SoC of all buses are constrained to 10% and 90% lower and upper boundaries respectively to preserve the battery's long-term health, as shown in Eq. (12). There is one charge opportunity defined per route. If the distance between charge opportunities is less than 18 miles, an 80-kWh battery capacity is used, with a consumption rate of 1.69 kWh/mile and a charge rate of 4.17 kWh/min, based on the Proterra Catalyst BEB model. If the distance between charge opportunities is 18 to 37 miles, a 200-kWh battery capacity is used, with a consumption rate of 2.16 kWh/mile and a charge rate of 4.17 kWh/min, based on the New Flyer XE40. Finally, if the distance between charge opportunities is greater than 37 miles, a battery capacity of 324 kWh is used, with a consumption rate of 2.14 kWh/mile and a charge rate of 3.33 kWh/min, based on the BYD 40-Electric. This selection ensures that fully charged (90% SoC) buses can skip a charge opportunity and still complete their routes. These consumption rates are based on an Altoona Bus Research and Testing Centre report that used an average of different driving cycle types (BYD-40E, 2014; New Flyer-XE40, 2015; Proterra-E40, 2015).

$$0.1 \leq S_{b,t} \leq 0.9 \quad \textit{for all } t \tag{12}$$

Each timestep, the bus manager determines the SoC of each bus in the system and defines which buses are able to charge. If the bus was charging during the previous timestep, the SoC increases by the charge rate r_b (kWh/min), as shown in Eq. (13). If the bus was running during that timestep, then the SoC decreases as a function of the consumption rate c_b (kWh/mile) and the average speed traveled during that timestep $v_{b,t}$ (miles/hour), as in Eq. (14). $S_{b,t}$ is the SoC at time *t* (between 0 and 1).

$$S_{b,t} = r_b * (1\ min) \tag{13}$$

$$S_{b,t} = c_b * v_{b,t} * \frac{1\ hr}{60\ mins} \tag{14}$$

Of the buses at charge opportunities at each timestep, the manager compiles a normalized priority list to determine the order in which buses should be charged. This list is ordered based on Eq. (15), where a higher value of $p_{b,t}$ (unitless) equates to a higher charging priority for bus *b* at time *t*. $E_{b,t}$ is the energy needed by bus *b* for the next route at time *t* (kWh), $T_{b,t}$ is the time until bus *b* must leave the charger at time *t* (minutes). Note that the first minute after the bus arrives and the last minute before the bus departs are not considered to be time available to charge, to account for the time it takes to plug in a charger. There are separate priority lists for each charging station

and for each charger type. The 80-kWh buses are constrained to charge at EVA080K chargers and the 200- and 324-kWh buses must charge at SAE J3105 chargers, based on bus model specifications.

$$p_{b,t} = \frac{E_{b,t}}{T_{b,t} r_b} \quad (15)$$

When $p_{b,t} = 1$, the bus is deemed in the critical charging category, and must charge during that timestep and all timesteps $T_{b,t}$ until the bus must leave the charger to make its route. Once buses are assigned chargers, they are removed from the priority list for that timestep. After all critical buses are assigned a charger, the bus manager looks at the power request from the utility manager in Eq. (16) to understand what to do next, where $z_{b,t}$ is a binary indicator of bus *b* charging (1) or not (0) at time *t*.

$$X_{buses,t} = R_{buses,t} - \sum_b z_{b,t} r_b \quad (16)$$

If $X_{buses,t}$ is positive, the bus manager aims to charge more than just the critical buses. In this case the bus manager looks at the top of the priority list and assigns that bus to a charger if there is a charger available at that bus's charging station and it would not violate the constraint in Eq. (12). If this is the case, Eq. (16) is updated and that bus is removed from the priority list for that timestep. If there is no charger available at that charging station, then the bus does not charge but it is still removed from the priority list for that timestep. The bus manager continues down the list so long as $X_{buses,t}$ is positive, there are still chargers available, and there are still buses that qualify to charge. If any of these are not true, this portion of the model terminates, and the achieved power for that timestep is sent to the utility manager.

In contrast, if $X_{buses,t}$ is negative after all critical buses are assigned a charger, the bus manager attempts to discharge some buses. The bus manager starts at the bottom of the priority list and assigns that bus to discharge if there is a charger available at that bus's charging station and if the bus will still have enough energy for its next route after it discharges at rate $-r_b$ for that timestep. If both of these are true and Eq. (12) will not be violated, Eq. (16) is updated and that bus is removed from the priority list at that timestep. If those conditions to discharge are not true, that bus does not discharge, and it is removed from the priority list for that timestep. The bus manager continues up the list so long as $X_{buses,t}$ is negative, there are still chargers available, and

there are still buses that qualify to discharge. If any of these are not true, this portion of the model terminates, and the achieved power is sent to the utility manager.

11.3 Cost Analysis

A cost analysis is completed for each model run. Bus capital and operating costs, utility operating costs, and GHG external costs are considered. Utility operating costs are detailed in Table 25 on page 80. The bus-related assumptions and costs are based on four different buses currently on the market: a standard 40 diesel bus, the 324-kWh Proterra Catalyst, the 200-kWh NewFlyer XE40, and the 80-kWh BYD 40-Electric. For GHG external costs, many estimates exist. These estimates are challenging due to many factors of uncertainty. Averages of several estimates are used in this analysis. Nuclear, wind, and solar are assumed to produce zero emissions. See Table 26 below for more details.

Table 26: Cost Assumptions for Scenario Cost Analysis

Bus capital and infrastructure costs (USD)	
Cost of new diesel bus ($/bus)	$280,000
Cost of new 80-kWh BEB bus ($/bus)	$491,000
Cost of new 200-kWh BEB bus ($/bus)	$553,000
Cost of new 324-kWh BEB bus ($/bus)	$700,000
Cost of 80-kWh BEB charger ($/charger outlet)	0*
Cost of 200-kWh BEB charger ($/charger outlet)	$250,000
Cost of 324-kWh BEB charger ($/charger outlet)	$250,000
Bus operating assumptions and costs	
Diesel bus fuel mileage (MPG)	4.2
80-kWh BEB energy consumption (kWh/mile)	1.69
200-kWh BEB energy consumption (kWh/mile)	2.16
324-kWh BEB energy consumption (kWh/mile)	2.14
Diesel fuel cost ($/gallon)	$2.50
Electricity cost ($/kWh)2	$0.06**
Diesel bus operating cost ($/mile)	$0.48
80-kWh BEB operating cost ($/mile)	$0.10
200-kWh BEB operating cost ($/mile)	$0.13
324-kWh BEB operating cost ($/mile)	$0.13
GHG emission assumptions and costs	
Diesel CO2 emissions (lbs/mile)	3.85
Diesel NOX emissions (lbs/mile)	4.84×10-4
Diesel SO2 emissions (lbs/mile)	2.38×10-4
Diesel PM emissions (lbs/mile)	1.10×10-3
Coal power plant CO2 emissions (lbs/kWh)	0.703
Coal power plant NOX emissions (lbs/kWh)	2.05×10-4
Coal power plant SO2 emissions (lbs/kWh)	3.41×10-4
Coal power plant PM emissions (lbs/kWh)	1.40×10-4
Natural gas (CC) power plant CO2 emissions (lbs/kWh)	0.399
Natural gas (CC) power plant NOX emissions (lbs/kWh)	2.56×10-5
Natural gas (CC) power plant SO2 emissions (lbs/kWh)	3.41×10-6
Natural gas (CC) power plant PM emissions (lbs/kWh)	1.92×10-7
Natural gas (SC) power plant CO2 emissions (lbs/kWh)	0.399
Natural gas (SC) power plant NOX emissions (lbs/kWh)	1.02×10-4
Natural gas (SC) power plant SO2 emissions (lbs/kWh)	3.41×10-6
Natural gas (SC) power plant PM emissions (lbs/kWh)	5.52×10-7
Total cost of CO2 ($/lb)	$0.06
Total cost of NOX ($/lb)	$1.40
Total cost of SO2 ($/lb)	$1.00
Total cost of PM (< 10 μm) ($/lb)	$2.15

*One charger is provided with each BYD 40-Electric bus, included in the cost of the bus.

**Assuming Austin's industrial-rated electricity cost.

Sources for this table: Austin Energy, 2018b; Biswas et al., 2009; BYD, 2015; Carpenter, 2019; Congress, 2014; Institute for Energy Research, 2009; Kane, 2016; Matthews et al., 2001; Mitchell, 2017; Muncrief, 2016; Proterra, 2016; Proterra, 2017; Proterra, 2018a; Proterra, 2018b; Proterra, 2019b; Reuters, 2010; U.S. Energy Information Administration, 2016; Van den Bergh & Botzen, 2015; Yasar et al., 2013.

Chapter 12: BEB Case Study[4]

12.1 Input Data

The Austin, Texas region is used to test the methodology outlined in the previous section. Austin, Texas is an advantageous location for this case study as Austin rarely gets below freezing, and EV ranges can decrease by up to 50% on the coldest days of the year in the Northern United States (Yuksel & Michalek, 2015). The Austin bus fleet currently consists of 423 buses. There are eighty-one bus routes of varying lengths operating over 88,000 bus-miles per day. General Transit Feed Specification (GTFS) data was used to define route schedules used as input to the BEB Simulation model (CapMetro, 2019). Thirteen charging station locations were defined across the Austin region and each bus route has one charging location defined on its route. See Figure 20 below for the location of these charging stations.

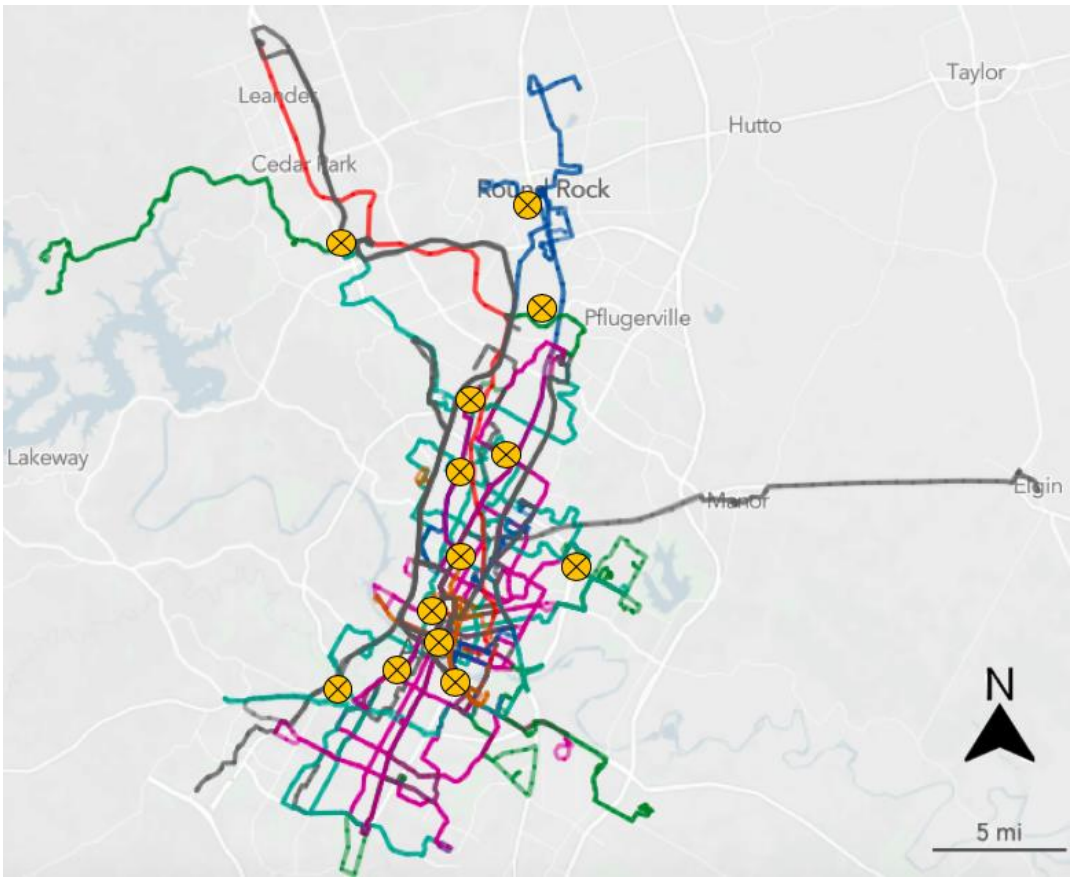

Figure 20: Austin Bus Transit Routes Map with Charging Stations Labeled in Yellow (Remix, 2019)

[4] This chapter is adopted from a publication submission that is under review for publication in the *Sustainable and Renewable Energy Reviews* with co-authors Joseph Griffin, Dr. Kara Kockelman, and Dr. Moataz Mohamed.

In addition to solar and wind power purchases, Austin's electricity comes from two coal plants each with capacities of 285 MW, two nuclear plants with capacities of 200 MW, and fourteen natural gas plants of varying capacities between 48 and 435 MW. The capacity factor of Austin's nuclear plants is 100.12% on average, and it is 78.00% for coal and 16.57% for natural gas (Austin Energy, 2018b). It is clear that Austin runs its coal and nuclear plants much more constantly than its natural gas plants, which might be attributed to the operational costs of each, shown in Table 25. Each plant's capacity rating is read in at the beginning of the model run and is matched with ramp rates and operational costs from Table 25 based on their fuel source.

One example of a solar and wind energy profile is tested in this case study. A standard idealized solar profile was approximated, centered at 2 pm, where it reaches its maximum capacity, and going to zero at sunset and sunrise. Real wind data from the Electricity Reliability Council of Texas (ERCOT) region was used, scaled to match Austin's capacity (ERCOT, 2019). The most frequent ERCOT data available was 5-minute data, so interpolation was used to get down to the 1-minute scale. Often times, wind production valleys align with solar production peaks, as happens in this example. It is an ideal situation from the utility manager's perspective because it means less ramping of traditional energy sources of coal and natural gas, which is costly and emitting. It is possible that wind and solar peaking can occur more simultaneously, which has the possibility of major traditional ramping implications, so this case should be tested in the future.

Finally, a simplified non-BEB energy consumption profile was assumed based on average daily energy consumption in the city of Austin in 2018, fit to a standard energy consumption model (Austin Energy, 2018a; Sargent, 2018). This was assumed to be the base energy demand, with additional loads coming from BEB charging. Note that the selected solar and wind production profiles made up 39.1% of the required energy needed for the non-bus consumption. This is close to the average of 37.5% mentioned previously, and thus these profiles were deemed reasonable for a typical day in Austin. See Figure 21 below for these consumption and production profiles.

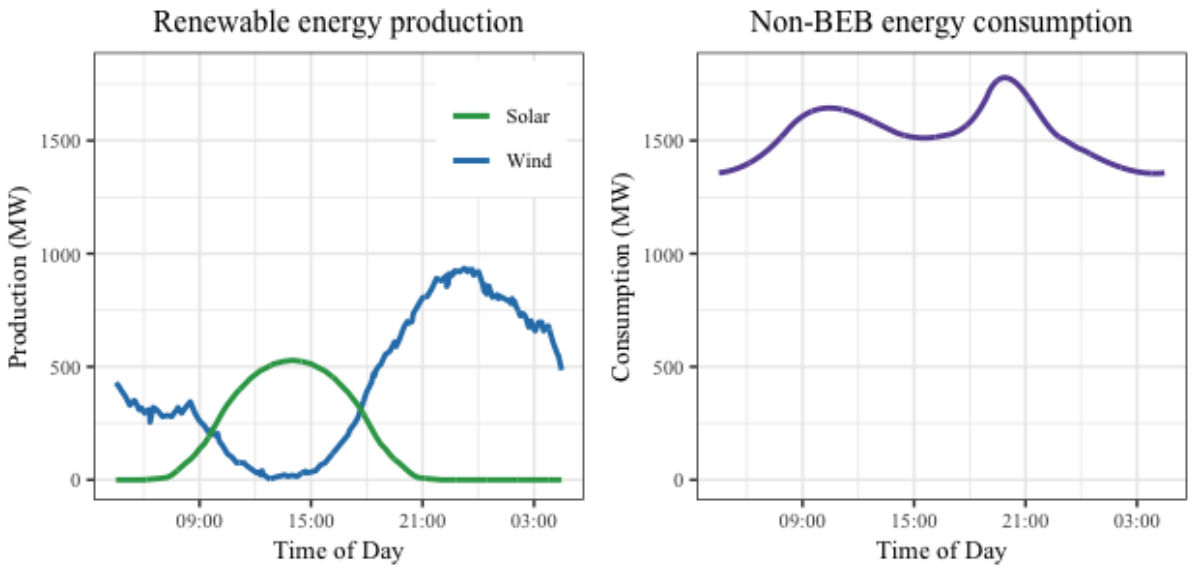

Figure 21: Solar and Wind Production and Non-Bus Electricity Consumption Tested

12.2 Scenario Definition

Three scenarios are considered in this study. In each scenario, bus routes run the same schedule and the same non-BEB energy demand/consumption is used. The first scenario is meant to reflect the current state in Austin where all buses are diesel. The second scenario is a non-SC BEB scenario, where the bus manager does not receive feedback from the utility manager. At each timestep in the non-SC scenario, buses at charging stations with the highest charge priorities are assigned to chargers (Eq. (12)-(15)). Finally, the third scenario is a smart-charging BEB scenario. This scenario charges based on Eq. (12)-(16), where buses aim to match power requests made by the utility manager at each timestep.

For both BEB scenarios, the number of chargers was not optimized, but several iterations were tested to determine the minimum number of chargers at each location where buses could always make their routes. In addition, bus chargers come in pairs, so an even number of chargers was required at each location. Also, because the 80-kWh buses include a charger with their purchase, those chargers did not need to be minimized.

Buses are assumed to last twelve years. We assume that there is the same number of inactive buses in the fleet in the diesel and BEB cases, though there are more active buses in the BEB scenarios because of additional time needed to charge. This inactive bus assumption is likely conservative because there is significantly less maintenance needed on BEBs than diesel buses

(due to fewer moving parts in EVs). The lifetime of charging stations is generally listed as thirty years. However, because this is a new technology, they are likely to be obsolete before then. Therefore, we assume that the lifetime of chargers is twelve years to accommodate the expected technological advancements in that time. We also assume that the bus manager would not be motivated to run the SC scenario, which helps the utility manager, unless they were given a discount on electricity costs. We assumed they were given a 50% discount on electricity in the SC scenario. This seems like a steep discount, but the Results section will show that this discount more than pays for itself from the utility manager's perspective.

Chapter 13: V2G Smart-Charging Battery Electric Bus Results[5]

A comparative analysis is performed for all scenarios based on cost and GHG emissions, shown in Table 27 below. Annual cost to the bus manager includes bus purchase, fueling, and infrastructure cost. Annual variable cost to the utility manager includes their variable O&M, startup, and ramping costs. It assumes each day is like the day detailed in Figure 21 which is a limitation, though the renewable production is representative of an average day in Austin. In the SC scenario, the bus electricity discount is included in the utility manager's cost.

The cost of purchasing a diesel bus is $280,000, and the total daily diesel fueling cost is $52,699. This results in an annualized cost of approximately $29.1M for the bus manager in this scenario. The total daily energy production in the diesel bus scenario is 36,760 MWh, with roughly equal amounts of energy coming from coal, nuclear, and wind power totaling to 81.3% of the overall energy generation. The remaining energy comes from solar power at 11.4%, and natural gas at 7.4% of the total. The annualized cost to the utility manager of this energy generation is approximately $398M.

Since diesel is more emitting per-unit energy than any power plant type, the total social cost of emissions is quite high in the diesel scenario, annualized to approximately $200M. Note that this study only considers emissions from the electricity grid and buses. It does not consider emissions from other forms of transportation or other sources, but it is assumed that those are constant across the three scenarios.

The capital cost for BEBs is more than twice that of diesel buses. However, the daily fueling cost is almost five times lower for BEBs because of the much lower cost of electricity compared to diesel. Given this, the bus manager's annual cost of owning this BEB fleet, which is larger than the diesel fleet and includes the cost of charging stations, is only $6.3M more in the non-SC scenario, annualized to approximately $35.4M. This annual cost assumes the buses and charging station costs are distributed over 12 years and does not include any interest payments. Of course, total electricity consumption increases slightly in both BEB scenarios relative to the diesel bus scenario.

[5] This chapter is adopted from a publication submission that is under review for publication in the *Sustainable and Renewable Energy Reviews* with co-authors Joseph Griffin, Dr. Kara Kockelman, and Dr. Moataz Mohamed.

Table 27: Summary of Bus Scenario Costs, Energy, and Emissions Results

	Current State	**Non-SC BEB**	**SC BEB**
Bus statistics and costs			
Number of daily active buses in the fleet	302	423	423
Total number of buses in the fleet	423	544	544
Average cost of buses in fleet	$280,000	$646,253	$646,253
Daily total diesel consumed (gallons)	21,080	0	0
Daily total net bus charging (MWh)	N/A	188.36	188.36
Total daily fueling/charging cost	$52,699	$11,370	$5,685
Infrastructure statistics and costs			
Number of EVA080K chargers	0	38	38
Number of SAE J3105 chargers needed	0	92	92
Annual charging infrastructure costs	0	$1.92M	$1.92M
Total energy production statistics and cost			
Total daily electric energy production (MWh)	36,760	36,940	36,940
Daily coal energy production (MWh & % of total)	10.2.k (27.8%)	10.2k (27.5%)	9.01k (24.4%)
Daily gas energy production (MWh & % of total)	2.71k (7.37%)	2.93k (7.94%)	4.53k (12.3%)
Daily nuclear energy production (MWh & % of total)	9.49k (25.8%)	9.47k (25.6%)	9.03k (24.4%)
Daily wind energy production (MWh & % of total)	10.2k (27.7%)	10.2k (27.6%)	10.2k (27.6%)
Daily solar energy production (MWh & % of total)	4.17k (11.4%)	4.17k (11.3%)	4.17k (11.3%)
Daily cost of production	$1.09M	$1.09M	$845k
Electricity grid and bus greenhouse gas emissions and costs			
Total daily CO_2 emissions (tons)	4,308	4,160	4,072
Total daily NO_x emissions (tons)	1.205	1.191	1.035
Total daily SO_2 emissions (tons)	1.756	1.740	1.546
Total daily PM emissions (tons)	0.7637	0.7128	0.6313
Daily external cost of CO_2 emissions	$538,500	$520,000	$509,000
Daily external cost of NO_x emissions	$3,373	$3,336	$2,899
Daily external cost of SO_2 emissions	$3,512	$3,480	$3,089
Daily external cost of PM emissions	$3,284	$3,065	$2,715
Summary of costs and savings			
Annual cost to the bus manager	$29.1M	$35.4M	$32.3 M
Annual variable cost to utility manager	$398M	$396M	$312M
Annual external cost of emissions	$200M	$193M	$189M
Overall annual net benefit relative to current state	N/A	$2.60M	$94.6M

The top pane of Figure 22 shows the total production by energy source in the non-SC scenario. Here, nuclear runs constant at full capacity until wind generation increases at night. Both coal plants also run at full capacity until about 1 pm, when solar production nears maximum capacity, and one of the coal plants dips in generation. Then around 9 pm when base load energy demands decrease and wind becomes strong, both coal plants dip to their minimum capacity. The SCNG plants are more variable because these are considered "peaker" plants. They are smaller plants that can ramp relatively quickly, so they can respond to sharp changes in production needs. Note that CCNG does not run in this scenario.

Numerically, the total daily energy production in the non-SC scenario is 36,940 MWh, with roughly the same energy generation percentages by type as the diesel scenario. The annualized cost to the utility manager of this energy generation is approximately $396M. The annual total social cost of emissions considered is $7M less in this scenario relative to the diesel scenario, due to Austin's energy grid burning cleaner than diesel. See Table 27 below for these details.

In the SC scenario, there are the same number of BEBs and charging stations as the non-SC scenario. However, the bus manager receives discounted electricity prices in this scenario, so the total charging cost is half the charging cost in the non-SC scenario. This means that the bus manager's annual cost of owning this BEB fleet in this scenario is only $3.2M more in this scenario compared to the diesel scenario, annualized to approximately $32.3M. The total daily energy production in the SC scenario is the same as the non-SC scenario (36,940 MWh) because buses are constrained to start and end the simulation with the same SoC in both scenarios. However, the main variation between the charge-as-needed non-SC and the managed SC BEB scenarios is in the power generation profile and the associated costs and emissions. The annual total social cost of emissions considered is $11M less in this scenario relative to the diesel scenario.

In the bottom pane of Figure 22, the change in production by source is shown for SC relative to the non-SC scenario, where positive values indicate that the SC scenario produces more, and negative values indicate that the SC scenario produces less than the non-SC scenario. In the SC scenario, nuclear ramps down a bit more around 9pm than the non-SC scenario. There are also some reductions in coal generation, although the seemingly major difference in coal in the middle of the day is due to the opposite plant ramping down at 1 pm in the SC scenario relative to the non-SC scenario, meaning there is not such a major difference there. What is most noteworthy in this

scenario is that instead of running many SCNG "peaker" plants, the utility runs its CCNG plant. CCNG plants have lower ramp rates, but they are cheaper to ramp. Because the SC scenario smooths the renewable production, the utility is able to substitute the emitting, costly, quick-ramping SCNG plants for the more efficient CCNG plant. It should also be noted that more of this energy is coming from natural gas than coal in the SC relative to the non-SC scenario.

Numerically, the SC scenario produces almost 1,200 MWh less from coal than the diesel scenario, and it produces almost 1,500 MWh more from natural gas, due to the use of the efficient CCNG plant. It also produces slightly less nuclear energy (about 450 MWh less) than the diesel scenario. However, this switch from coal to CCNG energy generation is responsible for the major GHG reduction in this scenario relative to the other two scenarios. For more details, see Table 27 above.

Figure 23 below quickly summarizes the information discussed above. The top pane of Figure 23 shows the electricity generation by type in the diesel scenario, and the bottom pane shows the change in electricity generation relative to the diesel scenario in the non-SC and SC cases, respectively. Positive values in the bottom pane of Figure 23 indicate that the scenario generates more of that energy type and negative values indicate that it generates less. Please note that the scales of the bar graphs are all different.

The figure shows that the non-SC scenario requires more SCNG than the diesel scenario because of the sharp changes in electricity generation from RESs and because of the uncoordinated increases in electricity demand from the BEB fleet. However, note the scale of the non-SC chart is not very large. In contrast, the SC scenario requires significantly less coal, SCNG, and nuclear, and replaces this with CCNG. The utility manager can do this in this scenario because the BEB fleet is buffering the sharp changes in renewable production, thus allowing the use of the slower-ramping SCNG. Ideally, there would not be a replacement of nuclear (which is zero emissions) for SCNG, but it is still a net benefit from a GHG emissions perspective because it reduces a lot of coal and CCNG, which are very emitting. See Figure 24 below for emissions results.

a. Generation by Fuel Type in the Non-SC Scenario

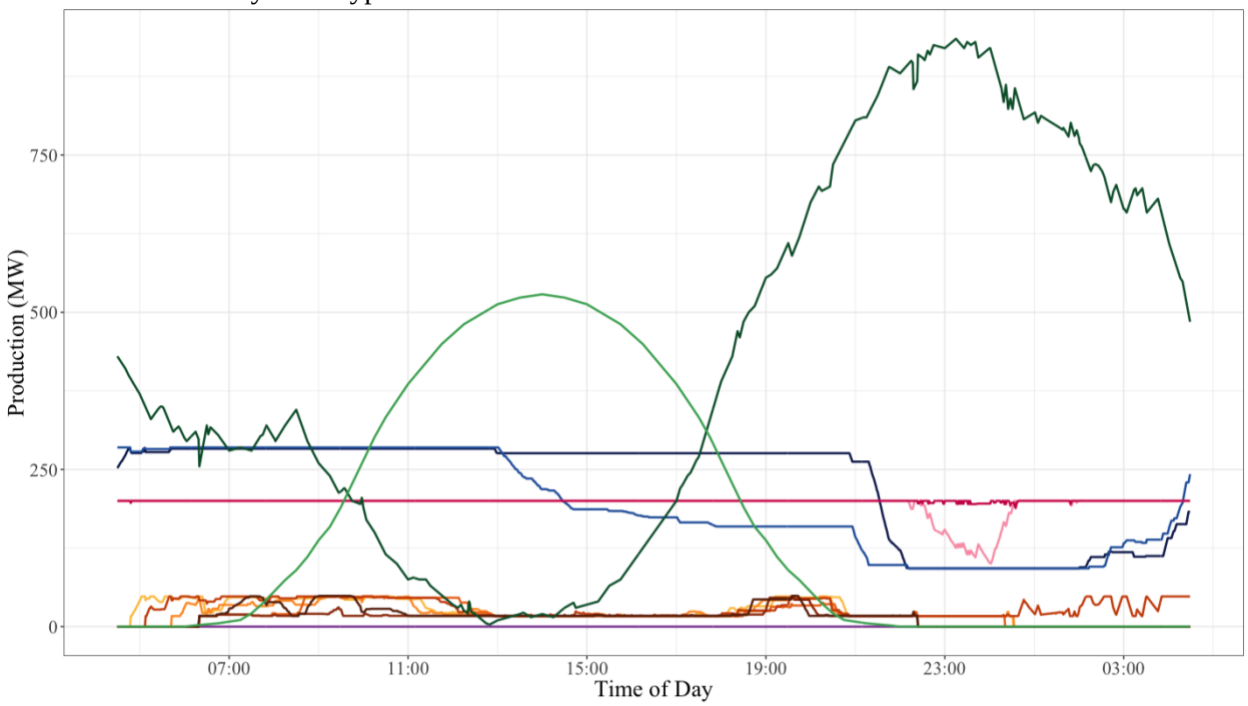

b. Change in Generation by Fuel Type in the SC Scenario Relative to the Non-SC Scenario

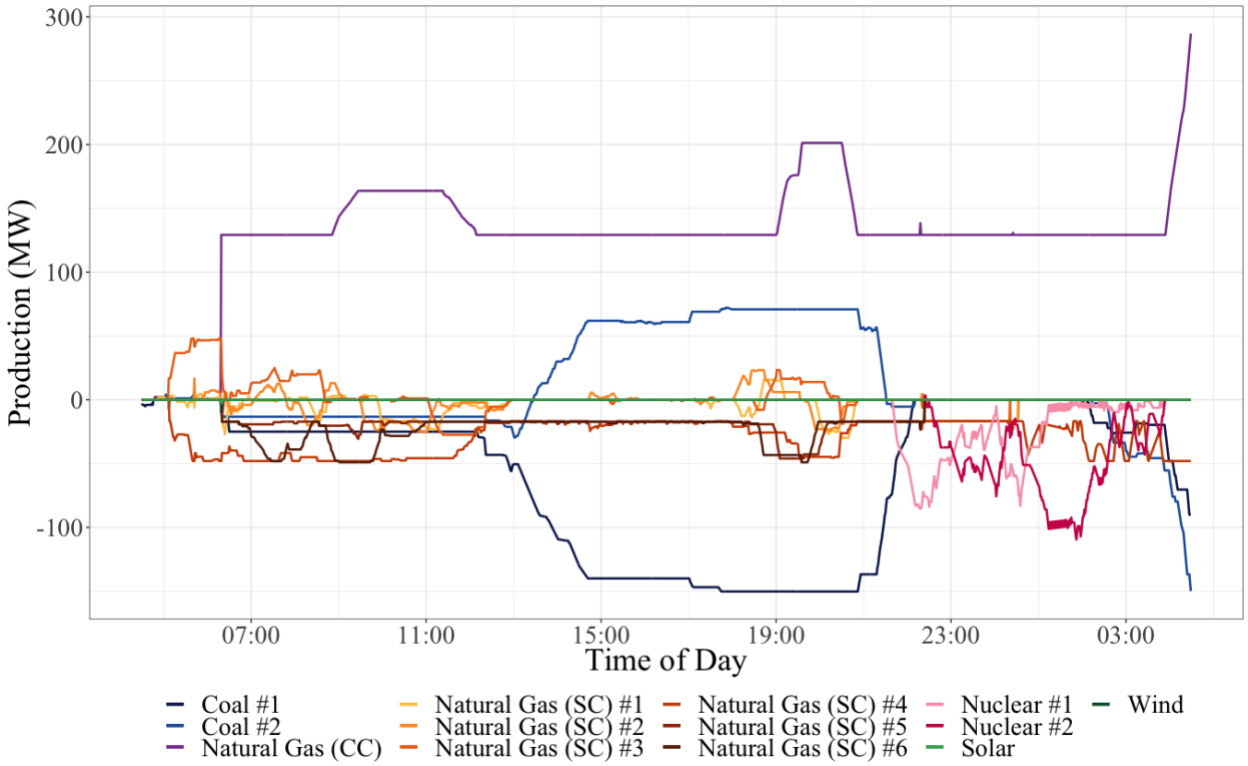

Figure 22: Production by Source in Non-Smart-Charging (Non-SC) Scenario and Change in Production in Smart-Charging (SC) Relative to Non-SC Scenario

a. Generation by Fuel Type in the Diesel Scenario

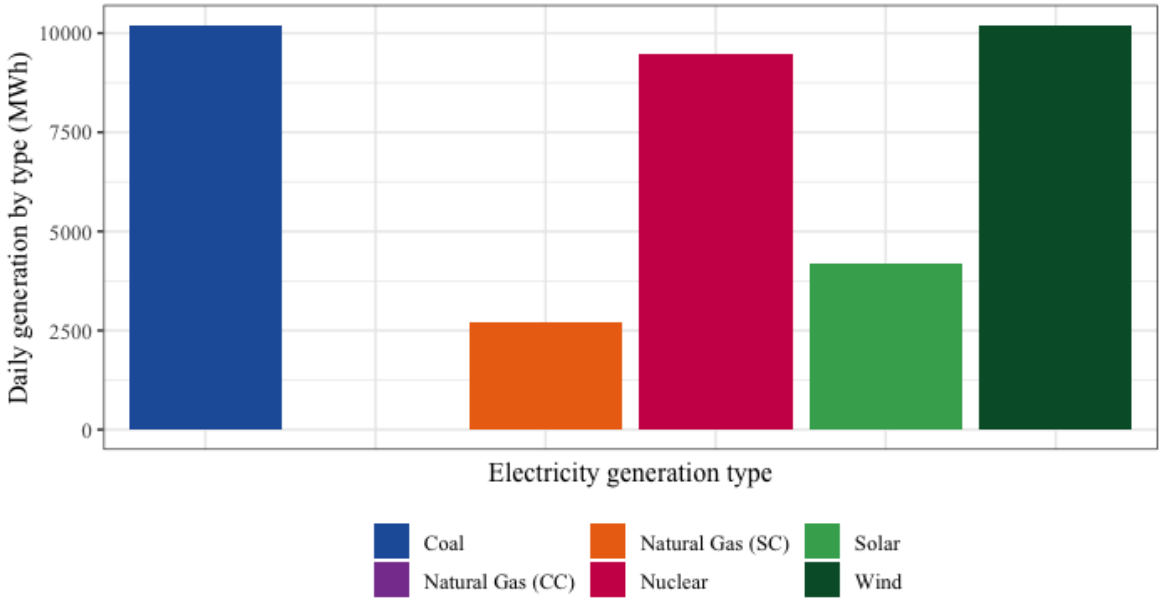

b. Change in Generation in Non-SC Relative to Diesel Scenario (note the different y-axis scale)

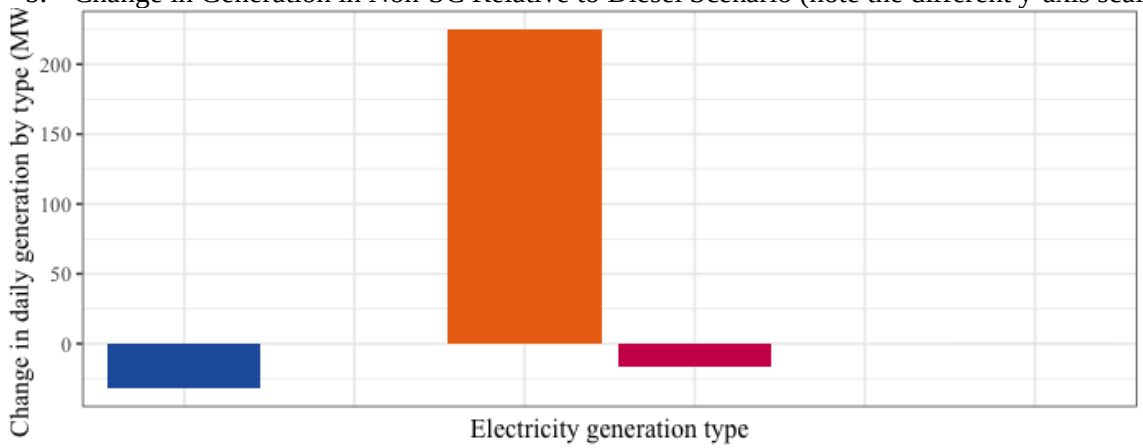

c. Change in Generation in SC Relative to Diesel Scenario (note the different y-axis scale)

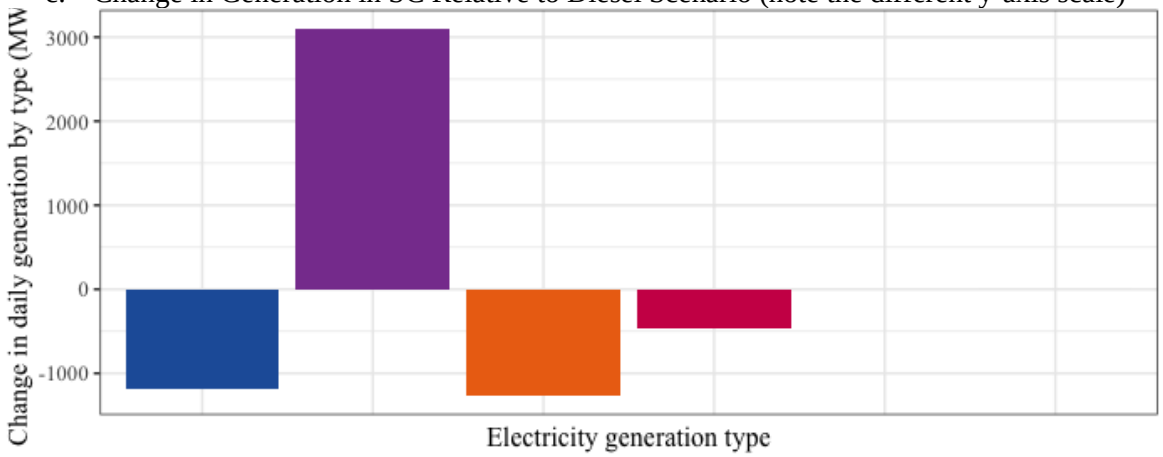

Figure 23: Electricity Generation by Type in the Diesel Case, Followed by Change in Generation by Type Relative to the Diesel Case in Non-SC and SC Scenarios

a. GHG Emissions by Type in the Diesel Scenario

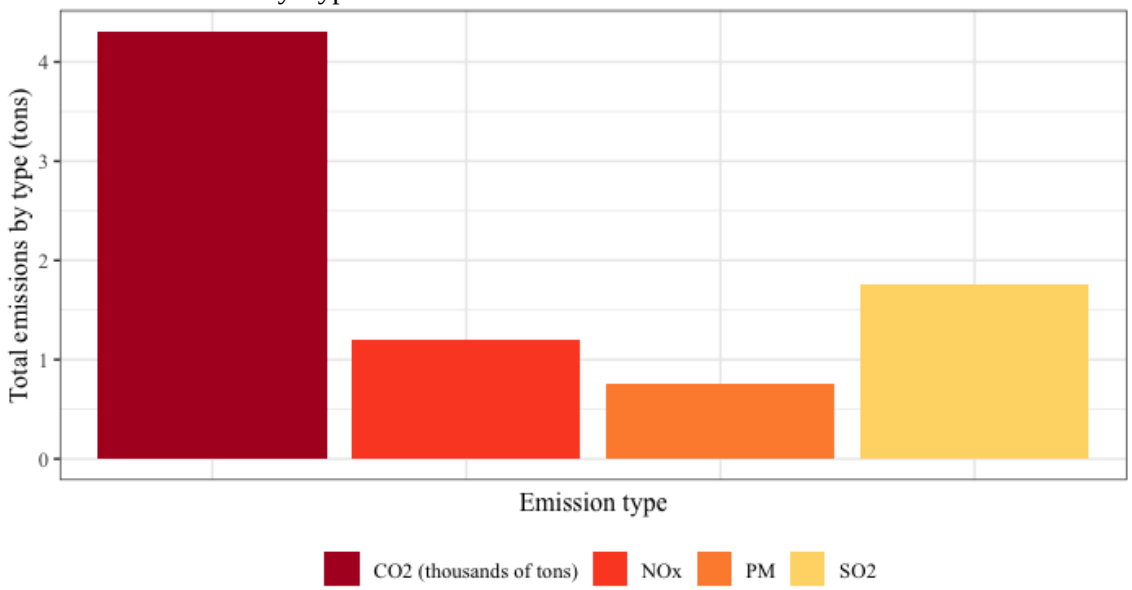

b. Change in GHG Emissions by Type in Non-SC Relative to Diesel Scenario

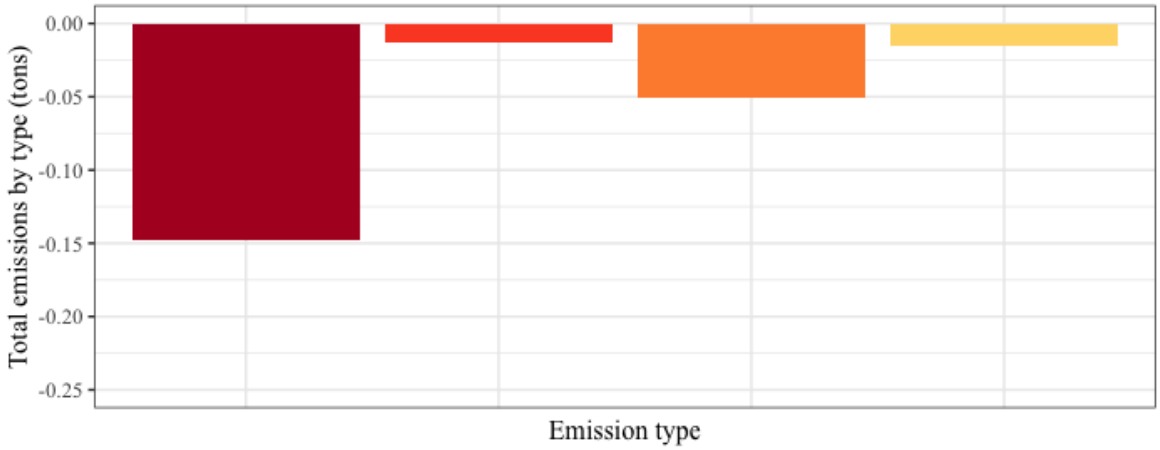

c. Change in GHG Emissions by Type in SC Relative to Diesel Scenario

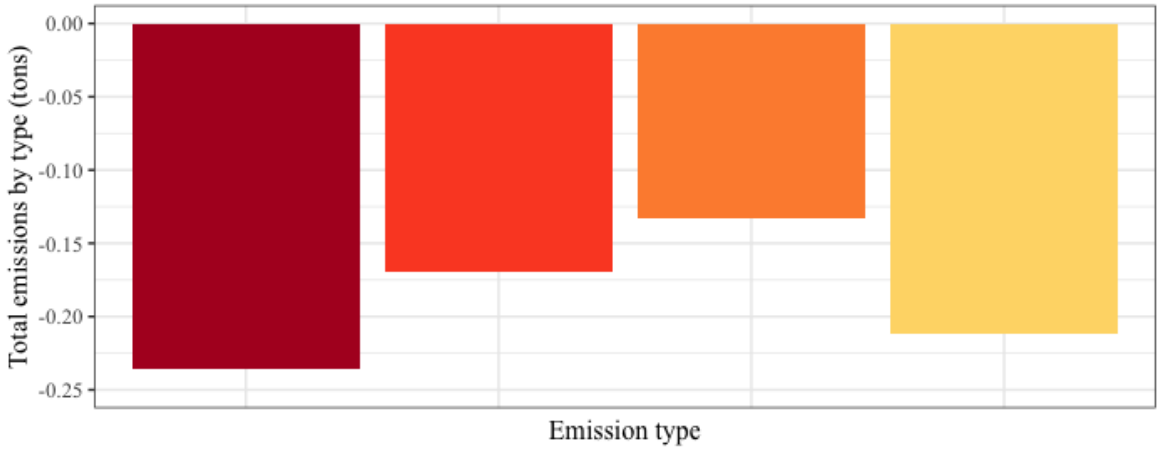

Figure 24: GHG Emissions by Type in the Diesel Case, Followed by Change in GHG Emissions by Type Relative to the Diesel Case in Non-SC and SC Scenarios

Recall that in the non-SC scenario, the bus manager receives no feedback from the utility manager and buses charge on a priority-basis. In the SC scenario, BEBs responds to power requests from the utility manager to smooth sharp changes in renewable production, mainly from wind production in this case study. In Figure 25 the power requested is plotted along with the actual power achieved by the bus manager in the SC scenario. The bus manager is not always able to fully meet the power requests, but it does quite well considering that buses must be sufficiently charged to make their routes and must remain within SoC limits of 10% to 90%. Figure 26 shows the difference in the net BEB system electricity consumption in the non-SC and SC scenarios. The SC scenario looks much noisier because it is attempting to smooth this noise from renewable generation.

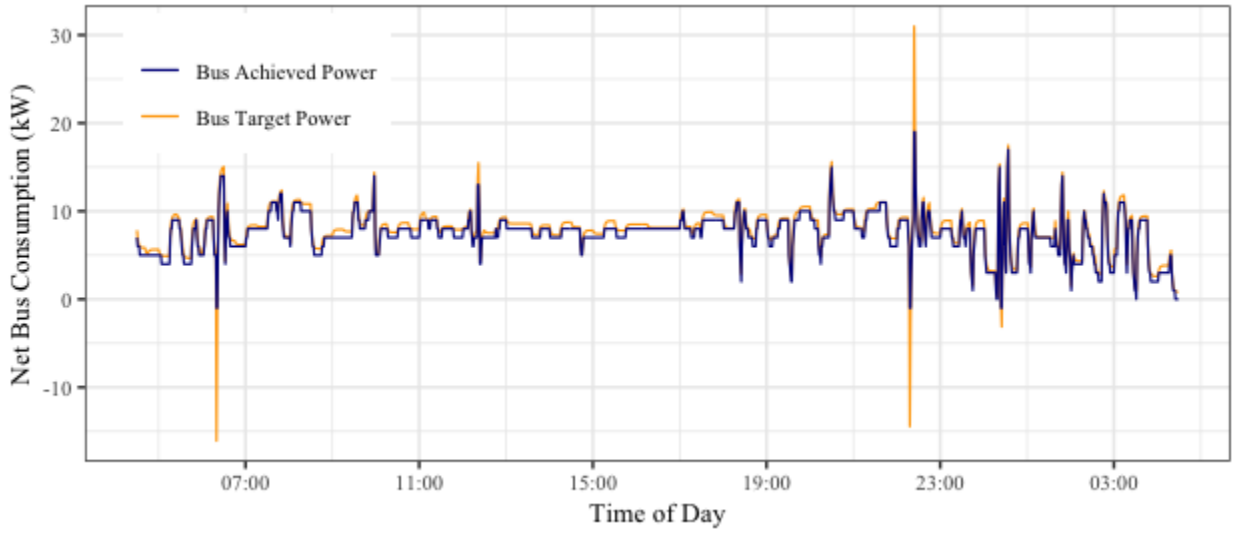

Figure 25: Battery Electric Bus (BEB) System Target vs. Achieved Consumption (from Eq. 9 & 16)

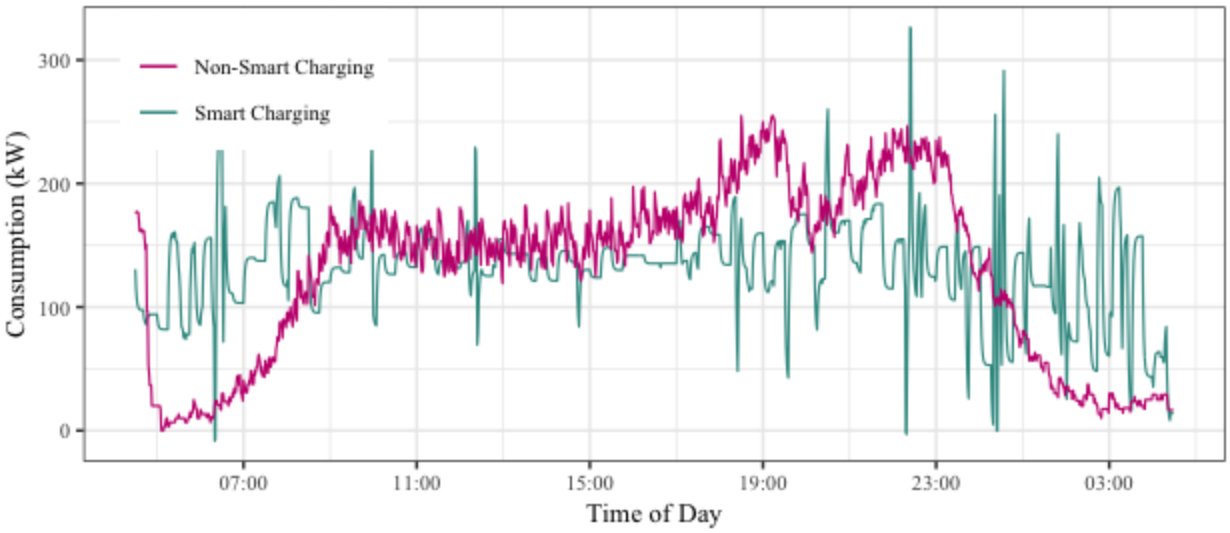

Figure 26: Net BEB System Energy Consumption in Non-SC and SC Scenarios

Chapter 14: Bus Costs, Energy, and Emissions Conclusions[6]

With the overall aim of promoting the use of RESs and electrified transportation systems, this study develops a methodology for V2G BEB systems to address utility operational challenges in utilizing RESs. Austin, Texas is used to test the proposed V2G model for a SC BEB fleet. Bus transit data and energy generation data for Austin are used to simulate the proposed model for a one-day operation.

Several important observations emerged from the analysis. This study finds that BEB annualized costs are more expensive than those of diesel buses from a transit agency's cost perspective, though this is not insurmountable. These costs could be offset by renewable energy or low-emission incentives, if carbon taxing, electric bus incentives, or similar legislature is passed in the future.

From the utility manager's perspective, the prospect is very encouraging. If Austin fully electrified its bus fleet and participated in V2G SC strategies, there is the possibility of substantial cost savings for the utility manager, even if they significantly reduce the cost of electricity for buses. When BEBs in this case study charged according to the proposed SC model, the fleet manager cut nearly 22% of their daily cost.

When considering the social costs of bus emissions, BEBs are more attractive yet. With Austin, and many other cities, planning to expand energy generation from solar and wind, this transition of transit technologies will only become more beneficial to human health. By simply electrifying Austin's buses, without any SC strategies, the total external cost of the considered emissions fell by 3.42%, and with SC strategies it fell by 5.64%. This is significant given that this only considers electrification of the bus fleet, though again the emissions from other on-road transportation systems are not considered.

It is worth noting that our results may have underestimated emissions from the utility across all scenarios because only emissions per MWh of each source were considered. It is intuitive that ramping and starting up plants would be less efficient than running a constant load, thus creating more GHG emissions. We could confidently argue that if we included this cost in the future, the SC scenario would look even more positive due to less ramping.

6 This chapter is adopted from a publication submission that is under review for publication in the *Sustainable and Renewable Energy Reviews* with co-authors Joseph Griffin, Dr. Kara Kockelman, and Dr. Moataz Mohamed.

Finally, all costs considered, both BEB scenarios are preferable compared to the diesel bus scenario. The non-SC scenario is $2.6M net positive (0.41% system-wide savings relative to diesel buses) and the SC scenario is $94.6M net positive annually (15.1% system-wide savings).

The focus of this study was to develop an SC framework that could be used to increase the practicality of heavily-renewable-dependent electricity grids by using electrified transportation as a buffer to the grid. Our case study applied this framework to the Austin bus transit fleet, which is limited in capability and scope. This framework could be applied to a wider range of electrified systems including school buses, trash and recycling trucks, mail delivery trucks, personal EVs, and other forms of battery ESSs. If more electrified systems are included in this analysis in the future, the response to fluctuations in renewable generation could be even more effective. In addition, with this increase in capacity, the methodology could go further in using electrified transportation systems to counteract daily cyclic power differences as well. In future studies, our proposed method could be adjusted to buffer daily fluctuations of wind and solar with the aim of leveling the generation of traditional sources to be constant all day.

Additionally, this study focuses on buffering supply-side renewable fluctuations, however there are also variations in demand that cause challenges and could be addressed in a similar manner. High-frequency energy consumption data would be needed, but if this were obtained then this would be another avenue to expand this methodology.

Appendix: Additional Spatial Maps for Part One

In Figures 30 – 32, higher positive values (shown in dark orange) indicate a greater increase in households in that zone in the final model year relative to the base model year in the respective scenario. Smaller positive values (shown in white) indicate a lesser increase in households in that zone in the final model year relative to the base model year in the respective scenario.

In Figures 33 – 35, smaller negative values (shown in dark green) indicate less available land that was used for construction in that zone between the final model year and the base model year in the respective scenario. Larger negative values (shown in white) indicate more available land that was used for construction in that zone between the final model year and the base model year in the respective scenario.

In Figure 36, darker blue indicates more jobs added to that zone between the base and final model year in all scenarios and lighter blue indicates fewer jobs added to that zone between the base and final model year in all scenarios. Employment increases and locations are provided as input based on CAMPO forecasts, and are exogenous to the model (Zhao, 2018).

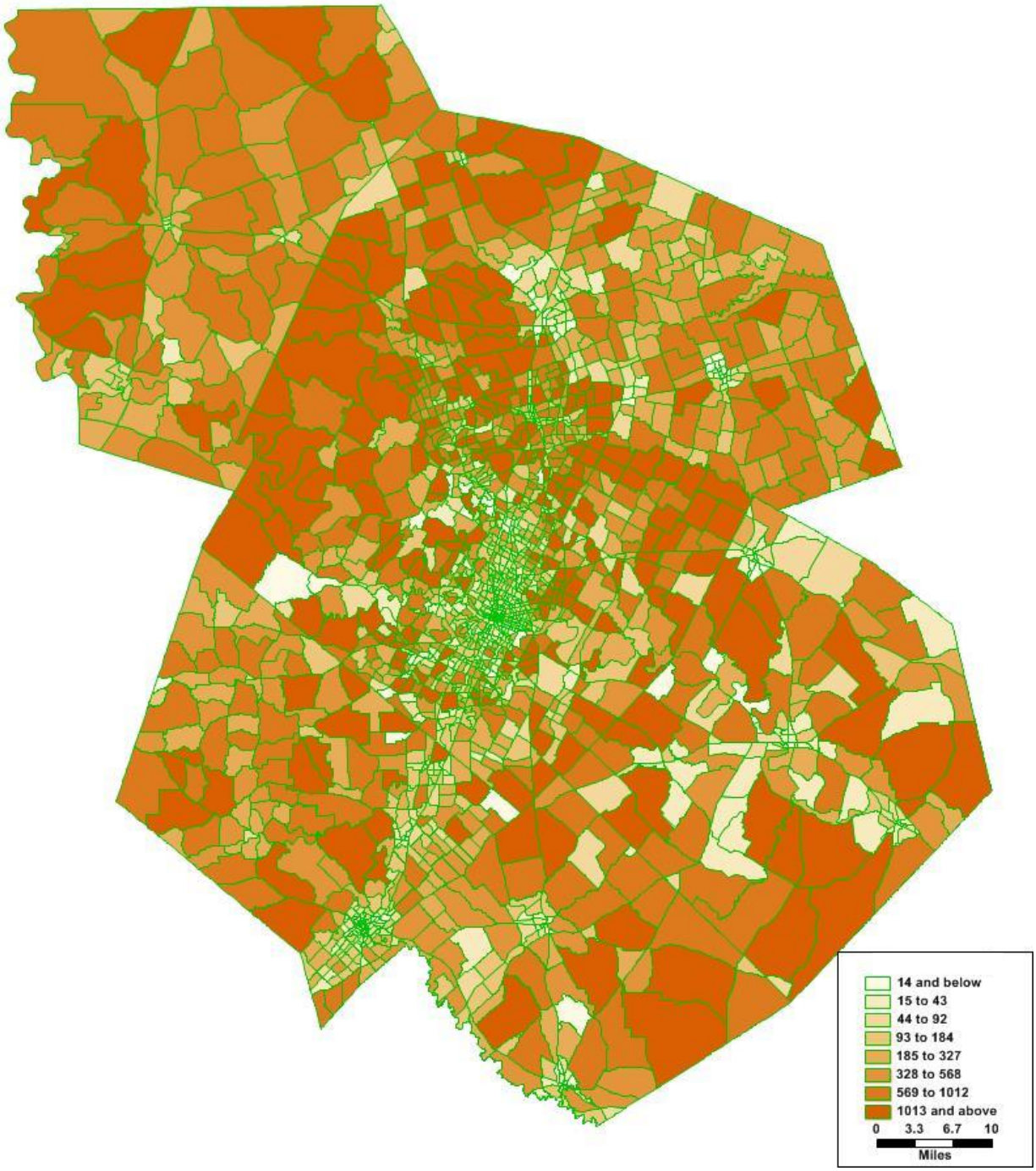

Figure 27: Change in Where Households are Located in the BAU Scenario from the Base Model Year to the Final Model Year

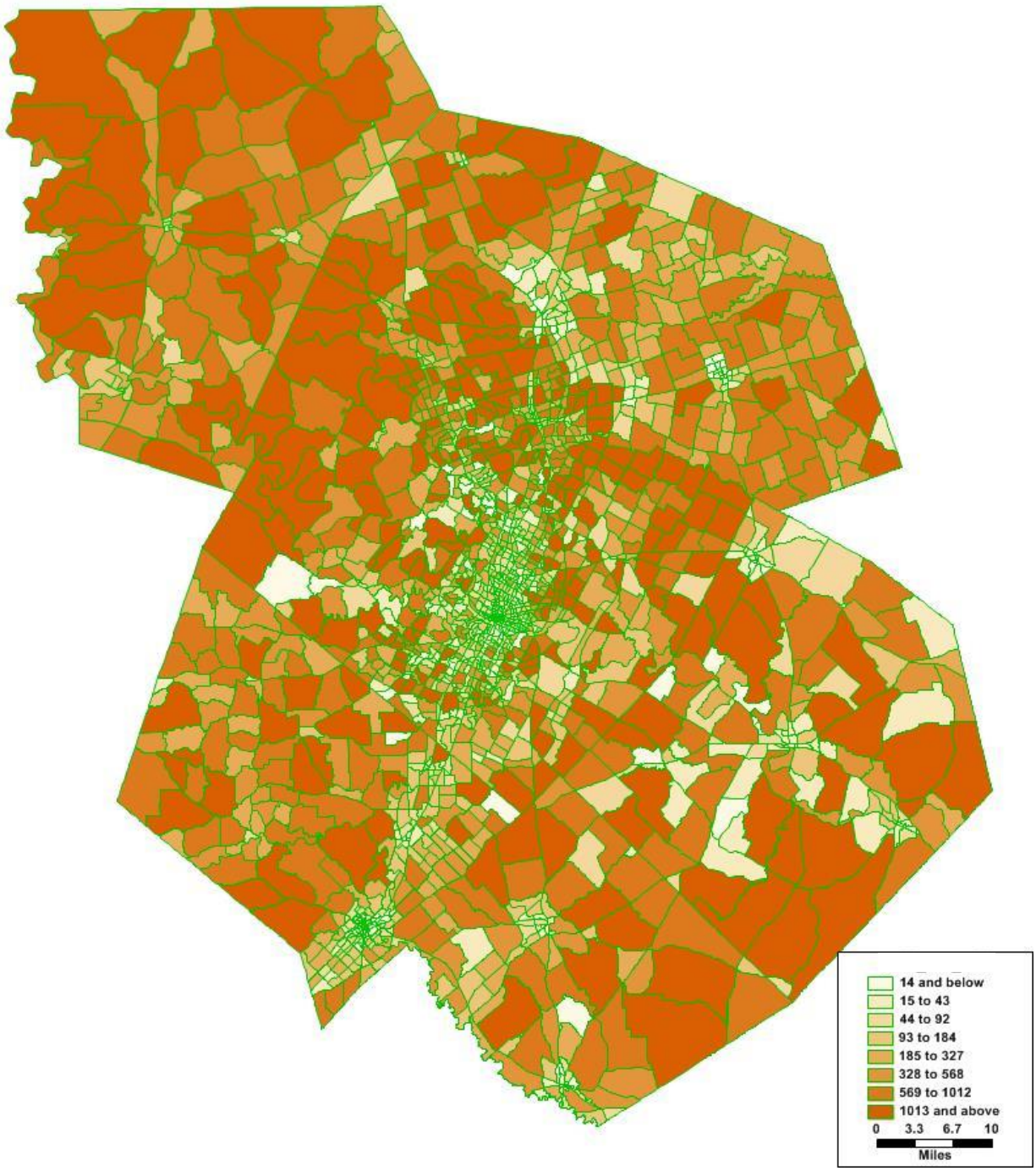

Figure 28: Change in Where Households are Located in the 100% AV Scenario from the Base Model Year to the Final Model Year

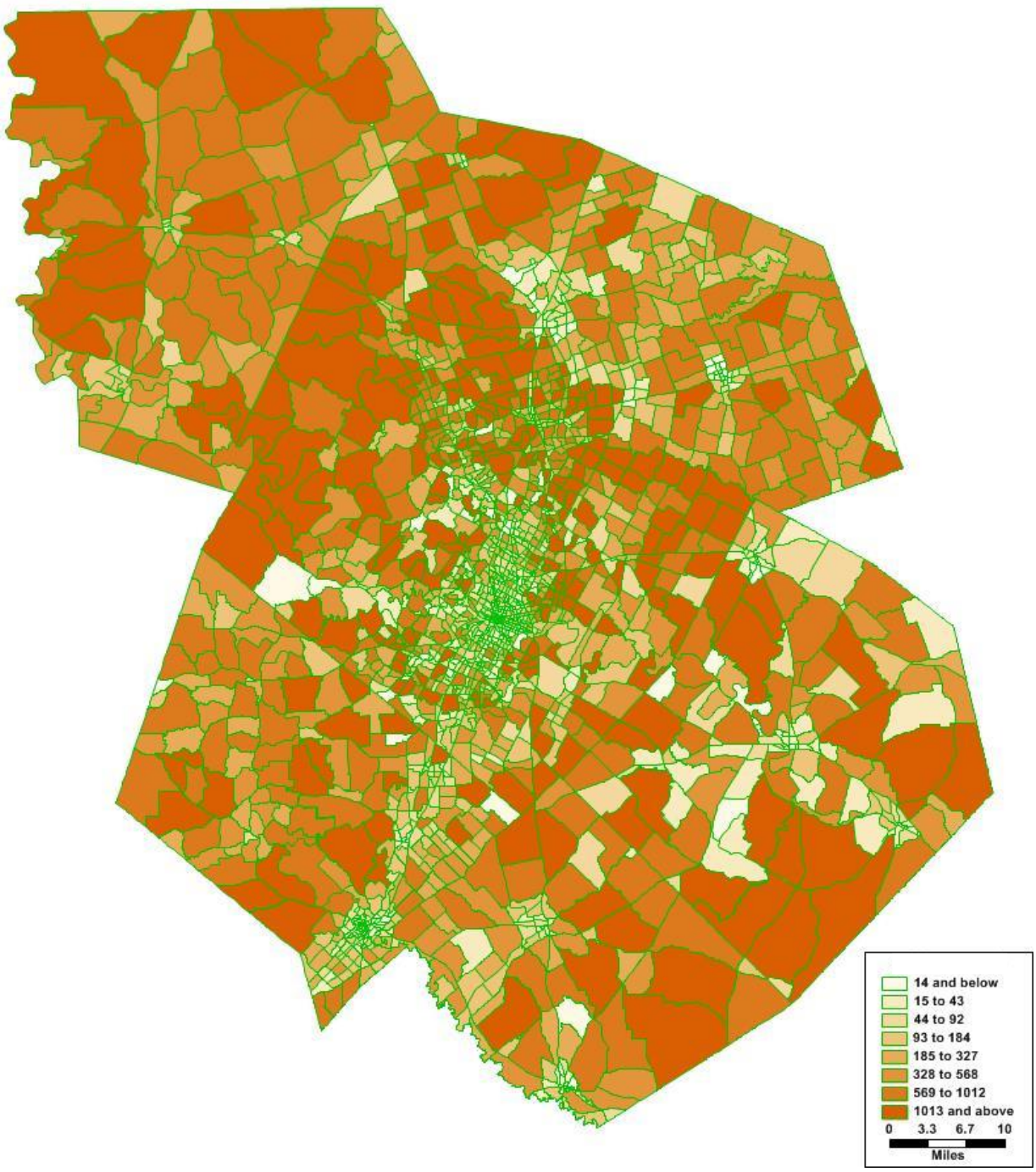

Figure 29: Change in Where Households are Located in the Hi-DRS SAV Scenario from the Base Model Year to the Final Model Year

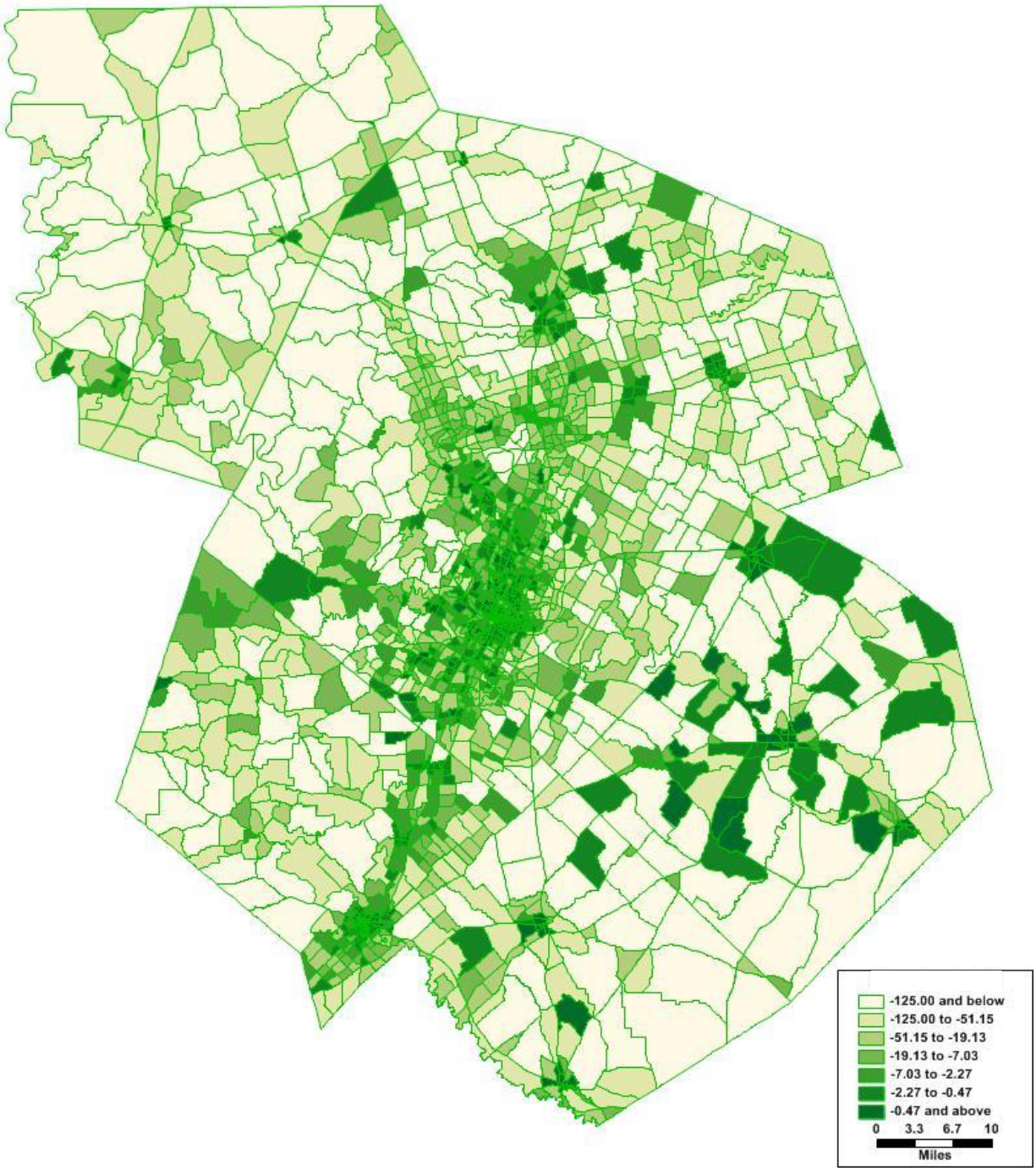

Figure 30: Change in How Much Available Land is Used for Construction in the BAU Scenario from the Base Model Year to the Final Model Year

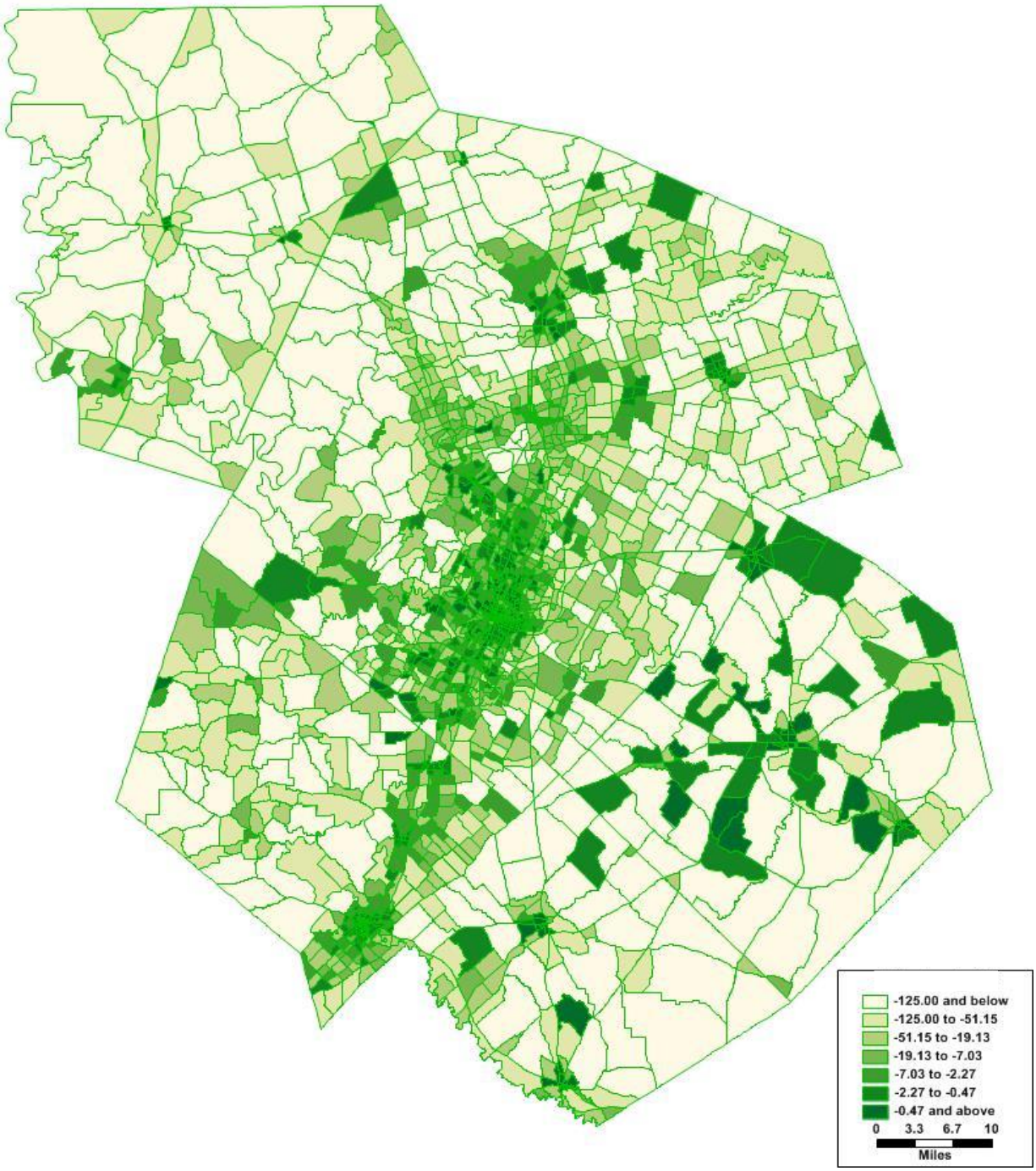

Figure 31: Change in How Much Available Land is Used for Construction in the 100% AV Scenario from the Base Model Year to the Final Model Year

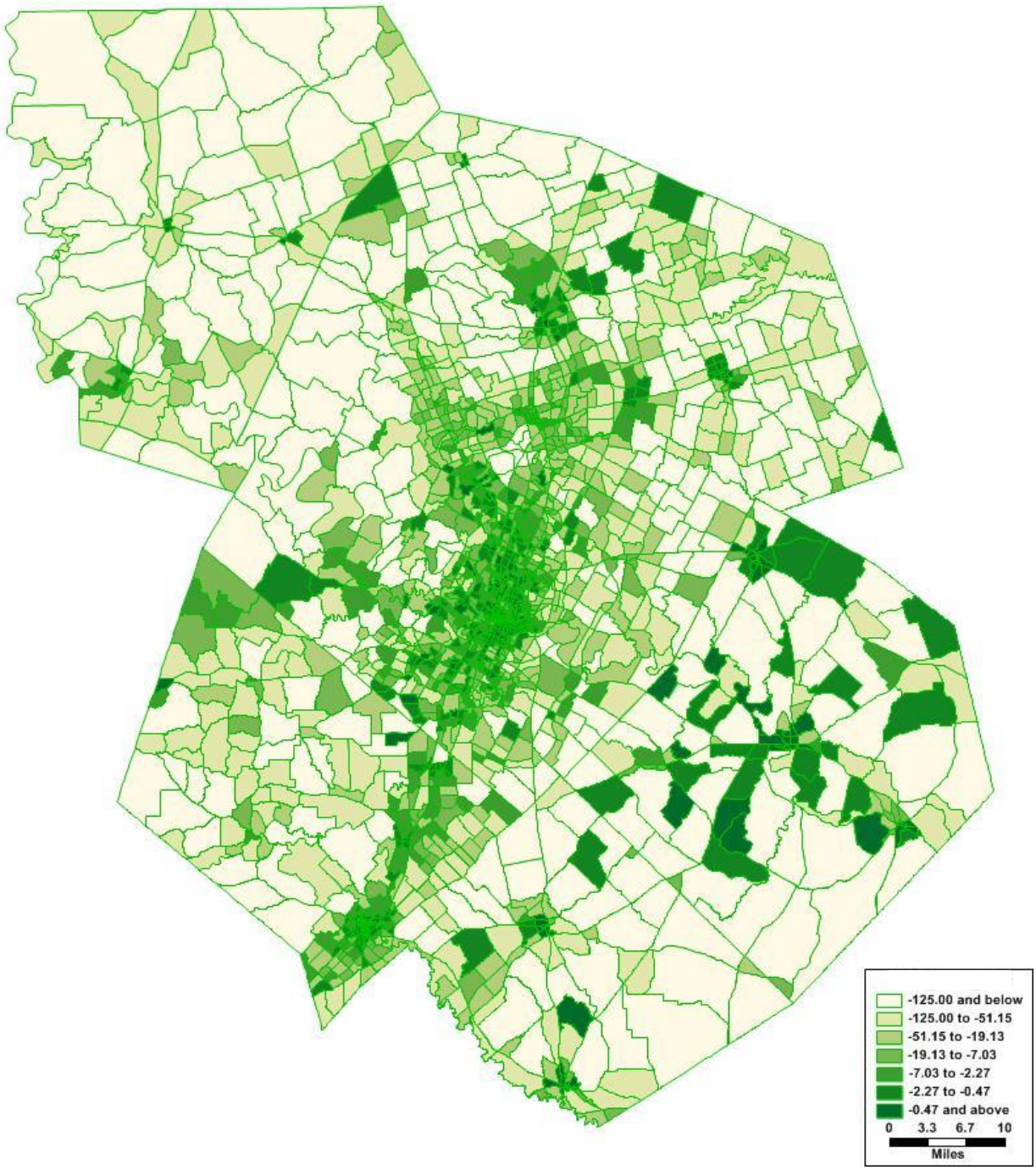

Figure 32: Change in How Much Available Land is Used for Construction in the Hi-DRS SAV Scenario from the Base Model Year to the Final Model Year

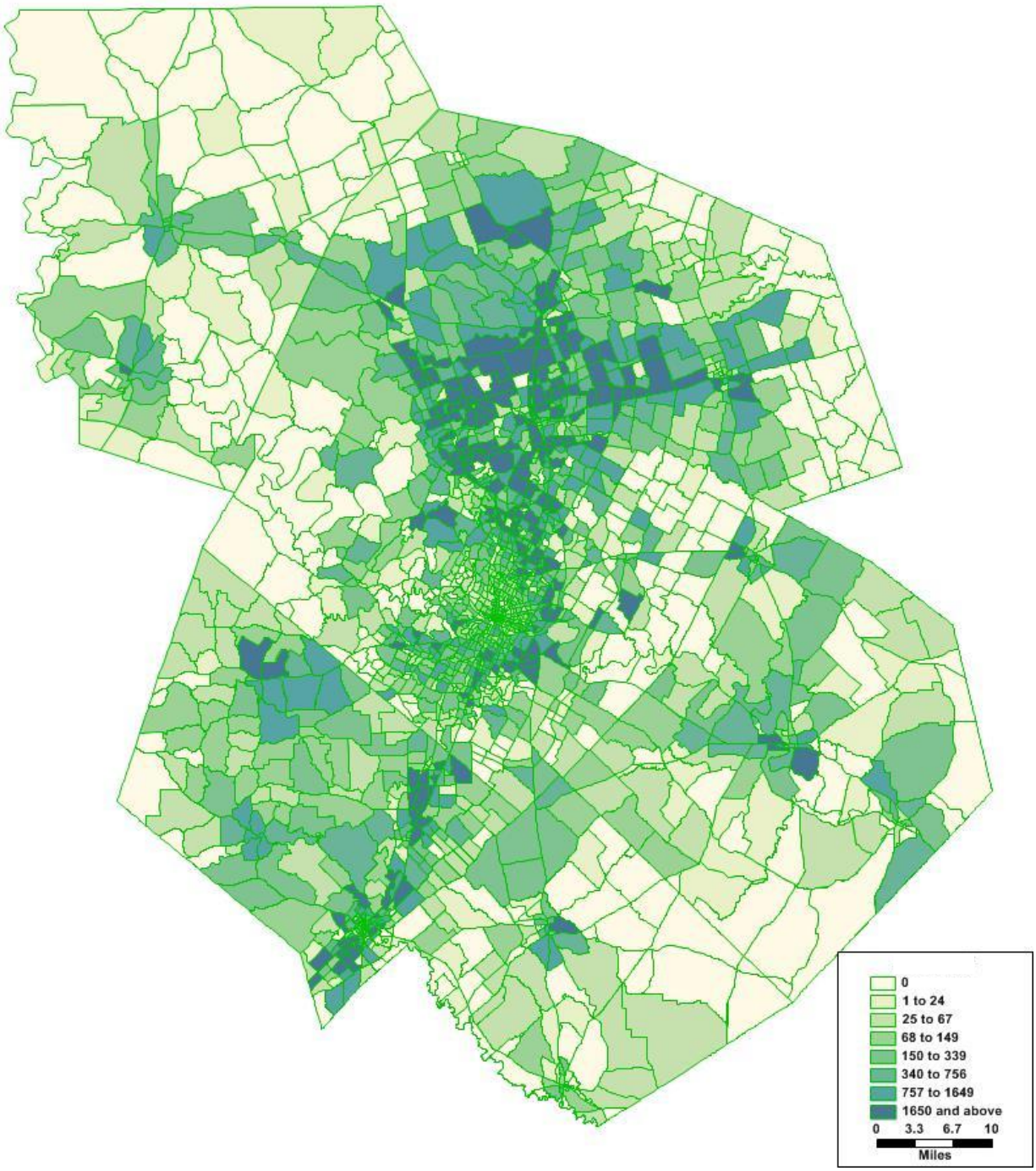

Figure 33: Job Growth Between the Base and Final Model Year

Abbreviations

AV	Autonomous vehicle,
BAU	Business-as-usual,
BEB	Battery electric bus,
CCNG	Combined cycle natural gas,
CAMPO	Capital Area Metropolitan Planning Organization,
ERCOT	Electricity Reliability Council of Texas,
ESS	Energy storage system,
EV	Electric vehicle,
GHG	Greenhouse gas,
GTFS	General Transit Feed Specification,
HEB	Hybrid electric bus,
ITLUM	Integrated transportation and land use model,
kWh	Kilowatt-hour,
lb	Pound,
LUM	Land use model,
MATSim	Multi-Agent Transportation Simulator,
MF2-4	Multi-family dwelling with up to four household residents,
MF5+	Multi-family dwelling with five or more household residents,
MH	Mobile home,
min	Minute,
MW	Megawatt,
MWh	Megawatt-hour,
MWmin	Megawatt-minute,
OSM	OpenStreetMaps,
O&M	Operating and maintenance,
PUMA	Public Use Microdata Area,
PUMS	Public Use Microdata Sample,
SAEV	Shared autonomous electric vehicle,
SAV	Shared autonomous vehicle,
SC	Smart-charging,
SCNG	Simple cycle natural gas,

SFA	Single-family attached (dwelling)
SFD	Single-family detached (dwelling)
SILO	Simple Integrated Land-use Orchestrator,
SoC	State of charge,
TAZ	Traffic analysis zones,
V2G	Vehicle-to-grid,
VMT	Vehicle miles traveled,
VHT	Vehicle hours traveled,
VO	Vehicle occupancy,
VTTS	Value of travel time savings,
µm	Micrometer

Nomenclature for Part One

u_d	Utility of the dwelling,
u_p	Utility of the price of the dwelling,
u_c	Utility of the commute time from the dwelling,
u_t	Utility of the transportation costs required for the dwelling,
u_{oth}	Utility of the non-essential factors of the dwelling,
$price_j$	Price that the household is considering paying,
$hhCount_{p;inc}$	Number of households in same income class that paid a mortgage/rent of p
et_h	Transportation expenditures for household *h*,
tc	Transportation costs,
el	Elasticity of travel demand on transportation costs, set to -0.25,
$e_{dis,h}$	Discretionary expenditures of household *h*,
s_h	Savings of household *h*,
u_{size}	Utility of dwelling size,
$u_{quality}$	Utility of dwelling quality,
$u_{autoAccess}$	Utility of auto accessibility,
$u_{transitAccess}$	Utility of transit accessibility,
$u_{crimeIndex}$	Utility of county-level crime index,

Nomenclature for Part Two

$\bar{B}$	Average bus energy consumption (MW),
c_b	Consumption rate of bus b (kWh/mile),
C_i	Variable O&M cost of energy source i ($/MWmin),
d_b	Total distance traveled by bus b over the course of the day (miles),
D_t	Total power required from bus and non-bus related loads (MW),
$E_{b,t}$	Energy needed by bus b for the next route at time t (kWh),
G_t	Total renewable energy generation at time t (MW),
$\widetilde{G_t}$	Filtered G_t using a low-pass filter (MW),
$L_{i,t,max}$	Maximum power that energy source i is capable of producing at time t (MW),
$L_{i,t,min}$	Minimum power that energy source i is capable of producing at time t (MW),
$O_{i,t}$	Binary indicator of energy source i being on ($O_{i,t} = 1$) or off ($O_{i,t} = 0$),
$p_{b,t}$	Charge priority of bus b at time t,
$P_{i,t}$	Power generation of energy source i at time t (MW),
$Q_{i,min}$	Minimum power capacity of energy source i (MW),
$Q_{i,max}$	Maximum power capacity of energy source i (MW),
$R_{buses,t}$	The power request from the utility manager to the bus manager at time t (MW),
R_i	Maximum change in power of energy source in one minute (MW),
$S_{b,t}$	SoC at time t,
RC_i	Ramping cost of energy source i ($/ΔMW),
S_t	Solar generation at time t (MW),
SC_i	Startup cost of energy source i ($/ΔMW),
$T_{b,t}$	Time until bus b must leave the charger at time t (minutes)
t_i	Initial model time (minute),
t_f	Final model time (minute),
$v_{b,t}$	Average speed traveled during time t (miles/hour),
W_t	Wind generation at time t (MW),
$z_{b,t}$	Binary indicator of bus b charging (1) or not (0) at time

References

Austin Energy. (2017, October 7). Austin Energy Resource, Generation and Climate Protection Plan to 2027. Retrieved from https://austinenergy.com/wcm/connect/6dd1c1c7-77e4-43e4-8789-838eb9f0790d/2027+Austin+Energy+Resource+Plan+20171002.pdf?MOD=AJPERES&CV.

Austin Energy. (2018a). Austin Energy Annual Report Fiscal Year 2018. Retrieved from https://austinenergy.com/wcm/connect/fc5e5028-8309-49f0-aae3-67db46bff892/2018corporate-annual-report.pdf?MOD=AJPERES&CVID=mFlnbMl.

Austin Energy. (2018b). Performance Report. Retrieved from https://data.austintexas.gov/stories/s/82cz-8hvk.

Barter, P. (2019). "Cars are parked 95% of the time". Let's check! Retrieved from https://www.reinventingparking.org/2013/02/cars-are-parked-95-of-time-lets-check.html.

BestPlaces. (n.d.). Texas: 254 Counties. Retrieved from https://www.bestplaces.net/find/county.aspx?st=texas.

Biswas, S., Verma, V., Schauer, J., & Sioutas, C. (2009). Chemical speciation of PM emissions from heavy-duty diesel vehicles equipped with diesel particulate filter (DPF) and selective catalytic reduction (SCR) retrofits. *Atmospheric Environment*, 43(11), 1917-1925.

Boyles, S., Lownes, N., & Unnikrishnan, A. (2019). Transportation Network Analysis. Version 0.8 (Public beta). Retrieved from https://sboyles.github.io/teaching/ce392c/book.pdf.

BYD. (2015). BYD Electric Vehicles. Retrieved from https://www.theicct.org/sites/default/files/BYD%20EV%20SEDEMA.pdf.

BYD-40E. (2014). Federal Transit Bus Test: BYD-40E Testing in Service-Life Category 12Year/500,000 Miles. Transport (Ed.), The Thomas D. Larson Pennsylvania Transportation Institute, Pennsylvania.

CapMetro. (2019). CapMetro GTFS. Retrieved from https://data.austintexas.gov/widgets/r4v4-vz24.

Carpenter, S. (2019, June 4). Country's Largest Transit Bus System on Electric Buying Spree. Retrieved from https://www.trucks.com/2017/10/17/la-metro-electric-bus-buying-spree/.

CarsDirect. (2012, March 15). How Does a CNG Engine Work? Retrieved from https://www.carsdirect.com/green-cars/cng-conversion-explained.

Chen, D., & Zhang, T. (2019). Smart Charging Management for Shared Autonomous Electric Vehicle Fleet: A Puget Sound Case Study. Under review in *Transportation Research Part D*.

Cheng, Y., Wang, W., Ding, Z., & He, Z. (2019). Electric bus fast charging station resource planning considering load aggregation and renewable integration. *IET Renewable Power Generation*, 13, 1132–1141. doi: 10.1049/iet-rpg.2018.5863.

CNG United. (n.d.). The Advantages and Disadvantages of CNG Conversion Kits. Retrieved November 5, 2019, from https://www.cngunited.com/advantages-disadvantages-of-cng-conversion-kits/.

Cohen, T., & Cavoli, C. (2019). Automated vehicles: exploring possible consequences of government (non)intervention for congestion and accessibility. *Transport Reviews*, 39(1), 129-151.

Congress, G. C. (2014, January 25). Initial results from first phase of road trails for 40-ft BYD electric bus in Canada. Retrieved from https://www.greencarcongress.com/2014/01/20140125-byd.html.

Dowling, R., & Morgan, A. (2019). Foreseeing the Impact of Transformational Technologies on Land Use and Transportation. National Academy of Sciences.

Environmental Protection Agency. (2017). Sources of Greenhouse Gas Emissions. Retrieved from https://www.epa.gov/ghgemissions/sources-greenhouse-gas-emissions.

ERCOT. (2019). Wind Power Production. Retrieved from http://mis.ercot.com/misapp/GetReports.do?reportTypeId=13071&reportTitle=Wind.

Foley, A., Tyler, B., Calnan, P., & Gallachoir, B. (2013). Impacts of Electric Vehicle charging under electricity market operations. *Applied Energy*, 101, 93-102. doi.org/10.1016/j.apenergy.2012.06.052.

Garcia-Olivares, A., Sole, J., & Osychenko, O. (2018). Transportation in a 100% renewable energy system. *Energy Conversion and Management*, 158, 266-285. doi.org/10.1016/j.enconman.2017.12.053.

Gent, E. (2019, November 4). New Battery Lets Electric Cars Go 200 Miles on a 10-Minute Charge. (SingularityHub) Retrieved November 4, 2019, from https://singularityhub.com/2019/11/04/new-battery-lets-electric-cars-go-200-miles-on-a-10-minute-charge/.

Gurobi Optimization, Inc. (2019). Gurobi Optimizer (Version 8) [Computer software].

Hawkins, J., & Habib, K. (2018). Integrated models of land use and transportation for the autonomous vehicle revolution. *Transport Reviews*.

He, Y., Song, Z., & Liu, Z. (2019). Fast-charging station deployment for battery electric bus systems considering electricity demand charges. *Sustainable Cities and Society*, 48, 101530. doi: 10.1016/j.scs.2019.101530.

Horni, A., Nagel, K., & Axhausen, K. W. (2016). The Multi-Agent Transport Simulation MATSim. London: Ubiquity Press.

Huang, Y., Kockelman, K., & Quarles, N. (2019). How Will Self-Driving Vehicles Affect U.S. Megaregion Traffic? The Case of the Texas Triangle. Under review for publication in *Journal of Transport Geography*.

Institute for Energy Research. (2009, June 1). The Facts About Air Quality and Coal-Fired Power Plants. Retrieved from https://www.instituteforenergyresearch.org/fossil-fuels/coal/the-facts-about-air-quality-and-coal-fired-power-plants/.

Kane, M. (2016, February 22). New Flyer Electric Bus Completes 1,150-Mile Demonstration in Florida. Retrieved from https://insideevs.com/news/327838/new-flyer-electric-bus-completes-1150-mile-demonstration-in-florida.

Kennedy, C. (2015). Key threshold for electricity emissions. *Nature Climate Change*, 5(3), 179-181. doi:10.1038/nclimate2494.

Land Use Inventory Detailed. (2019). The Official City of Austin Open Data Portal. Retrieved March 10, 2019, from https://data.austintexas.gov/Locations-and-Maps/Land-Use-Inventory-Detailed/fj9m-h5qy.

Legislative & Strategic Planning Committee (HART). (2017, May 15). Adapting New Fuel Technologies. Retrieved from http://www.gohart.org/Style%20Library/goHART/pdfs/board/Presentation%20CNG%20Verses%20Electric%20Bus.pdf.

Levy, A. (2019, January 1). The Verdict's Still Out on Battery-Electric Buses. (CityLab) Retrieved November 1, 2019, from https://www.citylab.com/transportation/2019/01/electric-bus-battery-recharge-new-flyer-byd-proterra-beb/577954/.

Li, X., Castellanos, S., & Maassen, A. (2018). Emerging trends and innovations for electric bus adoption—a comparative case study of contracting and financing of 22 cities in the Americas, Asia-Pacific, and Europe. *Transportation Economics*, 69, 470-481.

Litman, T. (2013). Changing North American vehicle-travel price sensitivities: Implications for transport and energy policy. *Transport Policy* 28: 2–10.

Madison BRT Transit Corridor Study Proposed BRT Travel Time Estimation Approach. (n.d.). Retrieved from http://www.madisonareampo.org/documents/DBRTTravelTimeEstimationApproach.pdf.

Matthews, H., Hendrickson, C., & Horvath, A. (2001). External Costs of Air Emissions from Transportation. *Journal of Infrastructure Systems*, 7(1), 13-17. doi:10.1061/(asce)1076-0342(2001)7:1(13).

Mitchell, A. (2017, July 11). Proterra and Greenville team up in $5.8M bus bid. Retrieved from https://www.greenvilleonline.com/story/money/2017/07/11/proterra-and-greenville-team-up-5-8-m-bus-bid/463964001/.

Moeckel, R. (2017). Constraints in household relocation: Modeling land-use/transport interactions that respect time and monetary budgets. *The Journal of Transport and Land Use*, 10(1), 211-228.

Moeckel, R. (2018a). NCHRP Synthesis 520: Integrated Transportation and Land Use Models: A Synthesis of Highway Practice.

Moeckel, R. (2018b). SILO Demography. Retrieved October 15, 2019, from https://silo.zone/demography.html.

Moeckel, R. (2018c). SILO Design. Retrieved October 21, 2019, from https://silo.zone/design.html.

Moeckel, R. (2018d). SILO Household Relocation. Retrieved October 15, 2019, from https://silo.zone/hhRelocation.html.

Moeckel, R. (2018e). SILO Modules. Retrieved October 15, 2019, from https://silo.zone/modules.html.

Moeckel, R. (2018f). SILO Real Estate. Retrieved October 15, 2019, from https://silo.zone/realEstate.html.

Moeckel, R. (2018g). Simple Integrated Land Use Orchestrator. Retrieved from https://silo.zone.

Moeckel, R. (2018h). SILO Introduction. Retrieved from https://silo.zone/introduction.html.

Moeckel, R. (2019a). SILO Model Java Code. Retrieved from GitHub: https://github.com/msmobility/silo/.

Moeckel, R. (2019b). Skype meeting.

Mohamed, M., Farag, H., El-Taweel, N., & Ferguson, M. (2017). Simulation of electric buses on a full transit network: Operational feasibility and grid impact analysis. *Electric Power Systems Research*, 142, 163-175. doi:10.1016/j.epsr.2016.09.032.

Mohamed, M., Garnett, R., Gerguson, M., & Kanaroglou, P. (2016). Electric buses: A review of alternative powertrains. *Renewable and Sustainable Energy Reviews*, 62, 673-684. doi:10.1016/j.rser.2016.05.019.

Muller, P. (2017). Transportation and Urban Form: Stages in the Spatial Evolution of the American Metropolis. In the Geography of Urban Transportation (pp. 57-85). New York: Guilford Press.

Muncrief, R. (2016, December). NOX emissions from heavy-duty and light-duty diesel vehicles in the EU: Comparison of real-world performance and current type-approval requirements. Briefing prepared by the International Council on Clean Transportation. Retrieved from http://www.theicct.org/sites/default/files/publications/Euro-VI-versus-6_ICCT_briefing_06012017.pdf.

Mwasilu, F., Justo, J. J., Kim, E. K., Do, T. D., & Jung, J. W. (2014). Electric vehicles and smart grid interaction: A review on vehicle to grid and renewable energy sources integration. *Renewable and Sustainable Energy Reviews*, 34, 501-516. doi:10.1016/j.rser.2014.03.031.

National Conference of State Legislatures. (2019, October 9). Retrieved October 15, 2019, from http://www.ncsl.org/research/transportation/autonomous-vehicles-self-driving-vehicles-enacted-legislation.aspx.

New Flyer-XE40. (2015). Federal Transit Bus Test: New Flyer-XE40 Testing in Service-Life Category 12Year/500,000 Miles. Transport (Ed.), The Thomas D. Larson Pennsylvania Transportation Institute, Pennsylvania.

New Residential Units: Summary by Calendar Year and Type. (October 23, 2019). Retrieved 24 2019, October, from https://data.austintexas.gov/Building-and-Development/New-Residential-Units-Summary-by-Calendar-Year-and/2y79-8diw.

Niche. (2019). Retrieved October 21, 2019, from https://www.niche.com/k12/search/best-school-districts/m/austin-metro-area/.

NREL. (2016, December 2). NREL Fuel Cell Bus Analysis Finds Fuel Economy to be 1.4 Times Higher than Diesel. Retrieved from https://www.nrel.gov/news/program/2016/nrel-fuel-cell-bus-analysis-finds-fuel-economy-to-be-14-times-higher-than-diesel.html.

Phuangpornpitak, N., & Tia, S. (2013). Opportunities and Challenges of Integrating Renewable Energy in Smart Grid System. *Energy Procedia*, 34, 282-290. doi:10.1016/j.egypro.2013.06.756.

Proterra. (2016). Catalyst:40 foot bus specifications. Retrieved from https://www.proterra.com/wp-content/uploads/2016/08/Proterra-Catalyst-Vehicle-Specs.pdf.

Proterra. (2017). Proterra 40 foot bus drivetrain performance. Retrieved from https://www.proterra.com/wp-content/uploads/2017/10/DT_PERF_HC-1.pdf.

Proterra. (2018a). Proterra introduces new high power interoperable EV charging technology. Retrieved from https://www.proterra.com/press-release/proterra-introduces-new-high-power-interoperable-ev-charging-technology/.

Proterra. (2018b). Proterra Catalyst Platform Introduction. Presentation to Plug-in NC Spring Summit. Retrieved from http://www.pluginnc.com/wp-content/uploads/2018/06/Proterra.pdf.

Proterra. (2019a). Catalyst: 40 Foot Bus Performance Specifications. Retrieved from https://www.proterra.com/wp-content/uploads/2019/06/Proterra-Catalyst-40-ft-Spec-Sheet.pdf.

Proterra. (2019b). The Proterra Catalyst 40-foot transit vehicle. Retrieved from https://www.proterra.com/products/40-foot-catalyst/.

Proterra-E40. (2015). Federal Transit Bus Test: Proterra-E40 Testing in Service-Life Category 12Year/500,000 Miles. Transport (Ed.), The Thomas D. Larson Pennsylvania Transportation Institute, Pennsylvania.

Quarles, N. and Kockelman K. (2019). Americans' Plans for Acquiring & Using Electric, Shared & Self-Driving Vehicles. under review for publication in Research in *Transportation Economics*.

Ramdass, N. (2017, May 30). 10 benefits of using Compressed Natural Gas (CNG). (Loop) Retrieved November 4, 2019, from http://www.looptt.com/content/10-benefits-using-compressed-natural-gas-cng.

Ranganathan, S. (n.d.). Hybrid Buses Costs and Benefits. Retrieved November 4, 2019, from https://www.eesi.org/files/eesi_hybrid_bus_032007.pdf.

Reichmuth, D. (2017, May 31). New Numbers Are in and EVs Are Cleaner Than Ever. Retrieved from Union of Concerned Scientists: https://blog.ucsusa.org/dave-reichmuth/new-numbers-are-in-and-evs-are-cleaner-than-ever?_ga=2.192964205.1361663491.1573771772-1383747918.1573069364.

Remix. (2019, August). August 2019 SC for Web. Retrieved from https://platform.remix.com/map/73e3cc9?latlng=30.39565,-97.94082,9.249.

REN21. (2018). Renewables 2018 Global Status Report. Retrieved from http://www.ren21.net/gsr-2018/chapters/chapter_01/chapter_01/.

Reschovsky, C. (2004). Journey to Work: 2000. U.S. Census Bureau.

Reuters. (2010, December 21). BYD focusing on electric buses and taxis. Retrieved from https://web.archive.org/web/20130310211205/http:/motoring.asiaone.com/Motoring/News/Story/A1Story20101221-253971.html.

SAE International. (2018, December 11). SAE International Releases Updated Visual Chart for Its "Levels of Driving Automation" Standard for Self-Driving Vehicles. Retrieved November 1, 2019, from https://www.sae.org/news/press-room/2018/12/sae-international-releases-updated-visual-chart-for-its-%E2%80%9Clevels-of-driving-automation%E2%80%9D-standard-for-self-driving-vehicles.

Sargent, J. (2018, February 26). Ten Years of Analyzing the Duck Chart. Retrieved from https://www.nrel.gov/news/program/2018/10-years-duck-curve.html.

Seteropoulos, A., Berger, M., & Ciari, F. (2019). Impacts of automated vehicles on travel behaviour and land use: an international review of modelling studies. *Transport Reviews*, 39(1), 29-49.

Silver, J. (2019, March 20). Here's how much Austin home prices have surged in the past 5 years. Retrieved October 23 2019, from http://austin.culturemap.com/news/real-estate/03-20-19-austin-home-price-increase-north-america-report/.

The Fuel Cells and Hydrogen Joint Undertaking. (2012, October 29). Urban buses: alternative powertrains for Europe. Retrieved from https://www.fch.europa.eu/node/790.

U.S. Census Bureau. (2017). Mean Travel Time to Work of Workers 16 Years and Over Who Did Not Work at Home. Retrieved October 21, 2019, from https://factfinder.census.gov/faces/tableservices/jsf/pages/productview.xhtml?src=CF.

U.S. Census Bureau. (2018). American Community Survey 2017 ACS 1-Year PUMS Files ReadMe.

U.S. Department of Energy. (2019, July 31). Alternative Fuels Data Center. Retrieved from https://afdc.energy.gov/fuels/prices.html.

(2003). U.S. Department of Health and Human Services: National Vital Statistics Reports. Vol. 51, No. 12.

U.S. Energy Information Administration. (2016, November). Capital Cost Estimates for Utility Scale Electricity Generating Plants. Retrieved from https://www.eia.gov/analysis/studies/powerplants/capitalcost/pdf/capcost_assumption.pdf.

Union of Concerned Scientists. (2018, March 12). How Do Battery Electric Cars Work? Retrieved from https://www.ucsusa.org/resources/how-do-battery-electric-cars-work.

University of Wisconsin-Milwaukee. (2006, September 5). Transit Cost Analysis. Retrieved from https://www4.uwm.edu/cuts/utp/cost.pdf.

USA Today. (2019, May 9). America's Fastest Growing Cities. Retrieved November 1, 2019, from https://www.usatoday.com/picture-gallery/money/2019/05/03/americas-fastest-growing-cities/39442563/.

Van den Bergh, J., & Botzen, W. (2015). Monetary valuation of the social cost of CO2 emissions: A critical survey. *Ecological Economics*, 114, 33-46. doi:10.1016/j.ecolecon.2015.03.015.

Van den Bergh, K., & Delarue, E. (2015). Cycling of conventional power plants: Technical limits and actual costs. *Energy Conversion and Management*, 97, 70-77. doi:10.1016/j.enconman.2015.03.026.

Weeberb, R., Mohamed, M., Higgens, C., Arain, A., Ferguson, M. (2018). How clean are electric vehicles? Evidence-based review of the effects of electric mobility on air pollutants, greenhouse gas emissions and human health. *Atmospheric Environment*, 185, 64-77.

Wellik, T., Griffin, J., Kockelman, K., & Mohamed, M. (2019). Utility-Transit Nexus: Leveraging Intelligently Charged Electrified Transit to Support A Renewable Energy Grid. Under review in the *Renewable and Sustainable Energy Reviews*.

Wood, L. (2019, September 4). Electric Bus Market Anticipated to Reach $71.9 Billion by 2024 - Key Players are BYD, CRRC, Alexander Dennis Limited, Solaris Bus & Coach, Zhengzhou Yutong, New Flyer, Volvo, and Proterra - ResearchAndMarkets.com. Retrieved November 1, 2019, from https://www.businesswire.com/news/home/20190904005502/en/Electric-Bus-Market-Anticipated-Reach-71.9-Billion.

Woodford, C. (2019, May 12). Diesel engines. Retrieved November 4, 2019, from https://www.explainthatstuff.com/diesel-engines.html.

Yasar, A., Haider, R., Tabinda, A., Kausar, F., & Khan, M. (2013). A Comparison of Engine Emissions from Heavy, Medium, and Light Vehicles for CNG, Diesel, and Gasoline Fuels. *Polish Journal of Environmental Studies*, 2, 1277-1281.

Yuksel, T., & Michalek, J. (2015). Effects of Regional Temperature on Electric Vehicle Efficiency, Range, and Emissions in the United States. *Environmental Science & Technology*, 49(6), 3974-3980. doi:10.1021/es505621s.

Zhao, Y. (2018). Modified CAMPO Model for Scenario Tests. Provided by Author.

Ziemke, D., Nagel, K., & Moeckel, R. (2016). Towards an agent-based, integrated land-use transport modeling system. *Procedia Computer Science*, 83, 958-963.